Radiometric Determination of Small Amounts of Potassium

By Tomitaro ISHIMORI and Yoshimasa TAKASHIMA

(Received May 29, 1953)

Sodium cobaltinitrite, the well-known reagent for both the gravimetric and the indirect colorimetric determinations of potassium[1], was used in the radiometric determination of potassium by R. Ehrenberg[2] and M. Ishibashi et al[3]. As it was difficult to obtain artificial radioactive substances, they were obliged to use natural radioactive indicators. Therefore, tedious chemical procedures were necessary before beginning the measurement of radioactivity. Their methods are schematically shown in Table I.

TABLE I SCHEMES OF RADIOMETRIC METHODS FOR POTASSIUM

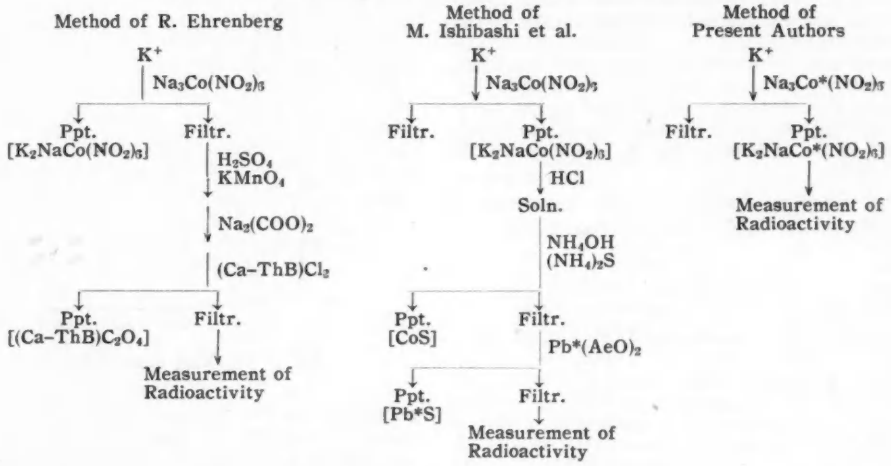

In recent years, the artificial radio-isotope of cobalt (cobalt-60) is easily obtainable from the Atomic Energy Commission of U.S.A., so the present authors investigated a simplified radiometric determination of small amounts of potassium using radioactive sodium cobaltinitrite labelled with cobalt-60 as precipitant.

(1) Determination of (8~0.3) mg. Potassium—Various amounts of the standard solution of recrystallised potassium chloride are taken and radioactive $K_2NaCo^*(NO_2)_6$ is precipitated according to the following procedure.

The relation between the relative intensity of the radioactivity of the precipitate and the amount of potassium taken is investigated.

(a) Preparation of the Radioactive Precipitant I—According to the usual method[1,3] a solution of sodium cobaltinitrite labelled with cobalt-60, $Na_3Co^*(NO_2)_6$, is prepared as the precipitant.

First, the following two solutions are prepared.

Solution (A)	cobalt nitrate	21 g.
	cobalt-60 chloride	about 0.7 mc.
	water	42 cc.
	acetic acid	10.4 cc.
Solution (B)	sodium nitrite	100 g.
	water	150 cc.

Next, the solution (B) is added to the solution (A) and the nitrogen oxide formed by the double decomposition of the salts is expelled by passing the air through the combined solution. Any precipitate formed is filtered off and the filtrate which contains sodium cobaltinitrite labelled with cobalt-60 is used as the precipitant.

In this paper, the precipitant thus prepared will be called the precipitant I.

(b) Procedure—According to the usual method[1], radioactive potassium-sodium cobaltinitrite,

1) R. Fresenius u. G. Jander, "Handbuch d. Analytischen Chemie", 3 Teil, Bd. Ia, Julius Springer, Berlin, 1940, p. 172.
2) R. Ehrenberg, *Microchem. Pregl Festschr.*, 61, (1929), *C.A.*, **24**, 2395; *Biochem. Z.*, **197**, 467 (1928), *C.A.*, **23**, 51.
3) M. Ishibashi and H. Kishi, *J. Chem. Soc. Japan*, **57**, 1039 (1936).

$K_2NaCo^*(NO_2)_6$ is precipitated by the precipitant described in (1, a). A definite amount of the standard solution of potassium chloride is poured slowly into a platinum or quartz crucible which contains 5 cc. radioactive precipitant I and 1 cc. of 1N nitric acid. Then some water is added until the total volume of the resultant solution amounts to 16 cc.

After standing over-night, the yellow precipitate of radioactive potassium-sodium cobaltinitrite is filtered on a glass filter and washed with about 20 cc. of 0.01N nitric acid and then with about 10 cc. of 95% alcohol. The washing solution is drained off by suction and the washed precipitate is dried at 110°C. in an air bath for about one hour. After cooling, the radioactivity of the precipitate on the glass filter is measured by a Geiger-Müller counter made by the Nuclear Instrument and Chemical Corporation, U.S.A.

The precipitate obtained from 3.145 mg. potassium is reserved as the standard of the radioactivity and the intensities of the activity of the precipitates obtained from the solutions containing various amounts of potassium are compared respectively with the standard. The relative intensity thus obtained is not affected by the decay of cobalt-60 or the daily variation of the sensitivity of the instrument for the measurement of radioactivity.

(c) **Results**—Results of the experiments are shown in Table II and Figure 1 and 2.

TABLE II RESULTS OF (1)

mg. K (Taken)	Relative Intensity of Radioactivity
7.863	2.27
6.291	1.82, 1.98
4.718	1.58, 1.47
3.145	1.00*, 0.98
1.573	0.45, 0.47, 0.48, 0.48
1.258	0.37, 0.40
0.943	0.28, 0.28
0.629	0.16, 0.16
0.315	0.04, 0.05

(*) Taken as the standard. The activity of the standard is about 1960 c/min. It shows slight variations according to the daily variation of the sensitivity of the counter.

In Figures 1 and 2, the almost linear relationships between the relative radioactivities and the amounts of potassium taken are shown in a fairly wide range of amounts of potassium, so we conclude that we can determine the amounts of potassium radiometrically according to the above-mentioned procedure, using Figures 1 and 2 as working curves.

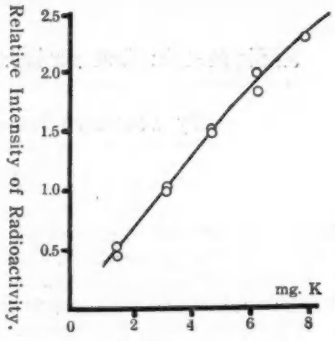

Fig. 1 Working curve of (1)

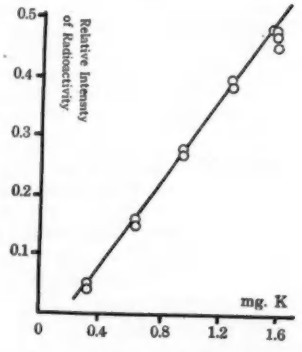

Fig. 2 Working curve of (1)

(2) **Determination of (0.8~0.16) mg. Potassium**—The relation between the relative intensity of the radioactivity of the precipitate formed and the amount of potassium taken is investigated following the same procedure as described in (1, b), and using the precipitant having a stronger specific activity, which is prepared as follows.

For the measurement of radioactivity, the same standard as (1, b) is used.

(a) **Preparation of Precipitant II**—The precipitant II is prepared from the following two solutions, (C) and (D), in the same way as described in (1, a).

Solution (C)	cobalt nitrate	15 g.
	cobalt-60 chloride	about 4.5 mc.
	acetic acid	7.5 cc.
	water	30 cc.
Solution (D)	sodium nitrite	72 g.
	water	108 cc.

(b) Results—Results are summarized in Table III and the relation between the relative intensity of the radioactivity of the precipitate and the amount of potassium taken is shown in Figure 3. As seen in Figure 3, the deviation of each experiment is larger than in Figure 1 or 2. The working curve of Figure 3 is shaped S, while those of Figure 1 and 2 are almost linear.

TABLE III RESULTS OF (2)

mg. K (Taken)	Relative Intensity of Radioactivity	Mean
0.786	2.00, 1.82, 1.88, 1.86	1.89
0.629	1.48, 1.39, 1.50, 1.54, 1.56	1.49
0.472	0.98, 0.85, 1.11, 0.92	0.97
0.315	0.29, 0.29, 0.34	0.31
0.157	0.05, 0.07, 0.13, 0.16	0.10

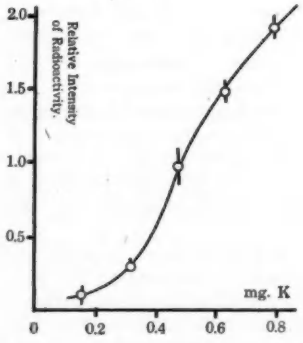

Fig. 3 Working curve of (2)

(c) Application of the Above Method to the Determination of Potassium in Silicate rocks—The determination of potassium contents in two kinds of andesite is tried by the above described radiometric method, combined with the method of J. Lawrence Smith for the isolation of alkali chlorides, using about 200 mg. of each sample. Comparison of the values thus obtained with those obtained by the usual gravimetric method as potassium chloroplatinate is shown in Table IV.

TABLE IV DETERMINATION OF POTASSIUM CONTENT OF ANDESITE

Sample	% K_2O obtained gravimetrically	% K_2O obtained radiometrically
(A)	0.46, 0.40	0.39, 0.39
(B)	0.40, 0.33, 0.37	0.32, 0.32

(3) Determination of (0.126~0.0016) mg. Potassium—In the experiments for the minute quantities of potassium, the precipitation and the filteration must be done microchemically, and the precipitant with a much higher specific activity must be used. Further, cautions against the contamination by potassium from glass-wares must be taken.

(a) Standard Solution of Potassium Chloride—The stock solution which contains 1.5010 g. potassium chloride per litre is diluted just before use and a series of dilute standard solutions of potassium chloride is prepared.

(b) Preparation of Radioactive Precipitant III—The precipitant III is prepared from the following two solutions, (E) and (F), in the same way as described in (1, a) in a smaller scale.

Solution (E)	cobalt nitrate	1 g.
	cobalt-60 chloride	about 6.7 mc.
	acetic acid	0.5 cc.
	water	2 cc.
Solution (F)	sodium nitrite	4.8 g.
	water	72 cc.

(c) Procedure—Five drops of the precipitant III and one drop of 1N nitric acid are put into the platinum crucible which contains 0.5 cc. of standard solution of potassium chloride prepared as described in (3, a). After leaving it over-night, the precipitate formed is filtered off with a micro filter-tube[4] and washed with 0.5 cc. of 0.01N nitric acid and then three times with 0.7 cc. alcohol. The washed precipitate in the platinum crucible is dissolved in hot water. The solution is transferred to a glass dish through the filter-tube and evaporated up on a water bath.

The radioactivity of the residue in the glass dish is measured with Lauritsen electroscope, made by the Scientific Research Institute, Tokyo. For the measurement of radioactivity, an arbitrarily selected specimen is used as the standard and the ratio of the intensities of the radioactivity of each specimen and the standard is calculated.

(d) Results—Results are shown in Table V and Figure 6. The relation between the relative intensity of the measured radioactivity and the amount of potassium is linear, so that the quantitative determination of the minute amounts of potassium can be carried out in the procedure described in (3, c).

4) E. Beryl Daw, "Quantitative Organic Microanalysis", J. & A. Churchill Ltd., 1937, p. 96.

TABLE V RESULTS OF (3)

mg. K (Taken)	Relative Intensity of Radioactivity
0.0000	0.003, 0.003
0.0016	0.004, 0.005
0.0047	0.023, 0.025
0.0094	0.052, 0.061
0.0236	0.14, 0.12
0.0394	0.23, 0.24
0.0630	0.36, 0.36
0.1260	0.69, 0.70

The activity of the standard is about 347 div./min. It shows slight variations according to the daily variation of the sensitivity of the electroscope.

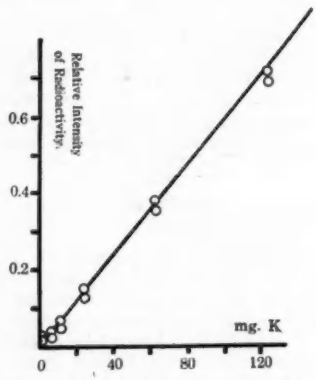

Fig. IV Working curve of (3)

(e) Applications of the Above Method— (i) The potassium contents of two samples of silicate rocks; andesite found in Kurofuyama, ASAMA[5] and the standard sample of diabase sent from the U. S. Geological Survey, W-I[6], are determined according to the following procedure:

About 20 mg. of the powdered sample is treated according to the J. Lawrence Smith method to obtain the total alkali chlorides. The chlorides are dissolved in a little water and treated as (3, c). A platinum or quartz crucible is used as a microbeaker and all filtrations are done with a micro filtertube.

In Table VI, the values thus obtained are

TABLE VI DETERMINATION OF POTASSIUM CONTENT OF SILICATE ROCKS

Sample	% K_2O obtained gravimetrically	% K_2O obtained radiometrically
Andesite (Kurofuyama)	0.85*	0.54, 1.07***
Standard Sample of Diabase	0.78**	0.77***, 0.88***

(*) Value given by I. Iwasaki.
(**) Value reported from our laboratory.
(***) Value obtained by the extrapolation of the working curve.

compared with those obtained by the usual method. The coincidences are fairly good and we conclude that this method will be effective for the microdetermination of potassium in silicate rocks.

(ii) The potassium content of the tap water which is supplied to our laboratory is determined in our micro-radiometric method.

The procedure is as follows: About ten grams of the tap water is taken in a platinum crucible and evaporated to about 0.5 cc. on a water bath. After cooling, the evaporate is treated as described in (3, c).

The determinations are done with 10 g. and 15 g. of the water, and potassium with the concentrations of 0.083 and 0.087 millimole per litre are obtained respectively. Although the presence of ammonium ion disturbs the determination, the ammonium content of the sample is estimated to be 0.006 millimole per litre by the colorimetric method, so that our value for potassium should be reliable.

The authors wish to express their sincere thanks to Prof. Sinnosuke Matuura for the facilities accorded to them during this investigation, to Prof. Iwaji Iwasaki for providing samples of andesite and to Mr. N. Kokubu for determining the ammonium content of the tap water.

Department of Chemistry,
Faculty of Science,
Kyushu University

5) I. Iwasaki, *J. Chem. Soc. Japan*, **57**, 1324 (1936).
6) W. G. Schlecht, *Anal. Chem.*, **23**, 1568 (1951).

On the Distribution of Nutrient Salts in the Equatorial North Pacific*

By Rinnosuke FUKAI

(Received May 30, 1953)

Introduction

Among the factors which govern the distribution of chemical constituents such as nutrient salts and dissolved oxygen in sea water, in addition to the hydrographical movements of sea water, it is clear that the biological factor, namely consumption or regeneration of the constituents by living organisms or from their corpses, play an important rôle in natural processes. Since 1937, various investigators[1] have discussed this problem in connection with the existence of the oxygen minimum layer in the oceans, and it has generally been accepted that the biological factor cannot be ignored in natural processes. As the author had an opportunity of analysing the water samples collected from the equatorial region of the North Pacific Ocean, where the movements of sea water represent a characteristic feature of the tropical region, the distribution of nutrient salts has been investigated taking the biological factor into consideration.

Samples and Analytical Methods

Water samples were collected by members of the Nankai Regional Fisheries Research Laboratory (Kôchi, Kôchi Prefecture, Japan) when the marine observations on the fishing ground of tunny were carried out aboard "F.R.S. Tenyô Maru" in the summer of 1951. The analysis of the samples except those of dissolved oxygen was carried out by the author at the Tôkai Regional Fisheries Research Laboratory (Tokyo, Japan) after about four weeks standing. The chemical constituents analysed were chlorine, phosphate-phosphorus and nitrate-nitrogen. Dissolved oxygen was determined by a member of the Nankai Regional Laboratory aboard the ship. As the area in which the observations were carried out was within a district of high temperature, the water samples to be analysed for phosphate and nitrate were carefully preserved by adding chloroform-toluol mixture and mercuric chloride solution respectively immediately after the sampling, in order to prevent bacterial growth. Although some changes in phosphate contents in the samples collected from the upper layers containing living organisms must be expected even if the above mentioned procedure has been adopted, serious errors will not be introduced since the phosphate contents of the upper layers are much lower than those of the deeper layers.

The analytical methods adopted were as follows: chlorine: titration method proposed by Fajans using uranine as the indicator[2]; phosphate: colorimetric determination by Denigès-Atkins using Beckman's Model DU Quartz spectrophotometer[3]; nitrate: colorimetric method with Harvey's reduced strychnine reagent[4].

Data for nutrient salts obtained from the equatorial region of the Pacific were accumulated through the observations made on board the "Carnegie" and the "Dana". But the data obtained from this region are much fewer than those from the equatorial Atlantic and there is a lack of systematic data in the Eastern Hemisphere. The data dealt with in this paper were obtained along the longitude 150°E and 160°E between the equator and latitude 20°N. Twelve samples were collected at each station from different layers above a depth of 1000 meters. Collection was carried out at about 50 stations, then about 600 samples were collected and analysed.

The distribution of the constituents was considered on the basis of the data obtained from longitudinal section along 150°E, since the conditions along 160°E did not differ significantly from those along 150°E.

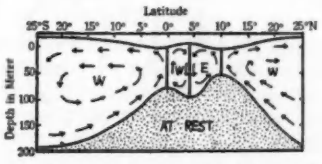

Fig. 1. Schematic representation of the vertical circulation within the equatorial region of the Atlantic. W: westward current. E: eastward current. (After Defant, 1936).

* Contribution B-No. 113 from the Tokai Regional Fisheries Research Laboratory, Tokyo, Japan.

1) H. R. Seiwell, *Papers in Phys. Oceanogr. and Meteor.*, **5**, No. 3 (1937); H. U. Sverdrup, *J. Conseil permanent intern. pour l'exploration de la mer*, **13**, 163 (1938).

2) Y. Miyake, This Bulletin, **14**, 29 (1939).

3) R. Fukai, *J. Oceanogr. Soc. Japan*, in press.

4) H. Wattenberg, *Rapp. et Proc.-Verb. des Reunions, Conseil permanent intern. pour l'exploration de la mer*, **103**, 1 (1937).

Results and Discussion

1. General Feature of Water Movements in the Region in Question—A. Defant[5] derived theoretically a schematic representation of vertical circulation of water within the equatorial region of the Atlantic as shown in Fig. 1. According to the schema, convergence (sinking of water) or divergence (upwelling of water) is developed at the boundary between the currents, and it is expected that the distribution of chemical constituents may fit with the schema. Based upon the data obtained on board the "Carnegie" (1929), Sverdrup et al[6]. recognised the close agreement between the water movements and the distribution of the constituents in the upper layers.

2. Chlorinity Distribution in the Longitudinal Section—The data for chlorine determination were given in term of chlorinity. In Fig. 2, distribution of chlorinity in the

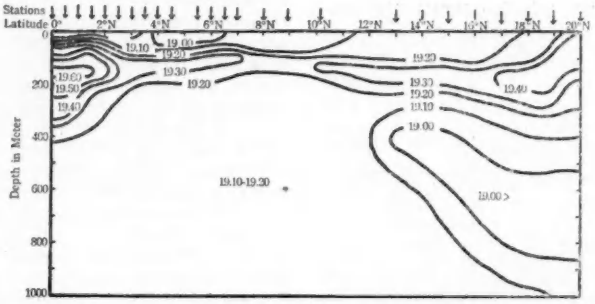

Fig. 2. Chlorinity distribution in the longitudinal section along 150°E. Units: ‰.

longitudinal section along 150°E is given. In this figure, it is obvious that the intermediate water of the North Pacific appears within the depths between 400 m. and 800 m. at lat. 12°N and northwards. As going to the south, the water below the intermediate layer becomes homogeneous and the characteristic water of the equatorial region having high chlorinity (Cl>19.30‰) appears in the upper layer. But whether the water movement has influence on the distribution of chlorinity is not clear.

3. Distribution of Dissolved Oxygen and Phosphate-phosphorus in the Section—The distributions of dissolved oxygen and phosphate are illustrated in Figs. 3 and 4, respec-

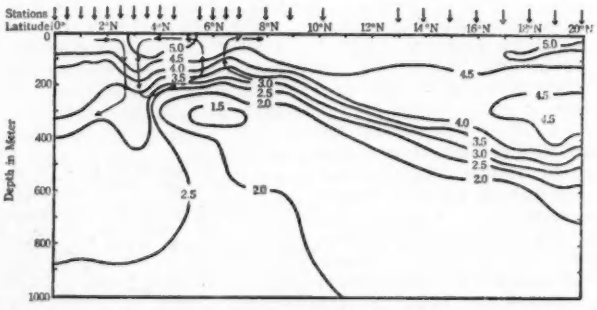

Fig. 3. Distribution of dissolved oxygen in the longitudinal section along 150°E. Units: O_2 ml. per liter.

tively. In these figures, the corresponding distribution of these constituents with the schema presented by Defant is clearly shown. The convergence occuring near lat. 3°N and divergence near 6°N are recognised. The water movements suggested by the distribution of the constituents are shown by the arrows. From these figures, it is concluded that the vertical movements of water affect

5) A. Defant, Deutshe Atlantische Expd. *Meteor*, Bd. VI, Teil I (1936).
6) H. U. Sverdrup et al., "The Oceans", Prentice-Hall, New York, 1946, p. 711.

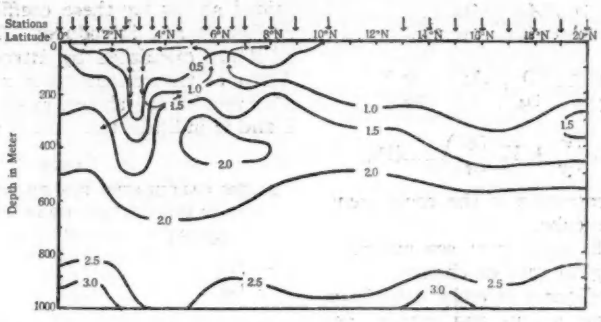

Fig. 4. Phosphate distribution in the longitudinal section along 150°E. Units: μg. -atoms PO_4-P per liter.

the distribution of the constituents at a depth as low as 500 m.

Although the water movements affect decidedly the distribution of the constituents in the region in question, it cannot be explained simply by the structure of water movements that a pool of minimum content of dissolved oxygen or maximum content of phosphate appears at a depth of about 300 m. The extreme value of the constituents in an enclosed domain should appear only when the decomposition of dead organisms, namely the consumption of dissolved oxygen or the regeneration of phosphate takes place within the domain[7]. It is a remarkable fact that the domain lies just below the divergence, for areas in which upwelling of water is taking place have high fertility due to the nutrient salts transported from the layers below, and are able to support larger populations of organisms than other areas. If a greater quantity of dead organisms in this area decomposes while sinking, decomposition processes occuring in this water column will be more vigorous than those in other areas. In consequence, it is probable that the maximum decomposition may occur in the above mentioned domain.

4. Relationship between Oxygen Minima and Maxima of Nutrient Salts—Before considering the decomposition processes quantitatively, the vertical distribution of the constituents is given in Fig. 5. From the figure, it can be seen that the extreme values of these constituents appear in close correlation with each other and are centered at a depth of 300 m. Although vertical distributions of phosphate and nitrate seem to be in parallel correlation, it is noteworthy that the gradient of phosphate increment is larger than that

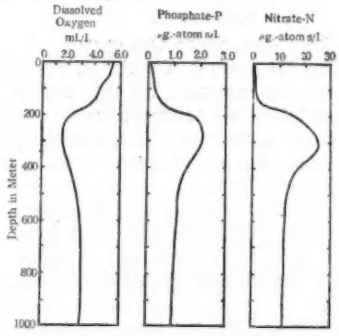

Fig. 5. Typical vertical distributions of dissolved oxygen, phosphate-phosphorus and nitrate-nitrogen in the Equatorial North Pacific based on the data obtained at Station 29 (lat. 4°30′N, long. 150°02′E).

of nitrate increment at depths within 200～300 m. This may be attributed to the difference in the rates of liberation between phosphate and nitrate *in situ*, as the author has recently pointed out[8]. Due to the lack of available data for nitrate, further detailed discussion concerning the vertical distribution of nutrient salts is impossible.

5. Quantitative Consideration on the Rate of Decomposition—In order to obtain quantitative knowledge upon the rate of decomposition in connection with the appearence of oxygen minima and nutrient salts maxima, computations were carried out introducing some simplifying assumptions.

If we consider a cube of sea water of a unit volume *in situ*, the change of concentration of the constituents affected by the biological factor in this cube can essentially be expressed[9].

7) G. A. Riley, *Bull. Bingham Oceanogr. Collection*, **8**, Article 1 (1951).

8) R. Fukai, This Bulletin, **25**, 123 (1952).

9) H. U. Sverdrup, *J. Conseil permanent intern. pour l'exploration de la mer*, **13**, 163 (1938).

$$\frac{\partial c_o}{\partial t} = R + \frac{\partial}{\partial x}\left(\frac{Ax}{\delta}\cdot\frac{\partial c}{\partial x}\right) + \frac{\partial}{\partial y}\left(\frac{Ay}{\delta}\cdot\frac{\partial c}{\partial y}\right) + \frac{\partial}{\partial z}\left(\frac{Az}{\delta}\cdot\frac{\partial c}{\partial z}\right) - \left(V_x\frac{\partial c}{\partial x} + V_y\frac{\partial c}{\partial y} + V_z\frac{\partial c}{\partial z}\right) \quad \cdots\cdots(1),$$

where, C_o: Concentration of the constituent in the cube,
δ: Specific gravity of sea water,
R: Biological rate of change,
A_x, A_y, A_z: Coefficents of eddy diffusivity along x-, y- and z-axis, respectively,
V_x, V_y, V_z: Current velocity components along x-, y- and z-axis, respectively.

We take x-axis from the east to the west, y-axis from the south to the north and z-axis from the surface to the bottom and make the following assumptions.

1. Steady state has been established. In other words, the distribution of the concentration is not altered in the course of time.
2. The distribution of the concentration is homogeneous along the east-west axis.
3. Current velocities except along the east-west axis, are negligibly small in the computation.

Under these assumptions, equation (1) is reduced as follows:

$$R = -\left[\frac{\partial}{\partial y}\left(\frac{Ay}{\delta}\cdot\frac{\partial c}{\partial y}\right) + \frac{\partial}{\partial z}\left(\frac{Az}{\delta}\cdot\frac{\partial c}{\partial z}\right)\right] \quad \cdots\cdots(2).$$

Assumptions 1 and 2 are supposed to be reasonable, because the difference between the distribution pattern along 150°E and that along 160°E is small. Assumption 3 is also likely correct since the vertical current velocity is nearly equal to zero at depths such as an oxygen minimum layer and horizontal current velocity along y-axis, V_y, may also be ignored because it does not exceed the order of 0.5 cm /sec.

Now let us assume that δ equals unity and A_y and A_z are constant and rewrite the equation (2) into a finite form. Then we may obtain.

$$R = -\left[A_y\frac{\delta^2 c}{\delta y^2} + A_z\frac{\delta^2 c}{\delta z_2}\right] \quad \cdots\cdots(3).$$

We cannot calculate the values of R unless the values of A_y and A_z are known. However, the derivation of physical coefficents, A_y and A_z, from the present data is difficult. Accordingly, the values which have been obtained so far for these coefficents in various regions[10] are introduced. Thus, the values of R are calculated by introducing the gradients of the concentration near 300 m. depth. The results are shown in the tables. Tables I and II indicate the rate of phosphate liberation and oxygen consumption, respectively. As it is considered that $A_y = 10^7$ C.G.S.[11] and $A_z \leqq 10$ C.G.S.[12] in the layer in question, the rate of $3\sim8\times10^{-8}$ μg.-atoms PO_4-P/1. sec. for phosphate liberation and of $3\sim12.5\times10^{-8}$ ml. O_2/1. sec. for oxygen consumption may be estimated. Knowledge concerning the biological rate of change *in situ* has scarcely been accumulated. The values here proposed are about ten times higher than those proposed by Riley in 1951.[7] But, these values are prolobly reliable, for they are estimated for a particular layer within the tropical region of high temperature, while Riley's values are those for the whole Atlantic Ocean.

TABLE I

VALUES CALCULATED FOR PHOSPHATE LIBERATION

Units: 10^{-8} μg.-atoms PO_4-P/1. sec.

A_z / A_y	10^6	10^7	10^8
0	0.3	3.4	34
10	5.1	8.2	39
50	24	27	58

TABLE II

VALUES CALCLATED FOR OXYGEN CONSUMPTION

Units: 19^{-8} ml. O_2/1. sec.

A_z / A_y	10^6	10^7	10^8
0	−0.4	−3.6	−36
10	−9.3	−12.5	−45
50	−45	−49	−81

Summary

The present author carried out the determination of nutrient salts of the water samples collected from the equatorial region of the North Pacific in 1951, and their distributions have been investigated taking the biological factor into consideration.

The author found that the distributions of nutrient salts were closely connected with the structure of the movements of sea water in this region and that the effect of water movements was extended to a depth of 500 m. On the other hand, it is suggested that the oxygen minima and nutrient salts maxima developed just below the divergence are caused by the biological factor.

10) H. U. Sverdrup et al., "The Oceans", Prentice-Hall, New York, 1946, p. 484.
11) R. B. Montogomery and E. Palmen, *J. Marine Res.*, 3, 112 (1940).
12) H. R. Seiwell, *Papers in Phys. Oceanogr. and Meteorol.*, 3, No. 1 (1935).

The estimations of biological rate of change of the constituents in the layer in which the decomposition processes might occur were made, introducing some simplifying assumptions. As the results, the values of $3\sim8\times10^{-8}$ μg.-atoms PO_4-P/1; sec. for phosphate liberation and $3\sim12.5\times10^{-8}$ ml. O_2/1. sec. for oxygen consumption were obtained. These values are probably reliable as the measure indicating the rate of decomposition processes which take place in the subsurface layer within the region in question.

The author desires to express his hearty thanks to Prof. Kenjirô Kimura of Tokyo University and Dr. Masao Migita of the Tokai Regional Fisheries Research Laboratory for their valuable advice. Many thanks are also due to Mr. Hiroshi Yabe and other members of the Nankai Regional Laboratory who have placed water samples at the author's disposal.

Tokai Regional Fisheries Research Laboratory, Tokyo, Japan

Spectrochemical Study of Microscopic Crystals. IV. The Dichroism of the Tetrahalogeno-Complex Type[1]

By Shoichiro YAMADA and Ryutaro TSUCHIDA

(Received June 25, 1953)

Previously the present authors[2,3] reported on the dichroism of tetra-co-ordinated planar complexes of platinum(II) and palladium(II), and reached the conclusion that the dichroisms of these planar complexes can be classified into two types; that is, the "tetrahalogeno-complex type" and the "tetracyano-complex type." Both the types have been found to show the following common rule as to the second band: the ∥-absorption[4] is hyperchromic to the ⊥-absorption[4] in palladium complexes, and the ∥-and ⊥-absorptions in platinum complexes show the band with maximum absorption coefficient of almost equal magnitude. The main difference between the two is that in the former type the second band of the ∥-absorption lies in the longer wave-length than the ⊥-absorption whereas in the latter it holds the relation reverse to the above. It seemed of interest to investigate the cases with other planar tetra-co-ordinated complexes. In the present work, the dichroisms of crystals of K_2PdI_4, $K_2Pd(SCN)_4$ and $K_2Pt(SCN)_4$ have been measured and the results of the measurements have been discussed in association with the previous data[2,3] on dichroisms of planar complexes.

1) Presented in part at the Symposium on Co-ordination Compounds, Tokyo, November 13, 1951.
2) S. Yamada, *J. Am. Chem. Soc.*, **73**, 1182 (1951).
3) S. Yamada, H. Yoneda and R. Tsuchida, *J. Chem. Soc. Japan*, **69**, 145 (1948).
4) ∥- or ⊥-absorption represents, respectively, absorption by polarized light with its electric vector parallel or perpendicular to the plane of the complex.

Experimental

Materials.—$K_2Pd(SCN)_4$ was prepared in red hexagonal prisms from potassium tetrachloro-palladate (II) and potssium thiocyanate. The crystal shows dichroism on the prism face, i. e., orange-red and yellow, and exhibits an oblique extinction. Dichroism measurements were made on the prism face by polarized lights with their electric vectors along the directions of extinction.

K_2PdI_4 was prepared in black, rhombic tablets with metallic lustre by adding a concentrated solution of potassium tetrachloro-palladate (II) to a hot solution of potassium iodide. The crystal exhibits a straight extinction. Dichroism can be recognized under the microscope with a thin crystal; that is, it appears brownish black and greenish black by polarized lights with their electric vectors along the c-and a-axes, respectively. Dichroism measurements were made in these directions; c-and a-absorptions represent absorptions by polarized lights with their electric vectors along the c-and a-axes, respectively.

$K_2Pt(SCN)_4$ was prepared in orange, hexagonal prisms by the method of Buckton[5]. The crystal exhibits an oblique extinction on the prism face, and appears yellow and yellowish orange by polarized light with electric vector along the directions of extinction. Dichroism measurements were performed along the directions of extinction, that is, the a-and b-directions in the figure (Fig. 3).

$K_2PdBr_4.2H_2O$ was prepared by the method of Gutbier and Krell.[6] The brown prismatic crystals obtained belong to the rhombic system, and

5) G. B. Buckton, *Ann.*, **92**, 236 (1854).
6) A. Gutbier and A. Krell, *Ber.*, **38**, 2385 (1905).

show a marked dichroism on the prism face. Dichroism measurements were made on this face by polarized lights with electric vectors parallel and perpendicular to the principal axis. Although the dichroism of the crystal had been reported in the previous paper,[2,3] measurements in the present work have been extended to the region of longer wave-length and smaller extinction coefficients. The crystal structure of the compound has not yet been analyzed. However, we concluded in the previous report[3] that the complex ions in the crystal are arranged parallel to each other with their planes perpendicular to the c-axis. ∥-and ⊥-absorptions are designated on the basis of the above presumption.

Measurements.—Quantitative dichroism measurements were performed by the microscopic method.[7] The crystals used in the measurements were several hundredths of mm. thick. α denotes extinction coefficient per mm. of the crystal. Molecular absorption coefficients, k, were estimated from the relation, $k=10M\alpha/\rho$, where M and ρ represent, respectively, the molecular weight of the compound and the density of the crystal. Results of the measurements are shown in the Figures 1~4 and tabulated in the Tables I~III.

Absorption spectra of aqueous solutions of $K_2PdBr_4.2H_2O$ and $K_2Pd(SCN)_4$ were determined by the photographic method using a sector-photometer, and that of $K_2Pt(SCN)_4$ was determined with a Beckman quartz-spectrophotometer model DU.[8]

Results and Discussion

Potassium Tetrathiocyanato-palladate (II).—A striking difference is observed between the two component absorptions in Fig. 1.

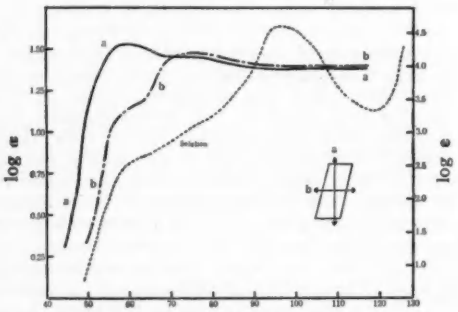

Frequency (ν), 10^{13}/sec.

Fig. 1. Absorption spectra of $K_2Pd(SCN)_4$

Comparing the result of the present measurements with existing data on absorption spectra of other palladium complexes,[2,3] it is reasonable to suppose that in the absorption spectra of the crystal the band at $\nu=60\times10^{13}$/sec. corresponds to the second band,[9] and that the flat absorption in the shorter wave-length region consists of the third[9] and SCN-specific bands.[10] The first band[9] may be so small that it is probably covered under the large second absorption band. The rule as to the dichroism of planar complexes of palladium, which was reported previously,[2] states that the second band of the ∥-absorption is hyperchromic to that of the ⊥-absorption. Therefore, the absorption curve "a" of the thiocyanato-complex may reasonably be assigned to the ∥-absorption. From the absorption curves, the following conclusion may be reached for the above complex-salt; the ∥-absorption is bathochromic to the ⊥-absorption. This is the case with the "tetrahalogeno-complex type.[2]" Consequently, tetrathioacyanato-palladium (II) complex is supposed to fall into the group of the tetrahalogeno-complex type."

Potassium Tetraiodo-palladate (II).—A rather remarkable dichroism can be recognized, as shown in Fig. 2. The band at $\nu=40$

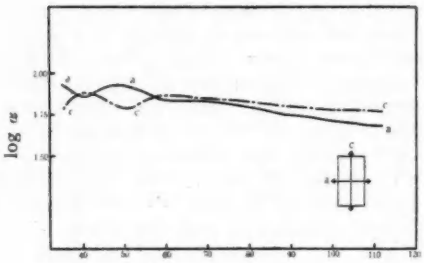

Frequency (ν), 10^{13}/sec.

Fig 2. Absorption spectra of K_2PdI_4.

in the c-absorption is considered to be the second band, and the broad absorption extending from $\nu=60$ to shorter wave-length region is supposed to be the superposition of the third and I-specific bands. With the a-absorption, the second band lies in the near infrared region. The broad absorption curve in the visible and shorter wave-length region consists of the third and I-specific bands. It is readily seen that for the second band the following relation exists; the a-absorption is bathochromic and hyperchromic to the c-absorption. With tetrachloro-and tetrabromo-palladate (II) ions, the following rule has been established[2]: the ∥-absorption of the second

7) R. Tsuchida and M. Kobayashi, "The Colours and the Structures of Metallic Compounds," Zoshindo, Osaka, Japan, 1944, p. 180; This Bulletin, **13**, 619 (1938); *J. Chem. Soc. Japan*, **60**, 769 (1939).

8) The authors are indebted to the Analytical Laboratory of our department for the measurement of absorption spectra of $K_2Pt(SCN)_4$ with a Beckman spectrophotometer.

9) About the first, second and third absorption bands, see R. Tsuchida, This Bulletin, **13**, 388 and 436 (1938).

10) R. Tsuchida and M. Kobayashi, This Bulletin, **13**, 476 (1938).

band is bathochromic and hyperchromic to the ⊥-absorption. Since it seems reasonable to assume that the tetraiodo-palladate (II) ion shows a dichroism of the same type as those of the tetrachloro-and tetrabromo-palladate (II) ions, the following presumption may be reached that the a-absorption corresponds to the ∥-absorption and the c-absorption to the ⊥-absorption. Moreover, comparing the dichroism of potassium tetraiodo-palladate (II) with those of tetrachloro- and tetrabromo-complexes and judging from the relation between the dichroisms and the external forms with the latter two crystals, in both of which the planes of the complex ions are perpendicular to the c-axis,[3] it may be concluded that in the crystal of potassium tetraiodo-palladate (II) the complex-ions are arranged at least almost parallel to each other with their planes perpendicular to the c-axis.

Potassium Tetrathiocyanato-platinate (II). (Fig. 3.)—In the b-absorption the small inflexion at $\nu=68$ corresponds to the second band and the broad absorption stretching over the

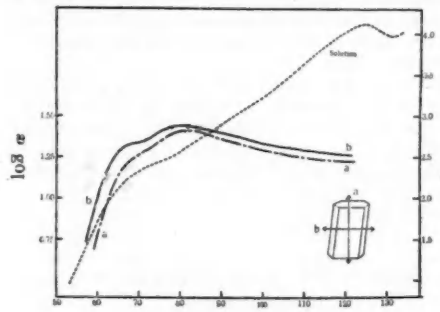

Fig. 3. Absorption spectra of $K_2Pt(SCN)_4$

shorter wave-length region consists of the third and SCN-specific bands. Similarly, in the a-absorption, the inflexion at $\nu=70$ corresponds to the second band and the broad absorption curve in the shorter wave-length region consists of the third and specific bands. The first band may be concealed under the large second band, as in the case of potassium tetrathiocyanato-palladate (II). No very great difference can be recognized between the a- and b-absorptions, but these absorptions seem to represent the characteristic feature of the dichroism of the planar tetrathiocyanato-complex. Thus for the second absorption band is found the following relation: the b-absorption is bathochromic and hyperchromic to the a-absorption.

Table II
Absorption Maxima of Tetrathiocyanato-Complex Compounds

		ν 10^{13}/sec.	log α	ν 10^{13}/sec.	log α
$K_2Pt(SCN)_5$	∥	67	1.31	80	1.44
	⊥	71	1.25	83	1.42
$K_2Pd(SCN)_4$	∥	58	1.54	73	1.44
	⊥	62	1.14	75.8	1.48

Since the tetrathiocyanato-platinate (II) ion is reasonably supposed to belong to the group of complexes which show a dichroism of the "tetrahalogeno-complex type," as in the case of the tetrathiocyanato-palladate (II) ion, it is considered that the b- and a-absorptions are abundant, respectively, with the parallel and perpendicular components of the planar complex ion, though the a- and b-absorptions may not completely coincide with the ∥-and ⊥-absorptions.

Potassium Tetrabromo-palladate (II) Dihydrate.—The absorption curve in the region for the low value of α was determined in the present measurement (Fig. 4). A slight

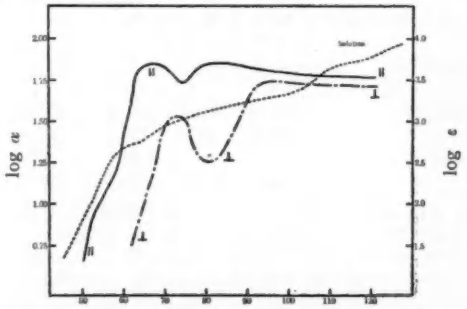

Fig. 4. Absorption spectra of $K_2PdBr_4\cdot 2H_2O$.

Table I
Absorption Bands of Tetrahalogeno-Complex Compounds

Compond		1st band ν 10^{13}/sec.	1st band log α	2nd Band ν 10^{13}/sec.	2nd Band log α	3rd Band ν 10^{13}/sec.	3rd Band log α
K_2PdCl_4	∥	51	0.45	64.0	1.68	(98)	(1.54)
	⊥	51	0.45	68.9	1,49	(108)	(1.51)
$K_2PdBr_4\cdot 2H_2O$	∥	(48)	(1.0)	58.8	1.85	(75)	(1.83)
	⊥	—	—	65.0	1.52	(90)	(1.75)
K_2PdI_4	∥	—	—	—	—	48.4	1.93
	⊥	—	—	40.4	1.88	(60)	1.86
K_2PtCl_4	∥	60.6	0.9	82.6	1.50	—	—
	⊥	60.6	0.9	89.1	1.45	—	—
$K_2PtBr_4\cdot 2H_2O$	∥	54.8	1.15	74	1.48	—	—
	⊥	54.8	1.15	84	1.43	—	—

inflexion is recognized in the longer wave-length part at a low value of α and at $\nu=$ about 53. This inflexion is supposed to correspond to the first absorption band. As in the case of the tetrachloro-complex, the first absorption band is found to be much week as compared with the other bands.

Comparison of Dichroisms of Planar Tetrahalogeno-Complexes.—Numerical data of the present measurements as to the dichroisms of the tetrahalogeno-complex type are tabulated in Tables I and III along with the other available data. For the tetrahalogeno-complexes of both palladium and platinum, the following relations are found to hold for the corresponding absorption bands: (1) $\nu_{Cl} > \nu_{Br} > \nu_I$ and $k_{Cl} < k_{Br} < k_I$;[11] (2) especially for the second band, the oscillator strength increases in the order, chloride<bromide<iodide.[12]

These tendencies are in accordance with those of cobaltic and chromic complexes, and they could be explained mostly in terms of the difference between the halogen atoms in their polarizability and, therefore, in the covalent character of the metal-halogen linkage

TABLE III

SECOND ABSORPTION BANDS OF TETRAHALOGENO-COMPLEX COMPOUNDS

		ν 10^{13}/sec.	half width 10^{13}/sec.	α	k
K_2PdCl_4	$\parallel$	64	12.2	47.8	57800
	$\perp$	68.6	10.4	30.9	37400
$K_2PdBr_4 \cdot 2H_2O$	$\parallel$	58.8	12	70.8	
	$\perp$	65.0	9	33.1	
K_2PdI_4	$\parallel$	—	—	—	
	$\perp$	40.4	—	76	
K_2PtCl_4	$\parallel$	82.6	18	31.6	38800
	$\perp$	89.1	14.4	28.2	34600
$K_2PtBr_4 \cdot 2H_2O$	$\parallel$	74	—	30.2	50700
	$\perp$	84	—	26.9	45200

Absorption Curves of $K_2Pd(SCN)_4$ and $K_2Pt(SCN)_4$.—Absorption curves of both the compounds show similar features. It is also found from the curves that the tetrathiocyanato-complexes show their absorption bands in the longer wave-length region, as compared with complexes of the same metals with other ligands; for example, they are bathochromic to the dioxalato-complexes[13] and show absorption in the longer wave-length region, comparable even to the tetrabromo- as well as tetrachloro-complexes. A similar tendency can also be noticed between potassium hexachloroplatinate (IV) and potassium hexathiocyanato-platinate (IV),[14] the former being hopsochromic to the latter. This fact seems, at first sight, inconsistent with the spectrochemical series for cobaltic complexes. Such anomalies might be attributed to the difference in the mode of co-ordination linkage between these complexes of platinum and palladium and of cobalt, and also possibly to the difference in the atom species which is bound to the central matallic ion. It may be assumed that in cobaltic and chromic complexes the thiocyanate ions co-ordinate with the metallic ion by means of the nitrogen atoms, while in the palladium and platinum complexes they co-ordinate by the sulphur atoms, since the complex, in which a thiocyanate ion co-ordinates with the central metal by its sulphur atom and which should consequently be called thiocyanato-complex, would be bathochromic to the complex, in which a thiocyanate ion coordinates by its nitrogen atom and which should consequently be called isothiocyanato-complex.[15]

The Dichroism of the Tetrahalogeno-Complex Type.—For all the planar tetrahalogeno-and tetrathiocyanato-palladium complexes shown in the table hold the following common rules.

(1) The first band: α is much smaller than that of the second or third band. $\nu_\parallel$ and $\nu_\perp$ are not greatly different from each other.

(2) The second band: $\parallel$-absorption is bathochromic and hyperchromic to $\perp$-absorption, the oscillator strength being larger for $\parallel$-ab-sorption than for $\perp$-absorption.

(3) The third band: $\alpha_\parallel$ is almost equal to $\alpha_\perp$ $\parallel$-absorption is bathochromic to $\perp$-absorption, $\nu_3 - \nu_2$ being larger for $\parallel$-absorption than for $\perp$-absorption.

For the planar platinum complexes hold similar rules to those for palladium complexes, but the former differ from the latter in the facts (1) that the second band of the $\parallel$-absorption has almost as strong intensity as that of the $\perp$-absorption, and (2) that in the $\parallel$ absorption its third band commences in almost the same wave-length region as in the $\perp$-absorption.

The fact that both $\parallel$-and $\perp$-absorptions show their first bands at almost the same wave-length suggests that the band is due to isotropic transitions. As such may be cited electronic transitions of *d*-electrons in the unsaturated shell of the central metal. The smaller value of α for the first band favours this view, suggesting that the transitions are forbidden ones. This agrees well with the idea on the origins of the bands, as advanced previously by one of the authors.[9]

The second absorption band is considered by the present authors to be originate from transitions of the electrons forming the co-ordination linkages. Therefore, in the planar

11) ν_{max} and k_{max} denotes, respectively, frequency and molecular absorption coefficient at maxima of the absorption bands of the tetrahalogeno-complex. Although the densities of the crystals $K_2PdBr_4 \cdot 2H_2O$ and K_2PdI_4 are not available, judging from the order of their magnitude and the values of α for the compounds, it seems quite clear that the above relation should hold.

12) Judging from the magnitude of k and the shape of the absorption bands, this relation seems evident.

13) R. Tsuchida and S. Yamada, unpublished.

14) H. Kuroya, unpublished.

15) The more detailed discussion related to such discrepancies will be submitted later.

complex, the electric moment responsible for the second should be larger in the direction along the plane of the complex than in the direction perpendicular to the plane. This accords well with the above rule that the oscillator strength of the second absorption band is greater in the ∥-absorption than in the ⊥-absorption. (Table III).

Diffierences between the platinum and palladium complexes are observed with respect to the second and third bands. Thus, in the palladium complexes the second band of ∥-absorption is very hyperchromic compared to that of ⊥-absorption, whereas in the platinum complexes they have almost equal magnitudes of absorption coefficients, and the oscillator strength of ∥-absorption is not so much larger than that of ⊥-absorption in the platinum complexes as in the corresponding palladium complexes. This tendency seems related to a similar discrepancy in the birefringence between complexes of the two metals, which was observed by Mellor and Quodling,[16] who reported that planar tetraco-ordinated compounds of platinum showed smaller double refraction than the corresponding palladium compounds. A completely explanation for the above fact can not be given for the present, but this phenomenon might be ascribed principally to the difference between the two metals in their polarizing powers and also in their polarizabilities.

16) D. P. Meilor and F. M. Quodling, *J. Proc. Roy. Soc. New South Wales*, **69**, 167 (1936); ibid., **70**, 205 (1936).

Summary

(1) Dichroisms of K_2PdI_4, $K_2Pd(SCN)_4$ and $K_2Pt(SCN)_4$ have been quantitatively determined by the microscopic method, and it has been found that all of them belong to the group which exhibits the dichroism of the "tetrahalogeno-complex type."

(2) For the tetrahalogeno-complexes, the following rules have been found: $\nu_{Cl}>\nu_{Br}>\nu_I$ and $k_{Cl}<k_{Br}<k_I$ for the corresponding absorption band, and the oscillator strength of the second band is larger for ∥-absorption than for ⊥-absorption.

(3) For tetrahalogeno- and tetrathiocyanato-complexes of platinum (II) and palladium (II), common regularities have been induced on the dichroisms of the tetrahalogeno-complex type.

This work was supported in part by a grant from the Ministry of Education.

Department of Chemistry, Faculty of Science, Osaka University, Nakanoshima, Osaka

Studies on Unsaturated Organosilicon Compounds. I.* Syntheses of Organovinylsilanes by Wurtz-Fittig Reaction

By Motonori KANAZASHI

(Received July 2, 1953)

Vinyl silicon compounds have been prepared by the elimination of hydrogen halides from haloethylsilanes,[1,2] and by the high temperature interaction of vinyl chloride and silicon in the presence of a catalyst such as copper or tin.[2,5] Recently Wagner[6] prepared vinyltrichlorosilane from acetylene and trichlorosilane at a high temperature and under pressure with platinized asbestos as a catalyst.

In this work, vinyl chloride and organohalosilanes were allowed to react with metallic sodium (in the shape of finely divided particles) in ethyl ether, to form organovinylsilanes. Trimethylchlorosilane, dimethyldichlorosilane, triethylbromosilane, and dimethylphenylchlorosilane were used as the organohalosilane.

The infrared spectra of these vinylsilanes are given in Fig. 1. From the spectra of cyclic tri- and tetra-siloxane,[7] it was found that the characteristic absorption bands for methyl, ethyl, and phenyl linked to silicon are remarkably constant in many compounds in the wave length shorter than about 11.0μ, that is 3.38, 7.08, and 7.94 μ for the methyl group, 6.84, 7.08, 7.26, 8.05, 9.9, and 10.4 μ for

* This paper was presented in the sixth annual meeting of the Chemical Society of Japan in April, 1953, at Kyoto.

1) S. N. Uschakov and A.M. Itenberg, *J. Gen. Chem. (U. S.S.R.)*, **7**, 2495 (1947).

2) D. T. Hurd, *J. Am. Chem. Soc.*, **67**, 1813 1945), U. S.P., 2,420,912 (1947).

3) *Brit. P.* 618,608 (1949).

4) C. D. Strother and G. H. Wagner, *U.S.P.*, 2,532,430 (1950).

5) D. T. Hurd and G. F. Roedel, *Ind. Eng. Chem.*, **40**, 2078 (1948).

6) G. H. Wagner and C. O. Strother, *Brit. P.*, 670,617 (1952).

7) C. W. Young, P. C. Servais, C. C. Currie and M. J. Hunter, *J. Am. Chem. Soc.*, **70**, 3758 (1948).

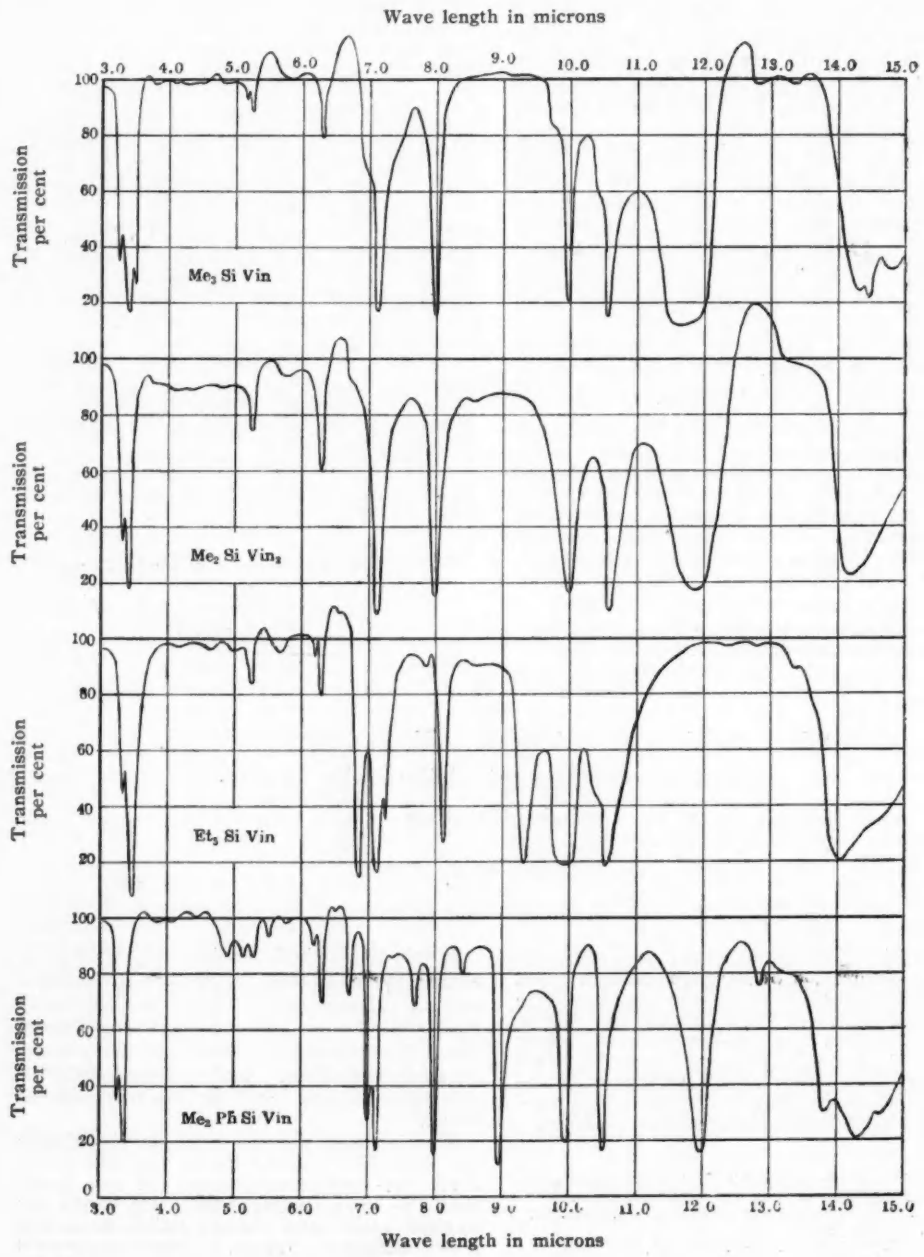

Fig. 1. The infrared spectra of organovinylsilanes

the ethyl group, and 6.28, 6.7, 6.98, 8.4, 8.9, 9.7, and 10.04 μ for the phenyl group, and allow a ready determination of the presence of these groups.

These bands are found at 3.39~3.43, 7.13~7.14, and 8.00~8.03 μ for methyl group in trimethylvinylsilane, dimethyldivinylsilane and dimethylphenylvinylsilane; 6.88, 7.12, 7.27, 8.11, 9.87 (not separated from 9.99 μ band) and 10.4 μ for ethyl group in triethylvinylsilane; and 6.21, 6.72, 7.01, 8.40, and 8.99 μ for phenyl group (9.7 and 10.04 μ bands were not found) in dimethylphenylvinylsilane.

The remaining bands common to four compounds are 5.27~5.28, 6.29~6.30. 9.94~9.99, and 10.50~10.54 μ. Of these, the bands at 6.29~6.30 and 10.50~10.54 μ were also found in vinyl siloxanediols at 6.2~6.3 and 10.3~10.4 μ and were assigned to C=C double bond and the vinyl group linked to silicon respectively, by Frisch and others.[8] The band at 5.28 μ in dimethyldivinylsilane is about twice as intense as in the other three compounds similar to the band at 6.3 μ, and it is doubtless due to the vinyl group linked to silicon. Probably the band at 9.95 μ is also believed to be assigned to the vinyl group.

Trichlorosilane was found to be added to these vinylsilanes in the presence of diacetyl peroxide like as to vinyltrichlorosilane, and the corresponding β-trichlorosilylethylsilanes were prepared.

Other reactions and properties of organovinylsilanes are under investigation in this laboratory.

Experimental

All yields reported are based on the amount of organohalosilanes or organovinylsilanes used.

Syntheses of Organovinylsilanes.

Trimethylvinylsilane I.—Ninety two grams (4.0 mole) of finely divided metallic sodium, 217 g. (2.0 mole) of trimethylchlorosilane (presented by the Shin-etsu Chem. Ind. Co.), and 250 cc. of ethyl ether were placed in a 1-l. three necked flask fitted with a mercury-sealed stirrer, a gas inlet tube and a 30 cm. Dimroth reflux condenser with a condenser sermounted with a cold finger, 4×15 cm., filled with a dry ice-aceton mixture.

Vinyl chloride gas, dried with phosphorus pentoxide, was introduced to the reaction mixture with stirring, at a rate of 10~20 l. per hour. About ten minutes after, 2 cc. of ethyl acetate was added to catalyze the reaction. When the reaction started the introduction of vinyl chloride was controlled so that a gentle reflux of ether was maintained. The reaction approached to the end in six hours then the introduction of vinyl chloride gas was stopped, and the reaction mixture was heated gently with stirring for one hour. The reaction mixture was allowed to stand overnight; then the ether layer was decanted and the residue was washed with ether and filtered. These ether solutions were mixed up and washed twice with water. After drying overnight over calcium chloride, the ether solution was fractionated through a 1-m. distillation column of about 30 theoretical plates. One hundred and fifty five grams of trimethylvinylsilane, boiling 53~56° at 767 mm. were isolated. Yield 77.5%.

The trimethylvinylsilane obtained in three runs was redistilled and the middle cut, b.p. 55.5° at 767 mm. was taken for analysis and determination of physical constants. See Table I.

Dimethyldivinylsilane II.—Ninety two grams (4 mole) of finely divided metallic sodium, 129 g. (1.0 mole) of dimethyldichlorosilane (presented by the Shin-etsu Chem. Ind. Co.), and 200 cc. of ethyl ether in a 1-l. flask reacted with vinyl chloride as indicated above, dimethyldivinylsilane were isolated, b.p., 80.8~81.6° at 760 mm., 26 g. yield 24%.

Triethylvinylsilane III.—Triethylbromosilane used in this synthesis was prepared from trichlorosilane *via* triethylsilane by the method of Whitmore and others[9] and Ladenberg,[10] and fractionated through a 30 cm. column, b.p., 78~79° at 50 mm.

Twelve grams of metallic sodium, 41 g. of triethylbromosilane and 100 cc. of ethyl ether in a 500 cc. flask reacted with vinyl chloride as outlined above, fractionation of the product through a 30 cm. column, gave triethylvinylsilane, b.p., 143.2° at 755 mm., 13.2 g., yield 45%.

8) K. C. Frisch, P. A. Goodwin and R. E. Scott, *J. Am. Chem. Soc.*, **74**, 4584 (1952).

9) F. C. Whitmore, E. W. Pietruza and L. H. Sommer, *J. Am. Chem. Soc.*, **69**, 2108 (1947).

10) Ladenberg, *Ann.*, **164**, 300 (1872).

TABLE I

THE PPOPERTIES OF ORGANOVINYLSILANES

Compound	b.p.		d_4^{20}	n_D^{20}	Molar ref.		Si %	
	°C	mm.			Calcd.	Obsd.	Calcd.	Found
I	55.5	767	0.6910	1.3914	34.44	34.50	28.02	27.8
II	80.8~81.6	760	0.7337	1.4176	38.60	38.52	25.03	24.9
III	143.2	755	0.7847	1.4330	48.33	47.47	19.60	19.6
IV	82.0	20	0.8919	1.5048	54.26	53.96	17.31	17.4

Dimethylphenylvinylsilane IV. — Dimethylphenylchlorosilane used in this synthesis was prepared from dimethyldichlorosilane and phenylmagnesium bromide in ether, and was fractionated through a 30 cm. column, b.p., 84~85° at 20 mm.

Twenty three grams (1 mole) of metallic sodium, 85 g. (0.5 mole) of dimethylphenylchlorosilane, and 100 cc. of ethyl ether in a 500 cc. flask reacted with vinyl chloride as outlined above, fractionation of the product through a 30 cm. column, gave 29.2 g. of dimethylphenylvinylsilane, b.p., 82.0° at 20 mm., yield 36%.

The physical constants and analytical data of these organovinylsilanes are given in Table I.

Addition of Trichlorosilane.

β-Trichlorosilylethyltrimethylsilane V. — A mixture of 5 g. (0.05 mole) of trimethylvinylsilane, 14 g. (0.1 mole) of trichlorosilane, and 0.25 g. (0.002 mole) of diacetyl peroxide (2.0 mole % to trichlorosilane used) in a glass sealed tube was heated for ten hours at 60° in a water bath. Then distilled in a 20 cc. Claisen flask, the excess trichlorosilane was recovered at atmospheric pressure and 10.5 g. of β-trichlorosilylethyltrimethylsilane, b.p., 94~96° at 50 mm. and 1 g. of residue was obtaind, yield 90%.

Bis(β-trichlorosilylethyl)dimethylsilane VI. —Heating a mixture of 3.5 g. (0.03 mole) of dimethyldivinylsilane, 13.6 g. (0.1 mole) of trichlorosilane, and 0.2 g of diacetyl peroxide for eleven hours in a sealed glass tube at 60°, gave 8.5 g. of bis(β-trichlorosilylethyl)dimethylsilane, b.p., 119~121° at 3 mm., yield 72%.

β-Trichlorosilylethyltriethylsilane VII.— Heating a mixture of 7.1 g. (0.05 mole) of triethylvinylsilane, 13.6 g. of trichlorosilane, and 0.2 g. of diacetyl peroxide for eight hours in a sealed glass tube at 60°, gave 6 g. of β-trichlorosilylethyltriethylsilane, b.p., 122~125° at 18 mm., yield 42%.

TABLE II

THE PROPERTIES OF β-TRICHLOROSILYLETHYLSILANES

Compound	f.p. °C	b.p. °C	b.p. mm.	d_4^{20}	n_D^{20}	Molar ref. Calcd.	Molar ref. Obsd.	Cl % Calcd.	Cl % Found
V	−18	94~96	50	1.1062	1.4473	57.32	56.96	45.13	45.0
VI	−4	119~121	3	1.2966	1.4838	84.36	84.52	55.52	55.4
VII		122~125	18	1.0713	1.4632	71.21	71.44	38.29	38.3
VIII		138~139	10	1.1553	1.5112	77.14	77.24	35.72	35.5

β-Trichlorosilylethyldimethylphenylsilane VIII.—Heating a mixture of 8.1 g. (0.05 mole) of dimethylphenylvinylsilane, 13.6 g. of trichlorosilane, and 0.2 g. of diacetyl peroxide for sixteen hours in a sealed glass tube at 60°, gave 3.5 g. of β-trichlorosilylethyldimethylphenylsilane, b.p., 138~139° at 10 mm., yield 24%.

The physical constants and analytical data of these β-trichlorosilyethylsilanes are given in Table 2.

Preparation of Spectra—The infrared spectra shown here were obtained using a Perkin-Elmer Model 12-C Spectrometer (rock salt prism) of Government Chemical Industrial Research Institute, Tokyo. All samples were run in potassium bromide cell, 0.1 mm. thick, as pure liquid.

Summary

1) Vinyl chloride and organohalosilanes were shown to react with finely divided metallic sodium in ethyl ether, and trimethyl-, dimethyldi-, triethyl- and dimethylphenyl-vinylsilanes were prepared. Of these, dimethyldi- and dimethylphenyl-vinylsilane are new compounds and their physical constants were given.

2) Infrared spectra of these four organovinylsilanes were obtained and certain characteristic absorption bands were discussed.

3) Trichlorosilane was found to add to these vinylsilanes at the presence of diacetyl peroxide and four new β-trichlorosilylethylsilanes were prepared and characterized.

The author is indebted to Mr. M. Yonemoto and Mr. S. Saeki for the spectra reported in this paper and the Shin-etsu Chem. Ind. Co. for the methylchlorosilanes used in this investigation. The author is also grateful to Dr. O. Shimamura and Dr. T. Yamada for much helpful advice in this investigation.

Electrotechnical Laboratory
Agency of Industrial Science and Technology, Tokyo

Sterols and Other Unsaponifiable Substances in the Lipids of Shell Fishes, Crustacea and Echinoderms. XII. Occurrence of Δ^7-Cholestenol as a Major Component of the Sterol Mixture of Chiton

By Yoshiyuki TOYAMA and Tatsuo TANAKA

(Received July 11, 1953)

The first report[1] of this series recorded the results of a brief examination of the sterol mixture of chiton, *Liolophura japonica*, and several other aquatic invertebrates. In those experiments, the sterol mixture of the fatty substances extracted with ether from the chitons, caught around Sugashima Island, Mie Prefecture, and also the acetate of sterol mixture were subjected to several recrystallizations. The highest melting points of recrystallized products were 119~121°C. for the free sterol and 125~127°C. for the acetate, though neither melting points were yet constant.

In the present experiments, the chitons caught around Osaki-Shimojima Island in the Inland Sea of Seto were extracted with ether, the ether-extract was freed from the acetone-insoluble portion, and the unsaponifiable matter was separated from the acetone-soluble portion. The crystalline fraction of the unsaponifiable matter, consisting of crude sterols, was acetylated, and the acetate obtained was recrystallized from ethanol. Unlike the results described in the previous report, the acetate showed, after 4 recrystallizations, a constant melting point of 118~119°C. which was unaltered by further recrystallizations. The free sterol obtained by saponification of the acetate showed also a constant melting point of 122~122.5°C. Both free sterol and acetate were optically inactive, and a spectrophotometric examination indicated the absence of conjugated diene. They reacted very rapidly with the Liebermann-Burchard reagent and developed a blue-green color almost immediately. The acetate had a saponification value and a degree of unsaturation, determined by perbenzoic acid titration, both of which agreed closely with the calculated values for a C_{27}-stenol. These facts seem to suggest that the sterol obtained above is Δ^7-cholestenol (γ-cholestenol). In order to gain a further confirmation, the isomerization of Δ^7-cholestenol (γ-cholestenol)→$\Delta^{3(14)}$-isomer (α-cholestenol)→Δ^{14}-isomer (β-cholestenol) and the hydrogenation of the last named isomer to cholestanol were performed. As shown in

TABLE I

	Free sterol		Acetate		Benzoate	
	m.p., °C	$[\alpha]_D^{\beta}$	m.p., °C	$[\alpha]_D^{\beta}$	m.p., °C	$[\alpha]_D^{\beta}$
Δ^7-Cholestenol	122~122.5	0	118~119	0	158~159; 177	+6.9
„ [2]	122~123	0	118~119	0	157~158; 176	+7.14
„ [3]	125~126	+5.7	118~119	+1.5	—	—
„ [4]	122	+5.65	118	—	153~154	—
$\Delta^{8(14)}$-Cholestenol	118~120	—	77~78	+9.5	115~117; 144	—
„ [2]	119~120	+20.36	77~78	+9.46	115; 140	+8.53
Δ^{14}-Cholestenol	130~131	—	90~91	—	168~169	+31.5
„ [2]	130~131	+34	91~92	—	168	+32.54
„ [5]	131~133	+30	90~92	+22.8	172~174	+31
Cholestanol	—	—	104~105	+14.2	—	—
„ [6]	—	—	109~110	+11.5	—	—

1) Y. Toyama and F. Shibano, *J. Chem. Soc. Japan*, **64**, 323 (1943).
2) Fr. Schenck, K. Buchholz and Q. Wiese, *Ber.*, **69**, 2686 (1936).
3) L. F. Fieser, *J. Am. Chem. Soc.*, **73**, 5007 (1951).
4) D. R. Idler and C. A. Baumann, *J. Biol. Chem.*, **195**, 623 (1952).
5) H. Wieland, F. Rath and W. Benend, *Ann.*, **548**, 19 (1941).
6) B. Heath-Brown, I. M. Heilbron and H. R. H. Jones, *J. Chem. Soc.*, **1940**, 1482.

Table 1, the respective products obtained in these experiments showed the same melting points and specific rotations as those recorded previously for the corresponding compounds, excepting that the hydrogenation product had a little lower melting point and higher specific rotation than cholestanol, possibly due to the contamination of unaltered Δ^{14}-cholestenol.

From sterol-free conponents of unsaponifiable matter, a small amount of saturated alcohols, possibly chimyl and batyl alcohols, was separated.

Δ^{7}-Cholestenol had been known as the reduction product of 7-dehydrocholesterol, but its occurrence among natural sterols was not known until quite recently. In 1951 Fieser[7] found this sterol, named lathosterol by him, as a companion sterol in various samples of crude cholesterol. Also Idler and Baumann[8] found a relatively large amount of this sterol in skin sterols of an albino rat, but the isolation of this sterol from skin sterols was attained by chromatography of the azoyl ester of sterol mixture, while repeated recrystallizations of the acetate of the sterol mixture were not efficient to concentrate this sterol. In contrast to these findings, it may be noted that only several recrystallizations of the acetate of sterol mixture of the chitons were sufficient to yield a pure Δ^{7}-cholestenol in the present experiments.

Since the acetate of sterol mixture of the chitons caught around Sugashima Island, as described in the previous report, did not yield an acetate of constant melting point, the authors have procured another lot of chitons caught at the same locality, and re-examined the sterol mixture from this lot of chitons. On repeatedly recrystallizing the acetate of sterol mixture, the melting point of the acetate became higher than that of Δ^{7}-cholestenyl acetate, as was the case with the previous experiments. The sterol mixture showed no ultraviolet absorption maximum, but it was positive for the Tortelli-Jaffé test, and formed a blue-green color very rapidly in the Liebermann-Burchard reaction. These facts seem to permit a presumption that the sterol mixture of the chitons caught around Sugashima Island contains Δ^{7}-cholestenol together with other sterol, and that the acetate of additional sterol is less soluble in ethanol and has a higher melting point than the acetate of Δ^{7}-cholestenol, so that repeated recrystallizations of the acetate mixture result in the concentration of the acetate of additional sterols with a higher melting point. Whether such a striking difference between the chitons from Sugashima Island and from Osaki-Shimojima Island in the content of Δ^{7}-cholestenol is a general case caused by the variation in the catching locality or a special case caused by some other factors, remains unknown.

7) l. c., (3).
8) l. c., (4).

Experimental

The chitons used in these experiments were caught around Osaki-Shimojima Island in the Inland Sea of Seto in August, 1952. Air dried chitons (4.98 kg.) were cracked to small pieces and lipid was extracted with ether, yielding 1.05% of lipid which was a dark reddish orange viscous liquid. The lipid (52.0 g.) was refluxed with 450 cc. of acetone, and the mixture was cooled and filtered, by which 42.0 g. of acetone-solubble oil with the following constants was obtained: d_4^{27} 0.9332, n_D^{20} 1.4784, acid value 110.2, saponification value 184.4, iodine value (pyridine sulfate dibromide method) 138.6, unsaponifiable matter 18.77%.

Unsaponifiable Matter—The acetone-soluble oil (36.8 g.) was saponified, and unsaponifiable matter was extracted with ether from the diluted soap solution. The unsaponifiable matter (7.2 g.) was an orange-yellow solid, and melted at 48~50°C. to a turbid liquid and at 92°C. to a clear liquid. The sterol content in the unsaponifiable matter was found to be 44.86% by the digitonide method. Recrystallization of the unsaponifiable matter from 250 cc. of methanol gave a crude sterol mixture (3.2 g.) of m.p. 113~118°C. It showed no characteristic absorption maximum in the region of 230~310 mμ. The acetate (3.1 g.), m.p. 112.5~114.5°C., prepared by refluxing the crude sterol mixture with acetic anhydride for one hour, was recrystallized from ethanol. After 4 recrystallizations, the melting point was raised to 118~119°C., which was unaltered by further recrystallizations from acetone and ether-acetone (1 : 2). The total yield of the acetate of m.p. 118~119°C. was 1.34 g. Further 0.94 g. of the acetate melting somewhat less sharply at 115~118.5°C. was separated from the mother liquor of recrystallizations. The remainder of the acetate recovered from the mother liquor showed a lower melting point.

The methanol filtrate from the initial recrystallization of the unsaponifiable matter was concentrated, and a solid deposit (0.67 g.) of m.p. 53~56°C. was separated and recrystallized from acetone, by which a crystalline solid (0.44 g.) of m.p. 61~63°C. was obtained. Since this solid was still contaminated with a minute amount of sterol, the latter was removed by digitonin. The sterol-free solid, after recrystallization from acetone, had m.p. 62.5~63.5°C., iodine value 0.8 and acetyl value 263.2 (calculated for chimyl alcohol 280.1; for batyl alcohol 261.8).

Acetate of m.p. 118~119°C.—This acetate showed saponification value 130.7 (calculated for $C_{29}H_{48}O_2$ 130.8) and number of ethylenic bond, determined by perbenzoic acid titration, 1.05.* It showed a positive Tortelli-Jaffé reaction, and developed a blue-green color very rapidly in the Liebermann-Burchard reaction. Free sterol obtained by saponification of the acetate showed, after recrystallization from ethanol, m.p. 122~122.5°C. and $[\alpha]_D^{12}=0$ (in chloroform). Benzoate was prepared by allowing free sterol to react with benzoyl chloride in pyridine; m.p. 158—159°C. (turbid), 176~177°C. (clear), $[\alpha]_D^{22}=+6.9°$.

$\Delta^{8(14)}$-Cholestenol—The acetate (0.65 g.) described above was dissolved in 30 cc. of acetic acid to which was added platinum black previously saturated with hydrogen. The solution was agitated in an atmosphere of hydrogen. No hydrogen absorption occured. After 3 hours, the solution was poured into 500 cc. of water, and was extracted with ether. The ether-extract, recrystallized from ethanol, gave $\Delta^{8(14)}$-cholestenyl acetate in lustrous leaflets; yield 0.56 g., m.p. 77~78°C., $[\alpha]_D^{10}=+9.5°$. Free stenol, after recrystallization from ethanol, melted at 118.5~119.5°C., and was positive for the Tortelli-Jaffé reaction. Benzoate prepared from free stenol had m.p. 115~117°C. (turbid) and 144°C. (clear).

Δ^{14}-Cholestenol — $\Delta^{8(14)}$-Cholestenyl benzoate (0.21 g.) was dissolved in 8 cc. of anhydrous chloroform, and dry hydrogen chloride was passed into the solution under cooling with ice for 2.5 hours. The solution was then washed successively with sodium bicarbonate solution and water, dried over anhydrous sodium sulfate, and the chloroform was distilled off. The residue contained no chlorine, and recrystallized from ethanol in lustrous needles; yield 0.13 g., m.p. 168~169°C., $[\alpha]_D^{22}=+31.5°$. Free stenol was obtained by saponification of the benzoate, and recrystallized from ethanol in fine needles; m.p. 130~131°C. Acetate was prepared from free stenol and recrystallized from acetone-ethanol (2:1) in fine needles; m.p. 89.5~91°C. It was negative for the Tortelli-Jaffé reaction.

Cholestanyl Acetate—Δ^{14}-Cholestenyl acetate (0.03 g.) was dissolved in 10 cc. of ether-acetic acid (1:1), and hydrogenated in the presence of platinum black as catalyst by stirring the solution in an atomosphere of hydrogen for 4 hours at room temperature. The hydrogenation product was extracted with ether from the solution diluted with water. After recrystallization from ethanol, it formed fine needles; yield 0.02 g., m.p. 104~105°C., $[\alpha]_D^{22}=+14.2°$. The final product still showed a violet color in the Liebermann-Burchard reaction.

Sterol Mixture of Chitons from Sugashima Island—Air dried material of the chitons (400 g.)* caught around Sugashima Island, Mie Prefecture, in April, 1953, yielded 7.9 g. of lipid by ether extraction, from which acetone-soluble oil was obtained in a yield of 86%; d_4^{20} 0.9356, n_D^{20} 1.4792, acid value 112.5, saponification value 185.6, iodine value 131.2, unsaponifiable matter 11.43%. Crude sterol mixture was separated by recrystallizing the unsaponifiable matter from methanol, and its acetate was repeatedly recrystallized from ethanol. The melting points of recrystallized products were121~123°C., 123.5~125.5°C. and 127~129°C., respectively, after 3, 4 and 6 recrystallizations. The final product showed a positive Tortelli-Jaffé reaction, and reacted very fast with the Liebermann-Burchard reagent. It showed no characteristic absorption maximum in the region of 230~310 mμ. The product after 3 and 4 recrystallizations showed $[\alpha]_D^{25}=+3.9°$ and $+6.5°$, respectively.

Summary

Sterol mixture of the chitons caught around Osaki-Shimojima Island in the Inland Sea of Seto contains predominantly Δ^7-cholestenol, the acetate of which is easily obtainable in a pure state by several recrystallizations of the acetate of sterol mixture. From sterol-free components of unsaponifiable matter, a saturated fraction, possibly consisting of chimyl and batyl alcohols, was separated.

The acetate of sterol mixture of another lot of chitons caught around Sugashima Island, Mie Prefecture, shows a higher melting point than Δ^7-cholestenyl acetate after several recrystallizations, as was the case with the chitons caught in the same locality which were described in the first report of this series.

Department of Applied Chemistry,
Faculty of Engineering,
Nagoya University, Nagoya

* The iodine value by the pyridine sulfate dibromide method showed an enormously high value of 232.4 against the calculated value 59.2.

* Supplied through the courtesy of Dr. E. Nakano, Biology Department, Faculty of Science, Nagoya University.

Rheology of Surface Films. I. Rheological Characteristics of Monomolecular Films of Ovalbumin and Serum Albumin*

By Kiyoshi INOKUCHI

(Received July 21, 1953)

Introduction

Recent interest in the study of surface films has been focused upon the problems of high molecular substances, such as proteins or synthetic high polymers. Since the most prominent characteristics of high polymers is their forming of viscoelastic films, excellent means for measuring the mechanical properties of surface films are now greatly needed. Although classical measurements of surface viscosity, based on the canal method[1-3] or damped oscillation method,[4-8] have shown considerable merits in the film studies of simple molecules, they were not so informative when applied to the viscoelastic films of high polymers. In view of the recent development of modern rheology with three-dimensional materials, the application of the method and concept of modern rheology to the two-dimensional systems would shed new light on the field of physical chemistry of surfaces. The aim of this series of works is to provide a set of standards of surface rheology and to achieve the analyses of mechanical properties of protein or synthetic polymer films from the modern rheological standpoint.

At the beginning of this work, the first attempt was started with protein monolayers at the air-water interface. At the present stage, it appeared necessary to make a careful preliminary study with some well-defined proteins. For this purpose, crystalline ovalbumin and serum albumin were mainly used. The present paper describes the mechanical characteristics of these protein films obtained by the method based on the analyses of deformation-time relation of the film subjected to shearing stress.

Experimental

Procedures—A static mothod was employed in this preliminary study. The apparatus is principally the same as used by Schwedoff and Hatschek[9] with three-dimensional gel. The illustration is given in Fig. 1. (A) is a platinum ring of

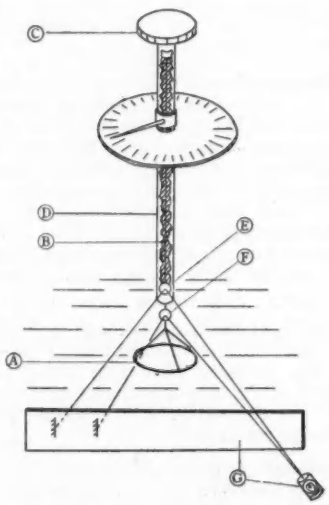

Fig. 1.—Diagrammatic illustration of the apparatus for measuring viscoelasticity of films

3.7 cm. in diameter. The suspending wire is enclosed by a protector (D) which is coaxial with the torsion head (C). The rotational angle of the torsion head and the deflection of the ring are measured by means of the mirrors (E) and (F) respectively, with lamp and scale (G). Care was taken that the experimental condition might not destroy the fine structure of films. For this purpose, both the moment of intertia of the ring

* Partly presented at the Annual Meeting of the Chemical Society of Japan, April, 1952.

1) M. Joly, *J. de phys.* **11**, 471 (1937), *Kolloid-Z*, **89**, 26 (1939).

2) E. R. Washburn and H.R.R. Wakeham, *J. Am. Chem. Soc.*, **60**, 1294 (1938).

3) R. J. Meyers and W. D. Harkins, *J. chem. phys.*, **5**, 601 (1937).

4) L. Fourt and W. D. Harkins, *J. Phys. Chem.*, **42**, 897 (1938).

5) I. Langmuir, and V. J. Schaefer, *J. Am. Chem. Soc.*, **52**, 2400 (1937).

6) L. Fourt, *J. Phys. Chem.*, **43**, 887 (1939).

7) M. Joly, "Surface Chemistry" (Supplement of Research) 157 (1949).

8) C. W. N. Gumper and A. E. Alexander, *Trans. Faraday Soc.*, **46**, 235 (1950).

9) V. E. Hatschek and R. S. Jane, *Kolloid-Z.*, **39**, 300 (1926).

and the torsion constant of a suspending wire which were chosen were sufficiently small. That is, a series of phosphor bronze wire of 25μ to 60μ in diameter and 30 cm. in length and the rotating system of moment of inertia of 0.8 g. cm^2 were used. Order of shearing stress ranged from 10^{-3} to 10^{-1} dyne per cm. The trough was 14.7 cm. wide and 60 cm. long. Wilhelmy dipping slide was applied to the one side of the trough to furnish the surface pressure-area curve (designated as F-A curve hereafter). The sensitivity of the balance was about 0.01 dyne per cm. To obtain maximum symmetry, the ring was suspended 7.3 cm. in front of the dipping slide. After the quick turn of the torsion head by a definite angle φ (less than 10 degrees), the deflection of the hanging ring ω during relaxation was measured with time t. As the surface film was distorted with the ring, ω was considered to be a strain of the film materials. When the ring was applied to a clean surface of water, the contribution of moment of intertia of the rotating system was found to be not small enough to be ignored. However, once the surface was covered by a certain amount of monolayer substance, the contribution of moment of inertia became negligible due to the increased film resistance against the motion of the ring. Under such conditions, if the film exhibits Newtonian flow, the rate of strain is given by the equation,

$$\dot{\omega} = \frac{K}{R}(\varphi - \omega) \qquad (1)$$

In case of ideal elastic films, where only the instantaneous elastic deformation occurs, the following equation holds:

$$\omega = \frac{K}{E}(\varphi - \omega) \qquad (2)$$

In above equations, K is the torsion constant of the suspending wire, R and E, the constants related to the surface viscosity coefficient η and surface shear modulus G expressed by the following formulas, (3) and (4), respectively

$$\eta = \frac{k}{4\pi}\left(\frac{1}{r_1^2} - \frac{1}{r_2^2}\right)\left(\frac{\varphi - \omega}{\dot{\omega}}\right) \qquad (3)$$

$$G = \frac{k}{4\pi}\left(\frac{1}{r_1^2} - \frac{1}{r_2^2}\right)\left(\frac{\varphi - \omega}{\omega}\right) \qquad (4)$$

where r_1 and r_2 are the radii of the ring, and of the circular films coaxial with the ring, respectively. In the present apparatus, r_2 may be assumed to be 7.3 cm., effective radius of the trough, which is sufficiently large compared with r_1. If the film under test is perfectly elastic, the film inside the ring would not affect the motion of the ring. Therefore, so far the instaneous elasticity is concerned, the shear modulus was calculated ignoring the film formed inside the ring. This assumption was checked to be valid within the experimental error*.

As will be described later, the mechanical properties of real films were generally neither a purely viscous, nor a purely elastic, but a more complicated one, superposed by both viscosity and elasticity. The deformation-time curve of such films were found to be quite similar to that of three-dimensional materials stressed, so that the mechanical properties of films would be analyzed by the usual method in rheology[10].

Materials—Ovalbumin was prepared from a fresh hen eggs by the sodium sulfate method and successive crystalization according to Kekwick[11]. Horse serum albumin was a crystalline product prepared by the sodium sulfate method[12] and horse hemoglobin by the alcohol method.

Results

ω-t Curve of Ovalbumin Film—When the ovalbumin aqueous solution was spread on 0.1 N hydrochloric acid solution, or on 5% ammonium sulfate solution, the following ω-t curve was observed (Fig 2). When the shearing stress was imposed, an instantaneous deformation (a-b) occurred, which follows time-dependent deformation (creep, b-c-d). At a later time, if the stress was removed, the instantaneous recovery of the first deformation occurred (d-e), preceding the time-dependent recovery of the creep (e-f). Complete recovery of the overall deformation, on the removal of the stress, was not generally observed, except the case under sufficiently

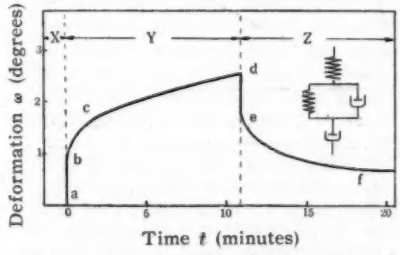

Fig. 2.—An example of ω-t curve for ovalbumin film on 0.1 N hydrochloric acid together with the illustration of the corresponding mechanical model. Range of (X) represents the dead time, (Y), the time in which the stress was imposed, and (Z), the time, the stress was removed.

* The ring, coated with paraffin, was applied to the elastic films of ovalbumin, and the shear modulus of instantaneous elasticity was obtained by equation (4). Next, after the film inside the ring was removed by being absorbed with filter paper, the same measurement was made again. Both results obtained were found to coincide each other within the experimental error.

10) T. Alfrey, "Mechanical Behaviors of High Polymers," Interscience Publishers (1948).

11) R. A. Kekwick and R. K. Cannon, *Biochem. J.*, **30**, 227 (1936).

12) R. A. Kekwick, *Biochem. J.*, **32**, 552 (1938).

small stress. Such mechanical behaviors may be approximately represented by the mechanical model of four elements with spring (elasticity) and dash pot (viscosity) as illustrated in Fig. 2. Such behavior was in common covering nearly the whole range of film areas. The instantaneous elasticity is the most definable in mechanical terms, since it mainly involves biased strain, and not any flow. So, with ovalbumin films, the main attention was directed toward the instantaneous elasticity of the film.

Relation between Stress and Instantaneous Elasticity—At a definite area, the stress-strain relation was obtained. As shown in Fig. 3, the strain was found to be proportional to the stress imposed. Such linearity holds covering almost the whole range of film areas. This means that the instantaneous elasticity obeys Hooke's law. When the shear

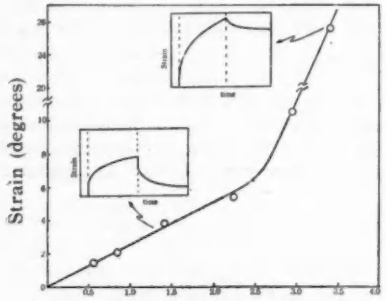

($\times 10^{-1}$) Shearing stress (dynes/cm.)

Fig. 3.—Stress-strain curve for ovalbumin films on 5% ammonium sulfate solution at 9.5 sq. m. per mg. Temperature, 10°C. Insets give the ω-t curves under the stress indicated by arrows.

stress was over a certain limit, however, the stress-strain curve became bent with the convex curvature against the stress axis. Further increase in the stress rendered the instantaneous elastic deformation obscure, causing the destruction of film structure (inset of Fig. 3). When the structure was once destroyed, reformation of the film took an appreciable time. In other words, ovalbumin film shows two-dimensional "thixotropy".

Relation between Instantaneous Elasticity and Film Area—In a sufficiently large area, ovalbumin film did not show any perceptible resistance against the motion of the ring. As the area was reduced, at a definite area, the ring suddenly received an appreciable resistance. In the case, the ω-t curve was not typical as shown in Fig. 2 and instantaneous elastic deformation was obscure. If the film was compressed a little more, however, the ω-t curve converted to give a typical instantaneous elastic response as shown in Fig. 2.

Shear modulus of instantaneous elasticity is obtained from the equation (4) at various areas, and the modulus vs. area curve (designated as G-A curve hereafter) was obtained. A typical example of the G-A curve is given in Fig. 4. The aqueous solution of 0.08 mg. per cc. was spread on 0.1 N hydrochloric acid at the initial spreading concentration of 0.2 mg. per sq. m. Twenty minutes were allowed to insure complete spreading.

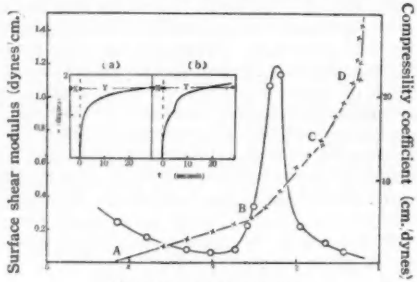

Area sq. m. per mg.

Fig. 4.—Surface shear modulus-area curve (crosses) and compressibility-area curve (circles) of ovalbumin film on 0.1 N hydrochloric acid, at 21°C. Insets give the ω-t curves. The region of (X) represents the dead time, and (Y), the time the stress is imposed.

The stepwise compression was extended to about 2 hours. Compressibility*-area curve, obtained from the F-A curve, was depicted in the same figure. It was found that the G-A curve starts at about 5 sq. m. per mg. (point A) and surface modulus increased

TABLE I

FLUCTUATION OF BOTH VALUES OF CRITICAL AREA (A) AND CRITICAL SHEAR MODULUS (G) AT BREAKS (A, B, C, D) OF SHEAR MODULUS-AREA CURVE OF OVALBUMIN FILMS ON 0.1 N HYDROCHLORIC ACID, AT 14–15°C.

	A	B	C	D
a (m^2/mg)	5.3	2.25	1.65	1.30
g (*dynes/cm*)		0.20	0.35	0.81
a (m^2/mg)	4.8	2.15	1.65	1.35
g (*dynes/cm*)		0.35	0.57	0.86
a (m^2/mg)	5.3	2.10	1.55	1.35
g (*dynes/cm*)		0.45	0.75	1.15
a (m^2/mg)	5.3	2.55		
g (*dynes/cm*)		0.37		

* Surface compressibility is defined as $-1/A(dA/dF)$, where F is the surface pressure in dynes per cm. and A, the film area in sq. m. per mg.

linearly with the decrease of the surface area, exhibiting several breaks at about 2.3 sq. m. per mg. (point B), 1.7 sq. m. per mg. (point C) and 1.3 sq. m. per mg. (point D). The extent of fluctuation of values of these breaks, obtained under the same condition, was shown in Table I. Although absolute values of shear modulus corresponding to the breaks were more or less scattered, the areas of breaking points were considerably reproducible.

It is to be noted that the minimum point of the compressibility curve appeared around the area corresponding to the breaks (point B) of the G-A curve. In addition, the particular state of the film phase in B-C range was also found from the corresponding ω-t curve. In A-B range, the ω-t curve was of such a type as in the inset (a) of Fig. 4, whereas it was converted into the type as (b) when the film was compressed to B-C range. Further compression down to C-D range made the ω-t curve into the same type as that in A-B range. From these facts it is strongly suggested that compression of the film exercises several steps of transformation of film phase which involves different modes of packing of film molecules.

In higher pressure region, the G-A curve was also obtained together with the compressibility-area curve (Fig, 5). Here, the shear modulus was found to increase steeply around the area of minimum compressibility. The type of the ω-t curve was almost similar to that of the low pressure region.

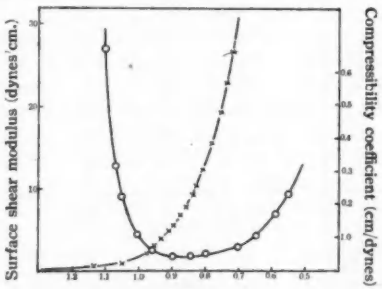

Fig. 5.—Surface shear modulus-area curve (crosses) and compressibility-area curve (circles) of ovalbumin film in high pressure region. Substrate solution, 0.1 N hydrochloric acid, and temperature, 13–14°C.

Effect of Various Experimental Conditions.—It was found that the ovalbumin film on 0.1 N hydrochloric acid, at elevated room temperature, did not exhibit an instantaneous elasticity until it was compressed down to the area of 1.7 sq.m. per mg. That is, elastic ovalbumin films at large areas underwent "melting" above certain temperature around 20°C. The film, once it was formed, showed reversible sol-gel transformation with "melting" range within 1°C, when the surface temperature was raised or lowered repeatedly by the intermittent exposure of infra-red lamp. If the film was newly formed under the same condition, however, the observed transition temperature was scattered considerably. The extent of the fluctuation was about ± 3°C. This may be due to some uncontrollable factors of the experimental conditions.

The films, when they were spread on 5% ammonium sulfate solution at pH 5.5, showed the instantaneous elasticity at the area above 15 sq.m. per mg., about three times as much area as on 0.1 N hydrochloric acid. In this case, "melting" of the film could not be observed at room temperature.

When the spreading solution of ovalbumin containing 10% formaldehyde was applied on 5% ammonium sulfate solution, at any temperature, only simple retarded elastic response was exhibited, without any instantaneous one. Although the reactions between formaldehyde and protein are complicated, in view of the fact that the amino or imino groups of protein molecules take a great part in this reaction, it seems probable that these groups are responsible for the instantaneous elasticity of the film.

Horse Serum Albumin and Hemoglobin—The proteins were spread under the same conditions with ovalbumin, but the mechanical behavior was found to be strikingly different from the case of ovalbumin. It was found that serum albumin did not exhibit any perceptible resistance against the motion of the ring, until the film was compressed to a considerably reduced area at the temperature from 5°C to 23°C. Below 1.0 sq. m. per mg., the film showed appreciable viscosity whose values increased gradually with the decrease of area, showing Newtonian flow (crosses in Fig. 6). Below 0.8 sq. m. per mg., the retarded elasticity appeared, which follows a simple viscous flow, but no sign of instantaneous elasticity was perceptible (inset of Fig. 6). This rheological behavior was referred to the compressibility-area relation obtained from the F-A curve. The compressibility curve is shown in Fig. 6 together with the illustration of the rheological behavior. It is noted that the minimum point of the compressibility curve just corresponds to the largest area

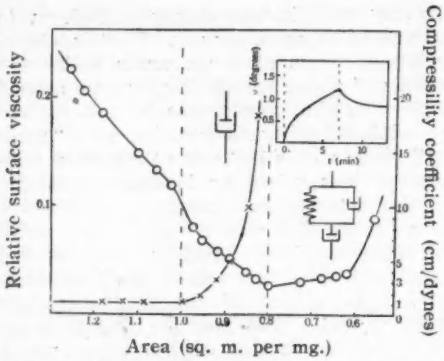

Fig. 6.—Compressibility-area curve (circles) and surface viscosity-area curve (crosses) for serum albumin film, together with the illustration of mechanical model corresponding to the film states. Relative surface viscosity is defined as the ratio of surface viscosity of the film to that of clean water. Temperature, 16°C. Inset gives the ω-t curve at the area of 0.78 sq. m. per mg. The region of (X) represents dead time, (Y), the time, stress is imposed, and (Z), the time, stress is removed.

where the film exhibited the retarded elasticity under stress, and the kink point of the compressibility at the area of 1.0 sq. m. per mg., is consistent with the largest area where the ring caught appreciable viscosity of surface film. Even though the film was extremely compressed below 0.3 sq. m. per mg., it failed to show instantaneous elasticity, exhibiting only the flow accompanied by the retarded elasticity.

Sasaki and Kimizuka[13] reported that an adsorbed layer of serum albumin aqueous solution exhibited an instantaneous elasticity, and the present author also observed this phenomenon with the solution of 10 to 50mg. per 100 cc. containing 0.1 N hydrochloric acid. It is noteworthy that the adsorbed layer exhibits an instantaneous elasticity, whereas the monolayer, as well as the polylayer made from the compression of a monolayer, fails to show any sign of instantaneous elasticity. Concerning the structural difference between a monolayer and an adsorbed layer, no work has been done, waiting for further research. Our rheological method of approach will also be promising for the solution of this problem.

The rheological behavior of horse hemoglobin was nearly similar to that of serum albumin. When hemoglobin was spread on 0.1 N hydrochloric acid solution at 14°C, it showed no elasticity at large areas, while below about 0.85 sq. m. per mg. the retarded elasticity appeared, accompanied by viscous flow. The correlation of rheological behavior with compressibility of the films was also similar to the case of serum albumin.

Discussion

The rheological method mentioned above enables the film properties to be quantitatively described in mechanical terms by the way of assigning absolute values of viscosity and elasticity to each element of corresponding mechanical model. Table II shows an example of the result obtained near the collapsing pressure of the film, i.e., at 6 dynes per cm. and 9 dynes per cm. For simplicity of computation, three element model was adopted as the mechanical model for ovalbumin film. The numbers in the table indicate the values of surface shear modulus and surface viscosity coefficient in c. g. s. unit. These values were computed approximately from the observed values corresponding to the instantaneous elastic deformation, the

TABLE II

COMPARISON OF MECHANICAL PROPERTIES OF OVALBUMIN AND HORSE SERUM ALBUMIN MONOLAYERS. *

Numbers indicate the values of surface shear modulus and surface viscosity coefficient of each element of the mechanical model in c. g. s. unit. At the bottom of the table, the Joly's data of surface viscosity are given, in which R indicates the surface viscosity coefficient in c. g. s. unit at the surface pressure of 6 dynes per cm., P_n, the critical surface pressure at which the nature of flow transforms from Newtonian to non-Newtonian by compression.

Surface Pressure in dynes/cm		Ovalbumin	Serum albumin
9		7.6 / 3.6 / 3030	0.1 / 7.5 / 22.5
6		6.0 / 2.4 / 550	0.8
Joly's data	R	0.038	0.076
	P_n (dynes/cm)	4	10

13) T. Sasaki and H. Kimizuka, This Bulletin, **25**, 318 (1952).

ultimate strain at infinite time, the rate of initial flow, and the rate of the stationary flow.[14] In this table, characteristics of ovalbumin and serum albumin films are quite clear at a glance. At the bottom of this table, Joly's[7] data on surface viscosity are tabulated; these date were obtained by the method of damped oscillation of ring. It is to be noted that Joly's measurement failed to show any difference in mechanical properties of these proteins. In addition, he reported the critical pressure (P_n), at which the nature of flow is transformed from Newtonian to non-Newtonian by compression, to be 4 dynes per cm for ovalbumin, 10 dynes per cm. for serum albumin. Such values, especially for ovalbumin, are hardly expected from the present method, since the films of these proteins exhibit distinct elasticity at such high surface pressures. Such large discrepancy may presumably be due to the too large shear stress employed by the oscillation ring method. The reason becomes apparent in view of the fact that ovalbumin film shows thixotropic behavior, that is, the film structure undergoes destruction and the film shows only simple flow under too large stress. It must be emphasized that sufficiently small stress should be applied to the film if the detailed information is wanted for the film structure.

From the view point of structural theory, the occurrence of the instantaneous elasticity is to be attributed to the exsistence of intermolecular bondings. The conclusion could, therefore, be drawn that even in a large area such as 5 sq. m. per mg., ovalbumin molecules are linked together with each other, making a two dimensional network covering the whole area of spread film.* It had been suggested that the protein molecule exists on surface in an unfolded structure, probably in the form of straightened β-configuration, and at low pressure, the side chains are lying flat on the surface.[15] The calculation based on the molecular model leads to the results that the area occupied by a polypeptide chain with the side chains flat on water surface is about 1.7 sq. m. per mg. In addition, according to Bull's[16] data the area of ovalbumin film available for the close packing state is not over 2 sq. m. per mg. under the best spreading condition. Our experimental result, therefore, shows that ovalbumin film forms a two-dimensional network before its spread molecules are closely packed, i.e., spread ovalbumin molecules have a marked tendency to combine with each other.

On the other hand, with serum albumin, it is to be noted that the film did not manifest any elastic behavior until it was compressed down to the area about 0.8 sq. m. per mg., and that the critical area is just consistent with the area of minimum point of film compressibility. It is commonly said that when the compressed film exists in a close packed state of molecules, whose side chains are oriented normal to the surfacee, compressibility-area curve exhibits a minimum point. Therefore, with serum albumin, it is considered that the closest packing state of film molecules just rendered the film viscoelastic and that the looser packing no longer brings about any elastic behavior. This shows that the interaction between the film molecules is very weak. Moreover, our experiments show that no perceptible viscosity of the film was observed until it was compressed to the area about 1. sq. m. per mg. The case is similar with hemoglobin. These facts may suggest that the film molecules of serum albumin exist with the side chains oriented normal to the surface even at the uncompressed film state as well as the compressed one. In these respects, the film structure of serum albumin and hemoglobin is considered to be in striking contrast to that of ovalbumin film, whose side chains lie flat on the surface in a large area forming the interchain bonds between the film molecules.

Summary

A static method of measuring the viscoelasticity of spread monolayers is presented, and the rheological study was carried out with the monolayers of ovalbumin, horse serum albumin, and hemoglobin. The deformation-time relations, obtained under the shear stress, were found to give very detailed information about the structure of films.

With ovalbumin films spread on 0.1 N hydrochloric acid, it was found that an instantaneous elasticity, accompanying retarded elasticity, appeared in an unexpectedly large area, i.e., in the area above 5 sq. m. per mg. Surface shear modulus of instantaneous elasticity increased linearly with the decrease of surface area, exhibiting several breaks in the slope.

The films of serum albumin and hemoglobin behaved differently from ovalbumin film, as they did not exhibit any viscoelasticity until they were compressed to a considerably small area. Compression down to the area

14) cf. T. Nakagawa, "Kagaku" (Science) **21**, 138 (1951).

* Complete spreading of the film was checked by the talcum test.

15) H. Neurath and H. B. Bull, *Chem. Revs.* **23**, 391 (1938).

16) H. B. Bull, *J. Biol. Chem.*, **185**, 27 (1950).

below 1.0 sq. m. per mg., however, makes a simple viscous film and further compression down to the area below 0.8 sq. m. per mg., just rendered the film viscoelastic. Such changes of film state were found to be consistent with the breaks in the compressibility-area curve obtained from the forcearea curve. Discussions of the characterization of these protein films were briefly made in terms of molecules.

The author wishes to express his hearty thanks to Prof. Taro Tachibana for his helpful advice and encouragement in the course of this work, and to Dr. Tsurutaro Nakagawa of the Chemical Laboratory of Tokyo University for his valuable discussions of the present experimental method. The author's thanks are also due to Dr. T. Shimanouchi of the Chemical Laboratory of Tokyo University and Takeda Pharmaceutical Industries Ltd. for a gift of horse serum albumin, and to Dr. S. Nagakura of the Scientific and Technological Institute of the Tokyo University for a gift of horse hemoglobin.

Department of Chemistry, Faculty of Science, Ochanomizu University, Tokyo

---

Studies on Amino-hexoses. III.[1] A New Synthesis of 2-Deoxy-D-ribose

By Yoshio MATSUSHIMA and Yujiro IMANAGA

(Received August 4, 1953)

The synthesis of 2-deoxy-D-ribose, a constituent of deoxy-ribonucleic acid, has been a matter of interest from the biochemical point of view. Of several methods of synthesis which have hitherto been reported, the glycal method[2] and the more recently discovered nitro-glycitol method[3] are best in yields. Here is reported another method of synthesis which we tried recently.

D-Arabinose was isomerized in hot pyridine to ribulose which was isolated as o-nitrophenylhydrazone.[4] The ribulose-o-nitrophenyl hydrazone was reductively decomposed into o-phenylene diamine on the one hand and 2-amino-2-deoxy-pentitols on the other, using Raney nickel as catalyst. As one of the authors has demonstrated,[5] α-amino-alcohols in sugar series undergo "semi-pinacolinic deamination" when treated with nitrous acid, thus glucosamine and glucosaminol affording chitose and 2-deoxy-glucose respectively. The 2-amino-2-deoxy-pentitols, as expected, were converted by treating them with nitrous acid to 2-deoxy-ribose which was isolated as its benzylphenyl hydrazone. The reaction sequence is represented as follows:

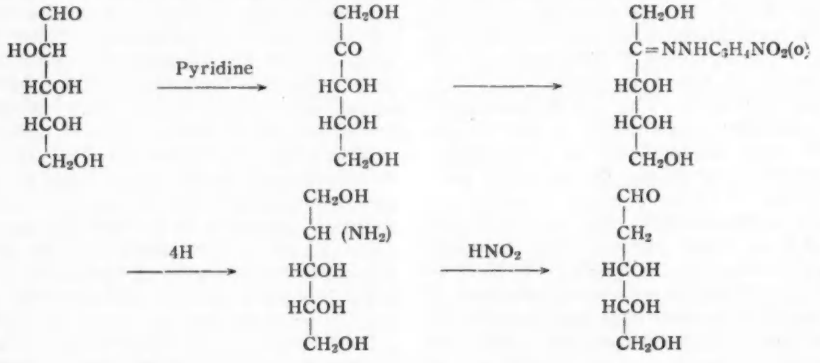

1) Previous reports of this series: This Bulletin, **24**, 17 (1951); ibid., **24**, 144 (1951); Preliminary report of this article: *Nature*, **171**, 475 (1953).

2) R. E. Deriaz, W. G. Overend, M. Stacey, E. G. Teece, L. F. Wiggins, *J. Chem. Soc.*, 1879 (1949); K. Ohta, *J. Biochem.* (Japan), **38**, 31 (1951).

3) J. C. Sowden, *J. Am. Chem. Soc.*, **71**, 1897 (1949).

4) C. Glatthaar, T. Reichstein, *Helv. Chim. Acta*, **18**, 80 (1935).

5) Y. Matsushima, This Bulletin, **24**, 144 (1951).

Experimental

Ribulose-o-nitrophenyl Hydrazone—23 g. of D-arabinose is gently boiled with 190 cc of anhydrous pyridine for 4 hours. The dark brown reaction mixture is evaporated *in vacuo*, water is added to the residue and redistilled in vacuo. After several repetitions of this operation, the syrupy material is separated with absolute alcohol from the unreacted crystalline arabinose. The alcoholic solution is seeded with arabinose and kept in an ice box in order to separate arabinose as far as possible. 17 g. of arabinose are recovered in almost pure state. After evaporation *in vacuo* of the alcoholic solution 7.25 g. of dark brown syrup is obtained.

The syrup above obtained is dissolved in 190 cc. of absolute alcohol and is boiled with 6.0 g. of o-nitrophenyl hydrazine for 10 minutes. The reaction mixture is concentrated to 75 cc. a few drops of acetic acid are added and it is placed in an ice box. The reddish yellow crystal separates and it is washed with water, absolute alcohol and then with ether-ethyl acetate (I : I). Ribulose-o-nitrophenyl hydrazone thus obtained weighs 5.2 g. and melts at 150°.

2-Amino-2-deoxy-pentitols—5.2 g of the ribulose-hydrazone above obtained is finely powdered and suspended in 70 cc. of water, 5 g. of activated Raney nickel are added, and shaken in the atmosphere of hydrogen. When the velocity of hydrogen absorption diminishes, the catalyst is added anew. 14 g. in all of the catalyst are necessary and 1970 cc. of hydrogen are absorbed in 16 hours. After the catalyst is filtered off, the solution is extracted with ether automatically for 20 hours. The ether extract, after evaporation, leaves 1.7 g. of o-phenylene-diamine. 3.2 g. of brown syrup of the 2-amino-2-deoxy-pentitols are obtained when the water solution is evaporated *in vacuo*.

2-Deoxy-D-ribose-benzylphenyl Hydrazone—3.2 g. of the syrup above obtained are dissolved in 20 cc. of 50% acetic acid and the solution of 2 g. of sodium nitrite in 5 cc. of water is dropped under ice cooling and in the atmosphere of cabon dioxide. After 20 minutes the nitrous acid is driven off by the stream of carbon dioxide and the solution is concentrated *in vacuo* to a syrup which is dissolved in 10 cc. of absolute alcohol; 2.15 g of benzylphenyl hydrazine in 2 cc. of absolute alcohol are added. The mixture is kept at 70° for 30 minutes in the atmosphere of carbon dioxide and concentrated *in vacuo*. The syrup thus obtained is extracted 3 times with each 10 cc. of benzene and the residue is once more extracted with 10 cc. of benzene after dilution with water. The benzene extract, after drying with sodium sulfate, leaves on evaporation crystalline needles mixed with syrupy matter. The crystal is separated by washing away the syrupy matter with ether and benzene. After recrystallization from benzene isopropyl alcohol and 40% ethyl alcohol, it melts at 125.5~126.5° and weighs 0.3 g. No melting point depression is observed when mixed with an authentic specimen. Colorless needle, $[\alpha]_D^{11}$ −15.25° (in pyridine).

Calculated for $C_{18}H_{22}O_3N_2$:	C, 68.79%; H, 7.01%; N, 8.92%
Found:	C, 68.86%; H, 6.56%; N, 8.98%

The authors are indebted to Prof. K. Makino and Mr. K. Ohta, of the College of Medicine, Kumamoto University, for an authentic specimen of deoxyribose, and are grateful to Prof. S. Akabori, of the College of Science, Osaka University, for his suggestions and encouragement. A part of the expenses was covered by the grant from the ministry of education in aid for fundamental scientific research.

Department of Science, Nara Women's University, Nara

Reactivity of Coke. I.
Absolute Reaction Rates of the Carbon Dioxide-Carbon Reaction

By Yoshio KAWANA

(Received August 16, 1953)

The reactivity of coke is very important in industry and so the reactions of carbon dioxide with charcoal and pure graphite have been extensively studied.[1-4] The mechanism of this reaction is at present considered as follows:

$$CO_2+C \longrightarrow CO+[CO] \quad \text{surface oxide} \quad (1)$$
$$[CO] \longrightarrow CO \quad (2)$$

The reaction (1) of the surface oxide for-

1) W. E. J. Broom and M. W. Travers, *Proc. Roy Soc.*, (London) **135A**, 512 (1932).
2) J. Gadsby, E. J. Long, P. Sleightholm and K. W. Sykes, *Proc. Roy Soc.*, (London) **A193**, 357 (1948).
3) I. Langmuir, *J. Am. Chem. Soc.*, **37**, 1154 (1915).
4) A. F. Semechkova and D. A. Frank-Kamenetzky, *Acta Physico. Chim.* (U.R.S.S.), **12**, 823 (1940).

mation is very rapid and only about 0.5% of sites on the total carbon surface seem to take part in the reaction (1). Desorption of [CO] is the rate-determining step.

In a recent paper, Bonner and Turkevich[5] discussed the carbon dioxide-carbon reaction using C^{14} as a tracer and supported the above mechanism.

More recently, Reif[6] discussed the mechanism of this reaction theoretically and Gulbransen and Andrew[7] questioned the surface oxide formation from their results using a sensitive microbalance. Gulbransen and Andrew, [7] Wynne-Jones and his coworkers[8] emphasized the effects of metal oxide impurities on the reaction rate of carbon dioxide with pure graphite.

In the present paper, the surface areas of eight carbons were determined by the adsorption of ammonia at 0°C by the B.E.T. method and, using these values, the absolute reaction rates of the carbon dioxide-carbon reactions were obtained and discussed from the absolute reaction rates theory.

Apparatus, Materials and Procedure

The apparatus is shown in Fig. 1. A is a reaction tube of quartz, F, a mercury reservoir, B, a gas burette and L_1~L_9, vacuum cocks. A was kept at 0°C with the surface area determination and regulated at a constant temperature in the range from 850° to 978°C within ±1°C with the reaction rate measurement.

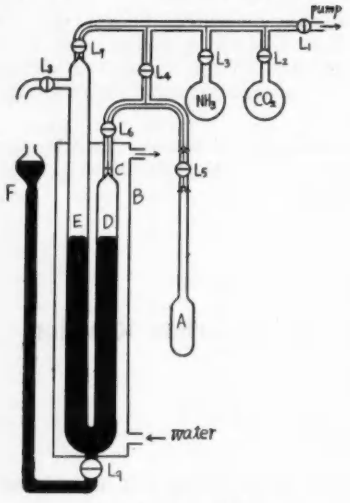

Fig. 1—Apparatus

Eight carbons as shown in Table I were used and their particle size is 10~20 mesh except for fine acetylene black and carbon for spectroscopic analysis. All carbons were previously treated with 6N-hydrochloric acid for about 40 hrs. and then washed by boiling distilled water during about 200 hrs. Analytical results and the density of all carbons using carbon tetrachloride at the end of all the experiments are shown in TABLE I.

TABLE I*

Sample	Moisture %	Ash %	Density g./cc.
Coke I	0.87	12.95	1.92
Coke II	2.03	11.18	1.79
Coke III	0.17	12.90	1.89
Pitch coke	0.30	2.32	1.90
Oil coke	0.17	0.39	2.00
Charcoal	4.82	0.70	1.27
Carbon for spectroscopic analysis	0.10	trace	2.25
Acetylene black	0.30	0.10	2.27

Ammonia was prepared by the thermal decomposition of 28% aqueous ammonia, dehydration by calcium oxide, potassium hydroxide and metallic sodium and lastly vacuum distillation at dry-ice temperature.

Carbon dioxide was prepared by the thermal decomposition of sodium bicarbonate and dehydration by both calcium chloride and phosphorus pentoxide.

Method for Determination of Surface Area.—The surface areas of carbon samples were determined using the adsorption of ammonia at 0°C following the simple B.E.T. method.[9,10]

The carbons were previously evacuated at 1100°C for 12~15 hrs. until 10^{-4} mmHg to eliminate some surface oxide and residual volatile matters. The adsorption of ammonia vapor was determined volumetrically at a series of P/Po values between 0.05 and 0.3. The B.E.T. plots of $P/v(Po-P)$ vs. P/Po were made and V_m and C in the B.E.T. equation were calculated.

$$P/v(Po-P) = \frac{1}{V_m C} + \frac{C-1}{V_m C} P/Po \qquad (3)$$

Where, V_m is the volume of monomolecular adsorption, C is a constant and approximately equal to $\exp(E_1-E_L)/RT$ where E_1 is the heat of adsorption of the first adsorption layer and E_L is the heat of liquefaction. P is the equilibrium pressure, Po, the saturation pressure, and v, the volume of gas adsorbed. From the value of V_m, the total surface area of the sample, S, can be calculated by the following equation, using the average

5) F. Bonner and J. Turkevich, *J. Am. Chem. Soc.*, **73**, 561 (1951).
6) A. E. Reif, *J. Phys. Chem.*, **56**, 785 (1952).
7) E. A. Gulbransen and K. F. Andrew, *Ind. Eng. Chem.*, **44**, 1048 (1952).
8) W. F. K. Wynne-Jones, H. E. Blayden and H. Marsh, *Brenn. Chem.*, **33**, 238 (1952).

* Samples were heated at 1100°C in vacua before surface area and reaction rates measurements and so subjected to vacuum treatment at 1100°C for about 20—60 hrs. in all.

9) S. Brunauer, P. H. Emmett and E. Teller, *J. Am Chem. Soc.*, **60**, 309 (1938).
10) S. Brunauer, L. S. Deming, W. E. Deming and E. Teller, ibid., **62**, 1723 (1940).

surface area per molecule of ammonia of 12.9×10^{-15} sq. cm. and then the specific surface area, A, of the sample can also be obtained,

$$S=(12.9\times10^{-15}\times V_m\times6.02\times10^{23})/22400\times10^4,\ m^2 \quad (4)$$

Method for Determination of Reaction Rates. After the surface area measurement, the sample was heated and the adsorbed ammonia was thoroughly desorbed. Carbon dioxide was introduced into the reaction tube A in Fig. 1 after regulating the temperature of the sample at a constant temperature in the range from 850° to 978°C and the increase of total pressure against time at constant volume was measured by cathetometer and the reaction rates of the system of carbon dioxide and carbons were determined.

After the reaction rate measurement was over and before the next surface area determination or the next reaction rate measurement, the sample was again evacuated at 1100°C for 3~15 hrs. until 10^{-4} to 10^{-5} mmHg to evaporate the surface oxide considered to be formed by the former reaction with carbon dioxide. The absolute reaction rates were obtained from the reaction rates measurement and the surface area determination.

Results and Discussion

(I) Surface Areas of Carbons. The B.E.T. plots of $P/v(Po-P)$ vs. P/Po are shown in Fig. 2 and monomolecular adsorption volume V_m, total surface area S, specific surface area A, B.E.T. constant C and the difference of the heat of adsorption of the first layer and the heat of liquefaction E_1-E_L are summarized in Table II. The surface areas and the weights of the coke I were determined before and after the reaction rate measurement with carbon dioxide as shown in No. 5-2, No. 5-3 and No. 5-4 in Table II and their differences were found to be so small that after the experiment with charcoal, No. 6 in Table II, the surface area determination was made at once and from these surface area values and kinetic data, the absolute reaction rates for various temperatures were obtained.

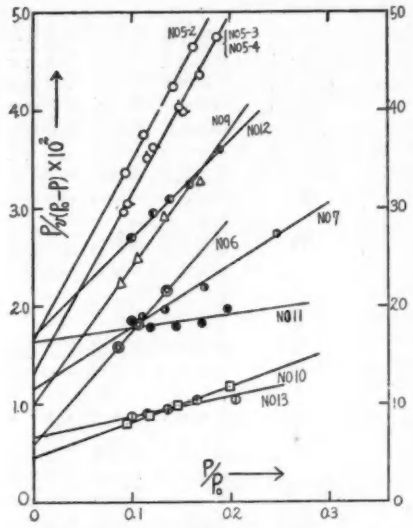

Fig. 2.—B.E.T. plots
Ordinate; left-hand, No. 5, No. 6, No. 9 and No. 12
right-hand, No. 7, No. 10, No. 11 and No. 13

The largest specific surface area of the samples investigated was 399 m^2/g of charcoal and the smallest, 0.41 m^2/g of oil coke and their ratio was about 10^3. If charcoal and acetylene black were excepted, the ratio of

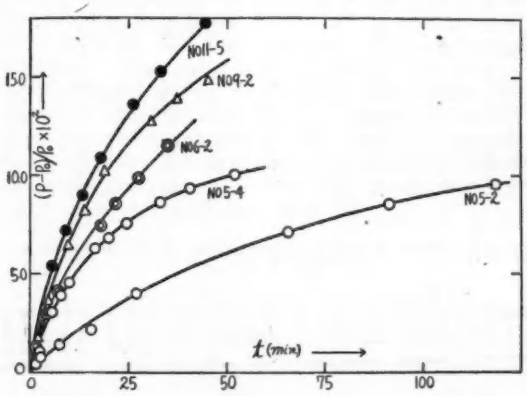

Fig. 3.—Relation between increase of total pressure and time
● acetylene black at 1230°K
△ coke II at 1173°K
◎ charcoal at 1173°K
○ coke I at 1173°K and 1223°K

TABLE II

Sample	Experimental number No.	Vacuum pretreatament at 1100°C hr.	Sample weights g	V_m cc	S m²	A m²/g	C	E_1-_1E cal/mol	Reaction temperature K	Number of moles of CO_2	Po mmHg	Slope	$1/2.303Po$	K	Ka_{obs} molecules cm^{-2} sec^{-1}	$Ka_{calc.}$ molecules cm^{-2} sec^{-1}
Coke I	5—2	15	8.0879	5.01	17.8	2.20	12.1	1360	1173	4.727×10^{-4}	784.0	5.44×10^{-4}	5.53×10^{-4}	0.0902	3.18×10^{9}	2.21×10^{9}
	5—3	15	8.0749	5.02	17.9	2.22	15.4	1490	1123	4.124 〃	665.4	6.47 〃	6.52 〃	0.00765	2.79×10^{8}	3.36×10^{8}
	5—4	15	8.0658	5.03	17.9	2.22	15.4	1490	1223	4.301 〃	719.0	5.98 〃	6.03 〃	0.298	1.08×10^{10}	1.30×10^{10}
	5—5	15	8.0590						1223	4.514 〃	752.0	5.73 〃	5.76 〃	0.311	1.11×10^{10}	1.30×10^{10}
Charcoal	6—1	15	0.0735	8.25	29.3	399.0	20.2	1640	1123	3.877 〃	573.0	7.18 〃	7.56 〃	0.0633	1.56×10^{9}	8.43×10^{8}
	6—2	3							1173	3.262 〃	495.0	8.45 〃	8.75 〃	0.342	8.19×10^{9}	5.06×10^{9}
	6—3	3							1223	4.664 〃	718.5	5.33 〃	6.04 〃	2.22	5.31×10^{10}	3.28×10^{10}
Oil coke	7—1	15	11.6119	1.34	4.76	0.41	6.43	1020	1223	4.157 〃	727.0	5.37 〃	5.97 〃	2.21	2.87×10^{11}	3.64×10^{11}
	7—2	10							1173	5.538 〃	635.0	6.65 〃	6.54 〃	0.220	4.10×10^{10}	7.32×10^{10}
	7—3	10							1123	4.493 〃	764.5	5.66 〃	5.66 〃	0.060	7.75×10^{9}	1.33×10^{10}
	7—4	10							1173	4.083 〃	700.1	6.07 〃	6.20 〃	0.393	5.04×10^{10}	7.32×10^{10}
	7—5	10							1223	3.649 〃	645.0	6.27 〃	6.72 〃	1.55	1.99×10^{11}	3.64×10^{11}
Coke II	9—2	15	6.9295	6.66	23.7	3.42	15.0	1480	1173	3.542 〃	562.0	7.55 〃	7.71 〃	0.492	1.19×10^{10}	1.30×10^{10}
	9—4	5							1223	4.415 〃	755.0	5.57 〃	5.75 〃	2.09	6.19×10^{10}	7.30×10^{10}
	9—5	5							1123	3.433 〃	535.0	8.25 〃	8.11 〃	0.0616	1.86×10^{9}	2.12×10^{9}
	9—7	5							1223	4.232 〃	703.0	5.90 〃	6.19 〃	1.94	5.70×10^{10}	7.30×10^{10}
	9—9	5							1223	4.254 〃	702.0	6.25 〃	6.18 〃	2.10	6.29×10^{10}	7.30×10^{10}
Coke III	10—1	15	10.1108	2.42	8.6	0.85	9.21	1210	1123	4.341 〃	700.0	5.95 〃	6.20 〃	0.0903	7.13×10^{9}	1.33×10^{10}
	10—2	10							1153	3.668 〃	600.0	6.80 〃	7.24 〃	0.360	2.86×10^{10}	3.70×10^{10}
	10—3	5							1183	3.946 〃	650.5	6.66 〃	6.69 〃	0.780	6.20×10^{10}	1.09×10^{11}
	10—5	5							1223	4.202 〃	713.0	5.88 〃	6.09 〃	2.23	1.76×10^{11}	3.82×10^{11}
Acetylene black	11—1	12	0.2309	3.36	12.0	52.0	1.81	326	1172	3.653 〃	552.2	7.58 〃	7.87 〃	0.089	6.07×10^{9}	5.55×10^{9}
	11—2	3							1212	4.768 〃	734.0	5.49 〃	5.91 〃	0.379	2.13×10^{10}	2.28×10^{10}
	11—3	3							1251	4.140 〃	642.0	6.60 〃	6.78 〃	1.18	6.58×10^{10}	7.46×10^{10}
	11—4	3							1193	4.148 〃	630.0	6.64 〃	6.88 〃	0.151	8.20×10^{9}	1.15×10^{10}
	11—5	3							1230	4.361 〃	675.0	6.16 〃	6.43 〃	0.870	4.85×10^{10}	3.95×10^{10}
	11—6	3							1216	4.906 〃	753.0	5.58 〃	5.76 〃	0.417	2.33×10^{10}	2.57×10^{10}
Pitch coke	12—1	15	12.2474	8.49	30.2	2.46	6.93	1055	1213	5.170 〃	681.0	6.21 〃	6.37 〃	0.366	1.00×10^{10}	0.91×10^{10}
	12—2	3							1252	3.544 〃	613.0	6.82 〃	7.07 〃	1.41	3.13×10^{10}	3.24×10^{10}
	12—3	3							1172	4.596 〃	774.0	5.58 〃	5.61 〃	0.117	2.58×10^{9}	1.97×10^{9}
	12—4	3							1143	3.839 〃	644.0	6.73 〃	6.74 〃	0.0296	6.58×10^{8}	7.30×10^{8}
Carbon for spectroscopic Analysis	13—1	12	9.0180	3.76	13.8	1.49	3.86	736	1223	3.722 〃	621.0	6.53 〃	6.99 〃	0.687	3.44×10^{10}	3.26×10^{10}
	13—2	3							1224	4.186 〃	691.0	5.86 〃	6.29 〃	1.15	5.76×10^{10}	6.62×10^{10}
	13—3	3							1192	3.930 〃	643.0	6.55 〃	6.75 〃	0.237	1.18×10^{10}	1.13×10^{10}
	13—4	3							1142	4.245 〃	680.0	6.33 〃	6.38 〃	0.0376	1.92×10^{9}	1.83×10^{9}

the largest specific surface area of cokes to the smallest was about 8.

(II) Reaction Rates of Carbons with Carbon Dioxide. Typical examples of the increase of the total pressure P against time t at constant temperature and volume are illustrated in Fig. 3. Po is the initial pressure. As time passes. the increase of the total pressure becomes smaller. It has been interpreted that this decrease was due to the retardation effect of the adsorption of carbon monoxide formed by the reaction of carbon dioxide with carbon; but more recently, Reif concluded that it was due to the reversible reaction of the reaction (1).

In the present paper, assuming that

a) the reaction (1) is rapid and always in equilibrium and the concentration of surface oxide is negligibly small compared with total active centers on the carbon surface,

b) the reaction (2) is the rate-determining step,

the following experimental equation is easily obtained,

$$dP/dt = K\ P_{co_2}/P_{co} \qquad (5)$$

where P is the total pressure, t, the time, K, a rate constant and Pco_2 and Pco denote the partial pressure of carbon dioxide and carbon monoxide respectively. From the assumption (a), there are the following approximate relations,

$$Pco_2 = 2Po - P, \qquad Pco = 2(P - Po) \qquad (6)$$

Integrating Eq. (5) under the initial condition that P is equal to Po at $t=0$ using the relation of Eq. (6), the following equation is obtained,

$$Y = K/4.606\ Po + X/2.303\ Po \qquad (7)$$

where Y is equal to $1/t \log Po/(2Po-P)$ and X equals $(P-Po)/t$. There must be a linear relation between Y and X from Eq. (7). The examples of these relations using experimental data in Fig. 3 are indicated in Fig. 4. Very good straight lines are obtained and $1/2.303Po$ must give the slope of these straight lines from Eq. (7). The comparison between the slope obtained from the figures and calculated values of $1/2.303Po$ are indicated in

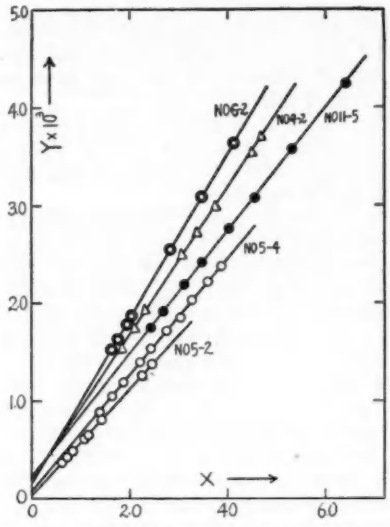

Fig. 4.—Relation between Y and X
○ coke I at 1173°K and 1223°K
● acetylene black at 1230°K
△ coke II at 1173°K
◎ charcoal at 1173°K

Table II and their differences are only a small percentage. Accordingly, Eq. (5) may satisfactorily represent the experimental data. The value of Y at $X=0$ is $K/4.606Po$ and then the rate constant, K, can be obtained. K represents the reaction rate when Pco_2/Pco equals unity. The number of molecules which react per sq. cm. per second at $Pco_2/Pco=1$, K_a, can be calculated by the following equation from K and the total surface area S,

$$K_a = a\ K \frac{273}{760} \frac{1}{60} \frac{6.02\times10^{23}}{22400} \frac{1}{S\times10^4} \qquad (8)$$

where, a *is* a constant determined by the volume of the reaction tube, the sample weight, the density of carbon and etc., and other figures are conversion factors.

K and $Ka_{obs.}$ are summarized in Table II. The plots of log Ka vs. $1/T$ are illustrated in Fig. 5 and Ka may by expressed in the form of

TABLE III

Sample	$A_{obs.}$ molecules cm^{-2} sec^{-1}	$A_{calc.}$ molecules cm^{-2} sec^{-1}	E, Kcal/mol
Oil coke	3.39×10^{27}	5.57×10^{27}	91
Coke III	〃	〃	〃
Coke II	5.12×10^{27}	〃	95
Charcoal	8.9×10^{27}	〃	97
Acetylene black	5.62×10^{27}	〃	〃
Carbon for spectroscopic analysis	〃	〃	〃
Pitch coke	5.75×10^{27}	〃	99
Coke I	〃	〃	〃

$$Ka = A\exp(-E/RT) \quad (9)$$

whe A and E are respectively the frequency factor and the observed activation energy. A and E obtained by the least squares are shown in Table III.

The values of A and E of oil coke, acetylene black and pitch coke coincide with those of coke III, carbon for spectroscopic analysis and coke I respectively.

The activation energy becomes smaller as the straight lines in Fig. 5 go upwards. It is very interesting that the line of charcoal does not deviate so much from those of coke II and carbon for spectroscopic analysis in Fig. 5 and that acetylene black and carbon for spectroscopic analysis fall exactly on the same line. Generally speaking, the ratio of the maximum value of Ka to minimum at the same temperature is about 16—20 for various carbons and is very small compared with the ratio of the largest specific surface area to the smallest, that is, 10^3, but among various cokes, except for charcoal and acetylene black, the difference of Ka is much greater than that of the speific surface area.

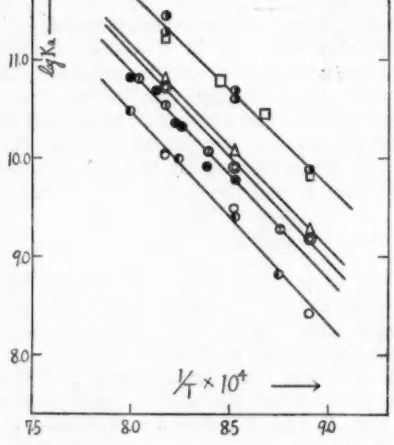

Fig. 5. Relation between log Ka and $1/T$

- ◑ Oil coke
- □ coke III
- △ coke II
- ◎ charcoal
- ● acetylene black
- ◫ Carbon for spectroscopic analysis
- ◐ Pitch coke
- ○ coke I

The systematic relations between the crystallographic structure of carbons and the values of Ka were not observed as shown in Fig. 5. This might be masked by the catalytic effects of impurities. From the above experimental results, it may be concluded that the difference of the specific reaction rates of pure amorphous carbon and pure graphite will be small and for carbons containing some impurities, the catalytic effects of the ash in carbons on the reaction rates may be much greater than that of the crystallographic structure of carbons that is, the degree of graphitization of carbons, and the difference of the observed activation energies may be due to the difference of the catalytic action of some impurities in carbons. These conclusions may be properly understood from various experimental facts that even small quantities of metallic oxide impurities usually play a very important part on the catalytic reactions. For example, Wynne-Jones and his co-workers[8] indicated that the addition of 0.1—0.02 per cent of sodium carbonates or elemental iron greatly affects the reactivity of pure graphite. In a recent paper, Parravano[11] indicated the change of the activation energies with the addition of some metallic oxide to nickel oxide in the reduction of nickel oxide by hydrogen. The activation energy of pure nickel oxide was 26.4 Kcal/mol, and with the addition of 1 mole per cent of alumina and 0.5 mole per cent of tungsten oxide, they became 35.2 Kcal/mol and 9.2 Kcal/mol respectively.

(III) A Theoretical Consideration of the Reaction Rates. The reaction mechanism of this system may be assumed as already mentioned and the absolute reaction rate theory[12] may be applied to this mechanism as follows,

$$\underset{P_{co_2}}{CO_2} + \underset{C_s}{C} \rightleftarrows \underset{P_{co}}{CO} + \underset{C_a}{[CO]} \quad \text{surface oxide} \quad (1')$$

$$\underset{C_a}{[CO]} \rightleftarrows \underset{C_a^*}{[CO]^*} \longrightarrow CO \quad (2')$$

The absolute reaction rates can be obtained from the following equation,

$$v = kT/h \cdot C_a \cdot f_a^*/f_a \exp(-E_1/RT) \quad (10)$$

where k, R, and h are universal constants, Ca, the concentration of the surface oxide, f_a^*/f_a, the ratio of the partition functions of the activated state and the surface oxide, E_1, surface activation energy and T, the temperature.

From the assumption (a) already stated, there is the following relation,

$$\frac{C_a}{C_s} = \frac{P_{co_2}}{P_{co}} \cdot \frac{f_{co}}{f_{co_2}} \cdot \frac{f_a}{f_s} \exp(-E_2/RT) \quad (11)$$

11) G. Parravano, *J. Am. Chem. Soc.*, **74**, 1194 (1952).
12) S. Glasstone, K. J. Laidler and H. Eyring: "The Theory of Rate Process," p. 369 (1941).

where, C_s is the concentration of the bare sites, P_{co_2} and P_{co}, the partial pressure of carbon dioxide and carbon monoxide, f denotes the partition functions of each species and E_2, the heat of reaction of the reaction (1'). From the assumption (a) C_s is also nearly equal to L, the concentration of the total active centers. When Eq. (11) is substituted for Ca in Eq. (10) using the relation of $C_s \fallingdotseq L$, some equations can be obtained as follows,

$$v = kT/h \cdot L \cdot P_{co_2}/P_{co} \cdot f_{co}/f_{co_2} \cdot f_a^*/f_s \exp\{-(E_1+E_2)/RT\} \equiv Ka\ P_{co_2}/P_{co} \quad (12)$$

where $$Ka = kT/h \cdot L \cdot f_{co_2}/f_{co} \cdot f_a^*/f_s \exp\{-(E_1+E_2)/RT\} \equiv A\exp(-E/RT) \quad (13)$$

here $$A = kT/h \cdot L \cdot f_{co}/f_{co_2} \cdot f_a^*/f_s \quad (14)$$

$$E = E_1 + E_2 \quad (15)$$

Eq. (12) is identical with the experimental reaction rate equation (5). A can be calculated from Eq. (14) and the calculated value using $L = 10^{15}$, $f_a^*/f_s = 1$ and $T = 1173$°K as the mean of the experimental temperatures is 5.57×10^{17} molecules cm^{-2} sec^{-1}. The calculated value of A is in satisfactory agreement with the observed values in Table 3. Ka can also be calculated from Eq. (13) using the activation energies obtained experimentally. $Ka_{calc.}$ for each temperature are tabulated in Table 2. The agreement of the calculated values with the observed is also very excellent. Accordingly, the mechanism presented in this paper may be interpreted by the absolute reaction rate theory.

Summary

The absolute reaction rates of carbon dioxide with eight carbons have been obtained from the surface area measurement by the B.E.T. method using ammonia adsorption at 0°C and the reaction rate measurement.

The activation energies ranged from 91 Kcal/mol of oil coke and coke III to 99 Kcal/mol of coke I and pitch coke.

The reaction mechanism that the reaction of the formation of surface oxide is rapid and always in equilibrium and the concentration of the surface oxide is negligibly small compared with total active centers and the rate-determining step is the desorption of surface oxide can be interpreted by the theory of absolute reaction rates.

It may be concluded that the difference of the activation energies will be due to catalytic effects of some impurities in carbons, and that the difference of the absolute reaction rates due only to the difference of the crystallographic structure of pure carbons without the catalytic effects of impurities will be small.

The author wishes to express his earnest thanks to Mr. A. Baba, Dr. H. Honda and Mr. Y. Yoshida (this institute) for their kind advice and interest in this study.

The author's thanks are also due to Mr. R. Sato (this institute) for his helpful assistance in this experiment.

Shigen-Gijutsu-Shikenjo
(Resources Research Institute)
Saitama-Kawaguchi, Japan

Studies on the Polarographic Analysis. XVII.* Electrolytic Reduction of Cyclohexanedionedioxime and its Application to Amperometric Titrations

By Masayoshi ISHIBASHI, Taitiro FUJINAGA, and Kazuo KAWAMURA

(Received May 6, 1953)

In a previous paper[1], the behavior of electrolytic reduction of 8-hydroxy-quinoline at the dropping mercury electrode and the amperometric titration using it have been described. In the present paper, polarographic and amperometric investigations of cyclohexanedionedioxime are reported. Cyclohexanedionedioxime (nioxime) was first employed by Wallach[2] as a reagent for nickel. It is very similar to dimethylglyoxime in its reac-

* Subtitle: Analytical Chemistry by Means of Organic Compounds XVII.

1) M. Ishibashi, T. Fujinaga, This Bulletin, **23**, 25, 27 (1950).

2) O. Wallach, *Ann.*, **437**, 148 (1924).

tion with nickel to form the red insoluble precipitate in an ammoniacal and weakly acid medium However, nioxime has many advantages over dimethylglyoxime in the sensitivity of reaction, in the smaller percentage of nickel in the precipitate and in the solubility of the reagent in water (0.824 g./100 ml. at 25°C). Together with its stable property, nioxime is an ideal organic reagent for the amperometric titration of nickel.

Experimental

Chemicals Used. Nioxime.—This product was synthesized according to the method of Rauh, Smith, Banks and Diehl[3], which was modified in some respects. The crude nioxime was recrystallized several times from alcohol.

Other Reagents.—Such reagents as nickel sulfate and buffer agents were all of analytical grade. They were all examined as to their purity by the polarographic method. Buffer solutions were prepared according to Kolthoff and Vleeschhower[4].

Apparatus Used.—The potentiometric manual polarograph designed by the authors[5] is used for the polarographic study, for the amperometric titration and for the determination of pH.

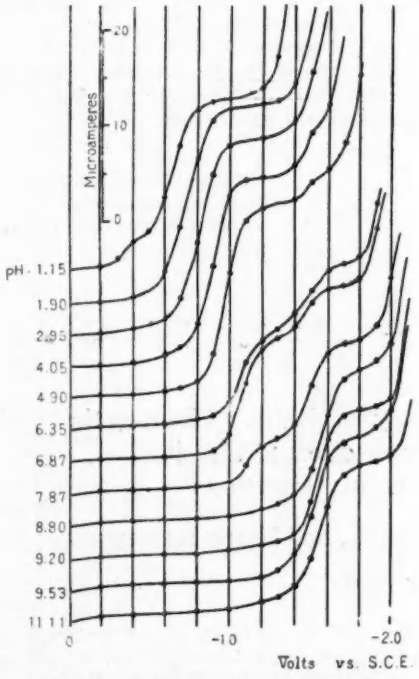

Fig. 1. Polarograms of nioxime at various pH

Polarographic Behavior of Nioxime.—Polarograms of nioxime at the dropping mercury cathode in various pH solutions are shown in Figure 1. These solutions have the composition of 10^{-3} M-nioxime, 10^{-2} M-KCl, and 0.01% gelatine except in the can of buffer agents. At a pH of 1.15, two waves appear at $E_{1/2}=-0.35$ and -0.65 volt vs. the saturated calomel electrode (S. C. E.) and in the pH range between 1.9 and 4.9, the first wave disappears and the second wave comes to predominate shifting to a more negative potential. At a pH of 4, the third wave appears at $E_{1/2}=-1.5$ volts vs. S. C. E. and above a pH of 8.8, the second wave disappears and the well-defined third wave predominates.

Amperometric Titration.—The general set-up was similar to that described in the previous paper[1]. For the performance of titration, a measured volume of the standard nickel solution in the proper medium was introduced into the cell, hydrogen was passed through for twenty minutes, the proper e.m.f. was applied to the cell and the current was measured. Successive amounts of nioxime standard solution were added from the burette. After each addition the contents of the cell were mixed by passing hydrogen through for half a minute and the current was recorded after it had become constant. In all cases the values of the current corrected for the volume change, were plotted against the amounts of reagent added.

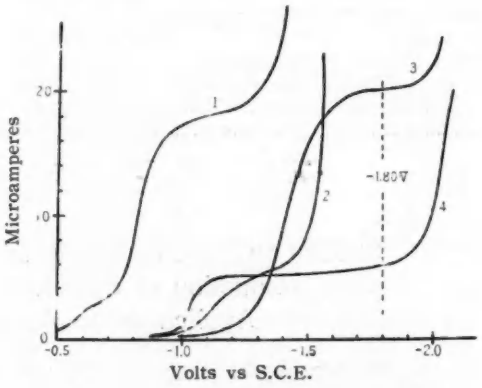

Fig. 2. Polarograms of nickel and nioxime in acetic acid medium and in ammoniacal medium
Curve 1. nioxime in 0.25M—CH_3CO_2Na, CH_3CO_2H
Curve 2. nickel in the same electrolyte
Curve 3. nioxime in 0.25M—NH_4Cl, NH_4OH
Curve 4. nickel in the same electrolyte
[nioxime]=1mM/l [Ni^{++}]=1mM/l

3) E. Rauh, G. F. Smith, C. V. Banks, H. Diehl, *J. Org. Chem.*, **10**, 197 (1945).
4) I. M. Kolthoff, "Acid-base Indicators", Macmillian Co., p. 251 (1937).
5) M. Ishibashi, T. Fujinaga, *J. Japanese Chem.* (in Japanese), 4, 554 (1950).

The most suitable titration medium for nickel was found to be an ammoniacal solution. Consequently, current voltage curves of nickel and nioxime were determined in order to find the most suitable condition for the titration. An applied e.m.f. of 1.80 volts was found to be the most suitable for the performance of the titration. See Figure 2.

In Figure 3 are given the data obtained in the titration of 0.000033M (1.955 mg.) nickel solution

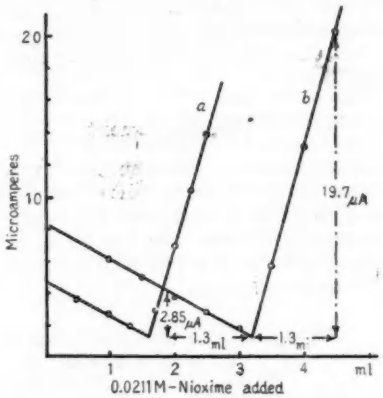

Fig. 3. Amperometric titration curves of nickel with nioxime
Curve a: 0.977 mg. of nickel in 20 ml. of 0.25M—NH_4Cl, NH_4OH.
Curve b: 1.955 mg. of nickel in the same solution

in 0.25M-ammonium chloride and ammonia with 0.0211M-nioxime at an applied e.m.f. of 1.8 v. The concentrations of ammonia and ammonium chloride could be changed within wide limits without affecting the results. In Table I is given a

TABLE I TITRATION OF NICKEL WITH NIOXIME

0.0667 N-Ni taken		0.211 N-nioxime used	Ni found	Error
0.50 ml.	(0.977 mg.)	1.59 ml.	0.987 mg.	+1.0 %
1.00	(1.955)	3.20	1.980	+1.2 %
2.00	(3.91)	6.35	3.92	+0.3 %
	"	6.36	3.93	+0.5 %
	"	6.37	3.94	+0.7 %
	"	6.39	3.96	+1.2 %
4.00	(7.82)	12.41	7.69	−1.7 %
Ni used		Nioxime taken	Ni found	Error
1.59 ml.	(3.12 mg.)	5.0 ml.	3.10 mg.	−0.7 %
3.17	(6.20)	10.0	6.19	−0.2 %
4.73	(9.27)	15.0	9.30	+0.3 %

summary of some results obtained in the titration of nickel with nioxime and in the reverse titration. In an acetic acid medium, it is difficult to select a proper e.m.f. riding over good plateaux of the diffusion currents of both nickel and nioxime. So good reproducibility in the titration curve is not expected.

Discussion

Numbers of Electrons Transferred in the Reduction of Nioxime.—The theoretical equation, derived by Ilkovic, for the diffusion current at the dropping mercury electrode is

$$i_d = 605 n D^{1/2} C m^{2/3} t^{1/6} = KC$$

where i_d is the average current in microamperes, n is the number of Faraday's transferred per mole, D is the diffusion coefficient in $cm.^2\ sec.^{-1}$, C is the concentration of reduced ion in millimoles per litre, m is the rate of flow of mercury from the dropping mercury electrode in $mg.\ sec.^{-1}$, t is the drop time in seconds, and K is the proportionality constant. Although diffusion coefficient D of nioxime is not known, by means of the Stokes-Einstein diffusion equation, it is computed to be about $5\times10^{-6}\ cm.^2\ sec.^{-1}$ from its molecular weight ($C_8H_{13}O_2N_2=142.16$). Substitution of experimental values to the equation (1) yields a value for n of approximately 8; e.g. in one experiment, using the mercury electrode of characteristics of m=0.641 and t=2.10, 0.9 mM/l-nioxime showed the diffusion current of 8.25 microamperes. Then

$$n = i_d/605 D^{1/2} C m^{2/3} t^{1/6}$$
$$= 8.25/605 \cdot (5\times10^{-6})^{1/2} \cdot 0.9 \cdot (0.641)^{2/3} \cdot (2.1)^{1/6}$$
$$= 7.65$$

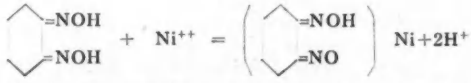

Again the number of electrons n was also calculated using the value of an amperometric titration curve of nickel with nioxime as they react according to the next formula.

At an applied e.m.f. of 1.8 volts, both nickel and nioxime are reduced at the dropping mercury electrode, thus the V-shaped titration curves are obtained in the present titrations. In such a case, the normal concentration of nickel at one point before the end point of titration is equal to that of nioxime at the point symmetric for the end point, in other words, at the point where the corresponding volume of the reagent is further added after the end point of titration, provided that the volume change in titration is negligible. As the reduction current, which is proportional to its concentration, is corrected for the volume change, the ratio of two reduction currents at the two points should follow the following equation assuming that the capillary characteristics at the two points are unchanged.

$$\frac{i}{i'} = \frac{n \cdot D^{1/2} \cdot C}{n' \cdot D'^{1/2} \cdot C'}$$

Here the numerators are of nickel and the denominators are of nioxime. As nickel ions are reduced to the metallic state at the applied e.m.f., $n=2$ and $C=C'/2$. Therefore,

$$n' = \frac{D^{1/2} \cdot i'}{D'^{1/2} \cdot i}$$

From the experimental data shown in Figure 3, $i'/i = 19.7/2.85 = 6.9$ and the diffusion coefficient of nickel calculated from its equivalent conductance at infinite dilution is 7.1×10^{-6} cm^2 sec^{-1}. Using the above numerical value,

$$n' = \frac{(7.1 \times 10^{-6})^{1/2}}{(5 \times 10^{-6})^{1/2}} \times 6.9 = 8.2$$

This value for n' is also very close to 8 and shows good coincidence with the value calculated according to the equation (1). This value for the number of electrons indicates that nioxime in an alkaline medium is reduced to 1,2-diaminocyclohexane at the dropping mercury cathode.

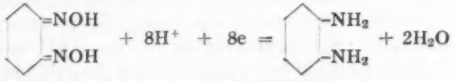

From the fact that oximes are generally reduced to the corresponding amines by metal reductants, the above inference is thought to be reasonable.

Summary

1. Cyclohexanedionedioxime (nioxime) was synthesized and its aqueous solution was used for the amperometric titration of nickel in ammoniacal medium, and the accurate results were obtained.

2. The polarographic behavior of nioxime was investigated and the reduction mechanism at the dropping mercury cathode was discussed.

Acknowledgement

It is a pleasure to these authors to express appreciation to Takeshi Kato and Manabu Matsuoka for their assistance in the measurement and also they wish to express their sincere thanks to the Ministry of Education for its financial grant.

Laboratory of Analytical Chemistry,
Faculty of Science,
University of Kyoto, Kyoto

This work was presented at the discussion on analytical chemistry held at Sendai in 1951 by the Chemical Society of Japan.

An Equation of State in Analytical Form (Continued)

By Tetsuya ISHIKAWA and Minoru IKEDA

(Received June 1, 1953)

In the previous paper[1] one of the authors (Ishikawa) proposed an equation of state slightly differed in its form from van der Waals' equation, but greatly improved in having a quantitative nature, i.e., for 1 mole of a gas the state is expressed by

$$p + \frac{a}{V^2 - \varepsilon} = \frac{RT}{V-b}, \quad a = 3p_c V_c^2, \quad b = V_c/3,$$

in which ε is an **analytically** determinable constant at each isotherm.

As clearly understood from the derivation of the equation, a and b are not the constants which satisfy $(\partial p/\partial V)_T = 0$ and $(\partial^2 p/\partial V^2)_T = 0$, so that at critical isotherm, the equation

$$p + \frac{a}{V^2 - \varepsilon} = \frac{RT_c}{V-b}, \quad a = 3p_c V_c^2, \quad b = V_c/3 \qquad (1)$$

should be combined with its critical condition:

$$p_c = \frac{3RT_c}{2V_c(1+3V_c\varepsilon)} \qquad (2)$$

where ε is not the value at the critical point, but the mean at the critical isotherm, or ε_c as denoted in the foregoing paper.

From the standpoint of the continuity of state, the unstable region of state at temperatures below the critical temperature has been supposed to consist of three portions of superheated liquid, supersaturated vapour and $\partial V/\partial p > 0$, the first and second portions being realizable, but the third being never realizable. Actually in the stable state these three

1) Tetsuya Ishikawa: This Bulletin, **26**, 78 (1963).

portion coincide on a horizontal straight line corresponding to a given temperature to realize a liquid-vapour coexistence region expressed by a well known relation:

$$\log_e \frac{p}{p_c} = A - B\frac{T_c}{T} \qquad (3)$$

A and B being constants of nearly equal magnitude, so that the state may be fully expressed by this relation in combination with an equation of state in a van der Waals' form which holds true even at temperature below the critical temperature.

We are fortunate to find the recent measurements done by Oliver and his collaborators on monomer of chlorotrifluoroethylene, C_2ClF_3, having average purity of 99.84%[2].

The molecular volumes of this substance at 25.0°C under high pressure range are all less than $b_{corr.}=b.(3RT_c/8p_cV_c)=RT_c/8p_c$, hence van der Waals' equation should be rejected.

Tests for the new equation are diagrammatically shown in Fig. 1, in which the curves in full and their connecting broken lines are plotted by taking $2-\varepsilon=1.861$, 1.879, 1.903 and 1.920 as the mean values at 25, 50, 75 and 100°C respectively, excluding the values in parentheses in Table I, which are far from

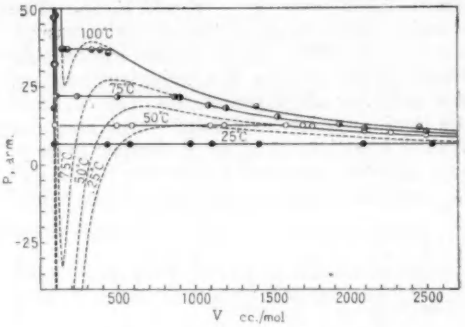

Fig. 1. Isotherms of C_2ClF_3.

TABLE I

$(2-\varepsilon)$ Values of C_2ClF_3 ($t_c=105.8$°C, $p_c=40.1$ atm., $d_c=0.55$ g./cc.)

$b=70.59$, $\log a=6.732021$

25.0°C			50.0°C			75.0°C			100.0°C		
p(atm.)	V(cc./mol.)	$2-\varepsilon$	p(atm.)	V(cc./mol.)	$2-\varepsilon$	p(atm.)	V(cc./mol.)	$2-\varepsilon$	p(atm.)	V(cc./mol.)	$2-\varepsilon$
47.29	89.34	1.862	47.30	95.74	1.908	47.91	105.88	1.902	37.05	142.92	1.923
32.26	89.57	1.861	12.81	99.01	1.888	32.27	108.67	1.904	37.02	150.02	1.925
18.24	89.80	1.860	12.73	99.36	1.889	22.14	111.70	1.907	36.93	179.77	1.927
6.774	90.97	1.866	12.66	497.71	1.868	22.20	112.05	1.907	36.91	335.80	1.915
6.796	91.78	1.871	12.53	594.27	1.857	22.06	241.69	1.918	36.82	389.97	1.915
6.766	94.93	1.888	12.50	1100.01	1.844	21.85	501.55	1.883	35.86	444.01	1.914
6.689	433.64	1.877	12.53	1190.04	1.848	21.74	868.57	1.900	18.80	1401.68	(1.941)
6.608	581.57	1.851	12.41	1591.31	1.882	21.61	902.00	1.904	11.91	2455.10	(1.995)
6.608	970.25	1.814	12.44	1705.22	1.904	21.58	905.03	1.904	8.629	3490.35	(2.038)
6.564	1109.56	(1.807)	12.42	1705.92	1.904	19.02	1088.82	(1.902)	6.650	4520.70	(2.015)
6.563	1418.57	(1.798)	12.16	1763.00	(1.906)	18.19	1200.76	(1.910)			
6.526	2093.09	(1.803)	10.68	2101.36	(1.913)	15.26	1535.98	(1.916)			
6.488	2537.80	(1.820)	10.05	2269.79	(1.916)	12.75	1935.38	(1.923)			
			9.311	2497.38	(1.920)	10.52	2498.66	(1.953)			
	mean	1.861		mean	1.879		mean	1.903		mean	1.920

having uniform pressures in unstable portions and those probably due to errors coming from the samples of different purity as noticed by the experimenters. These values together with the value at the critical point, 1.925, directly calculated by means of formula (2), are on a straight line as expected from the previous study. This proposition, therefore, serves as a supplemental test for estimating a probable value of $(2-\varepsilon)$.

The fair coincidences between the observed points denoted by ●, ○, ◑ and ◒ at 25, 50, 75 and 100°C respectively and the calculated curves outside of liquid-vapour coexistence regions are quite satisfactory.

The liquid-vapour coexistence regions can be represented by the following relation with less than 1.6% error:

$$\log_e \frac{p}{p_c} = 6.743 - 6.729\frac{T_c}{T},$$

which fits better than $\log p_{mm}=7.75412-1392.82/(t+319.70)$ proposed by the same experimenters.

Next we shall consider critical isotherms with two examples of hydrogen and carbon dioxide[3]. According to the classical theory, the critical point has been treated as a mathematical point of inflexion, e.g., applying van der Waals' equation, the condition of it is

2) G. D. Oliver, J. W. Grisard. C. W. Cuningham: *J. Am. Chem. Soc.*, **73**, 5719 (1951).

3) Adopted from "International Critical Tables" III, p. 5, 12.

$(8p_cV_c-3RT_c)^3=0$, or $V_c=3RT_c/8p_c$. The actual volume range at the critical pressure, however, is always found to be appreciably longer than that in the neighbourhood of this point, or diagrammatically, the curve of the liquid portion calculated from van der Waals' equation is situated farther from p-axis than the observed points (see Fig. 2 and 3, in which dotted curves are van der Waals' equation and ○ are observed points). This divergency needs another reasonable explanation.

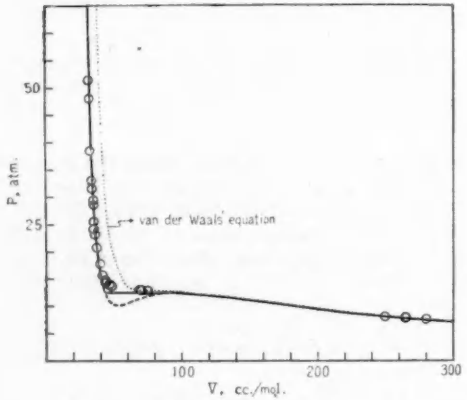

Fig. 2. Critical isotherm of H_2.

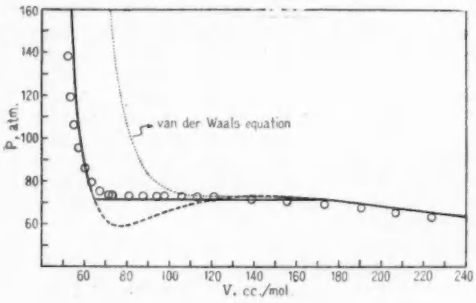

Fig. 3. Critical isotherm of CO_2.

Draw a horizontal straight line passing through the critical condition, $p_c=3RT_c/2V_c(1+3V_c^{\varepsilon})$, where ε is taken to be ε_c as stated above, i.e., $2-\varepsilon=1.928$ for H_2 and 1.912 for CO_2 (compare with Table 4 in the preceding paper). We see that experimental points lie near the line, and that by so doing the portion of supersaturated vapour almost disappears but a realizable portion of superheated liquid still remains. Further tests at other temperatures show that similarity though flat in its form happens even at a few or a few tens degrees above the critical temperature.

The above elucidation is no other than an extension of the already explained liquid-vapour coexistence to a critical region where p must tend to p_c, but $\log_e p/p_c=A-BT_c/T$ fails since A is not exactly equal to B.

The indefiniteness of the critical state (which means that even after the meniscus has disappeared, the density of the system is not uniform) since 1904, has long been the subject of investigation and the present recognition is that there exists a critical region between the temperature at which the meniscus disappears and that at which liquid can no longer exist[4].

Taking this recognition into account, the conception of combination of equation (1) with p_c from formula (2) which is elongated horizontally as a limiting case of relation (3) for the volume range between two portions of liquid and vapour states may be permissible.

Trials show that the calculated curve by use of the new equation passes on or by the observed points in both portions of liquid and vapour states (full line and its connecting broken line in Fig. 2 and 3 denote the calculated curves taking the same values of $(2-\varepsilon)$ as above).

This and foregoing results lead to the conclusion that the new equation of state, which is valid for gases, is also available for liquids.

Sasebo Commercial Junior College
Sasebo, Nagasaki

4) e. g., S. Glasstone "Textbook of Physical Chemistry", p. 433 (2nd Edition).

Microscopic Studies on Fused Catalysts for Ammonia Synthesis. III. Weak Ferromagnetic Inclusions and Their Isolation for X-ray Study

By Yoshio Ōsumi

(Received September 4, 1953)

Introduction

Iron catalysts for ammonia synthesis have been studied by different workers from different view-points. For these several years in our laboratory, microstructures of the polished surfaces of these catalysts have been examined using the optical, the surface-electron and the surface-ion microscopes.

As reported in our first paper[1] the unreduced polished surfaces of usual catalysts with potash addition, when optically observed, consist of two different sorts of grains. A grains are large and each of them is filled with fine regular cleavage surfaces peculiar to magnetite. B grains, much less abundant than A grains, are found mainly along the grain bonudaries of A and are more capable of fine polishing, less markedly changed by hydrogen reduction, but more easily attacked by hydrochloric acid than A grains.

It was found that unreduced surfaces of these catalysts emit enough electrons at about 1000°C to permit observations with the surface-electron microscope. Such observations made with twelve sorts of catalysts showed that potash-promoted catalysts generally gave brightest electronic images, and in particular, those with well developed crystal grains gave almost exact patterns of B grains (Phot. 1a, 1b).

1a ×40

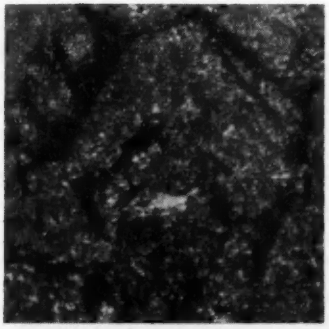

Optical image of polished surface (Cat. No. 10)

1b ×40

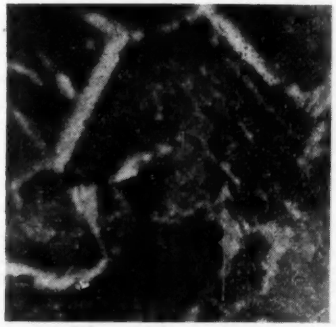

Thermo-electronic image of the same sample using a magnetic lens

The second paper contains observations with the surface-ion microscope of our own construction[2]. The catalysts, when reduced, emit positive ions mainly from B at about the same temperature as they do electrons (Phot. 2a, 2b). These ions could be identified

2a ×20

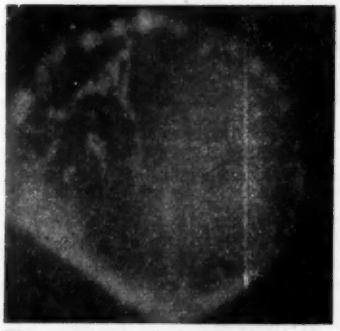

Thermo-electronic image of another sample using electrostatic lens (Cat. No. 10)

1) N. Sasaki, Y. Ōsumi, *J. Chem. Soc. of Japan*, (Pure Chemistry Section, Japanese), **73**, 808 (1952).

2) Y. Ōsumi, *J. Chem. Soc. of Japan*, (Pure Chemistry Section, Japanese), **74**, 308 (1953). More details of the results of optical-microscopy and of electron-microscopy are found in 3) and 4) respectively.

2b ×20

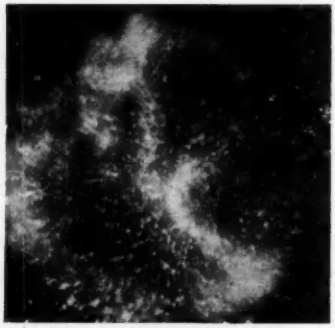

Thermo-ionic image of the same sample

with potassium ions, because the application of a magnetic field transversal to the ion path displaced the ionic image to the same extent as the image of a potassium ion source[2].

These potash-rich regions (B grains) seem to have become segregated from the ground magnetite mass of the potassium-promoted catalysts during its solidification.

In the present third paper[5], it will be reported that B grains have been found sufficiently less ferromagnetic than A grains to be magnetically separated from A grains and that they have been studied for their chemical and x-ray crystallographic properties in comparison with A grains.

Isolation of Weak Ferromagnetic B Grains for Surface-electron Microscopic Studies

From the polished surfaces of catalysts no. 4 and 10 (Table I) where B grains were relatively clearly observable, a small amounts of A and B were scraped off with the tip of a needle under an optical microscope. When a pole of a bar magnet whose strength was about 500 gausses was approached from above, it began to attract A powder at the distance of 2–3 cm., while B powder remained unattracted even at the distance of 2–3 mm.

TABLE I

Catalyst No.*	Promoter Added in %				Polished Surface as Observed		X-ray Diffraction Pattern of Powder	
	Al_2O_3	K_2O	CaO	MgO	Optically	Surface-Electronically	A	B**
1	—	—	—	—	no B	faint emission from whole surface	magnetite with slight α-Fe_2O_3	—
2	5	—	—	—	ditto	ditto	magnetite	—
3	—	1	—	—	B	strong emission from B	magnetite with slight FeO	FeO with slight magnetite
4	5	1	—	—	ditto (distinct)	ditto	magnetite	M
8	4	—	1	—	no B	somewhat bright emission from whole surface	ditto	—
9	4	—	—	1	ditto	faint emission from whole surface	ditto	—
10	10	1	1	—	B (distinct)	strong emission from B	ditto	M
11	4	1	1	—	ditto	ditto	ditto	M
12	4	1	—	1	ditto	ditto	ditto	M

* The catalyst numbers are the same as those used in the first report.
** In the column of X-ray diffraction pattern of B powder, blanks mean that weak ferromagnetic substance is not separable, and M indicates a peculiar diffraction pattern mentioned in the text.

A small piece of the catalyst as a whole was ground in an agate-mortar to a fine powder. It was then all attracted to the underside of a sheet of paper horizontally held, by placing the end surface of the magnet pole on the upper side of it. When the magnet was then moved about slowly along the sheet, weakly magnetic particles fell down from the paper, while the strong magnetic ones remained attached to it. From the powder made from pure magnetite no particles fell off during this treatment irrespective of the

3) Y. Osumi, "Ammonium Sulphate Engineering" (Japanese) **16**, 13 (1952).
4) Y. Osumi, ibid., **17**, 8 (1953).
5) Details about this work will soon be published in "Ammonium Sulphate Engineering" (Japanese).
6) N. Sasaki, K. Mitani, *Proc. Imp. Acad.*, (Tokyo) **17**, 36 (1941); N. Sasaki, *J. Applied Phys.*, **19**, 1050 (1948).

way and degree of pulverization. All the fallen particles must have come from B grains. Actually these were not attracted by the magnet 2–3mm from them.

One may suppose that B grains are inherently non-magnetic and the observed weak magnetism of B particles is due to the presence of a very small amount of A not separated from B particles by the process of pulverization. But the fact that even extrafine powder of B can finally be attracted to the last particle shows the magnetism is inherent in B. Incidentally the Curie point has been estimated to about 520°C for A powder and about 580°C for B powder made from catalyst no. 4.

By the magnetic separation, no. 4 and 10 catalysts respectively gave 3 and 5 per cent of B powder. These figures almost agreed with those calculated from the relative areas of A and B in the optical photographs of the polished surfaces.

A and B powders each in a small amount were kneaded with a drop of liquid paraffin, and placed side by side on a small disc cathode of nickel in our surface-electron microscope. Phot. 3a and 3b show that B powder is as good an emitter as

3a ×25

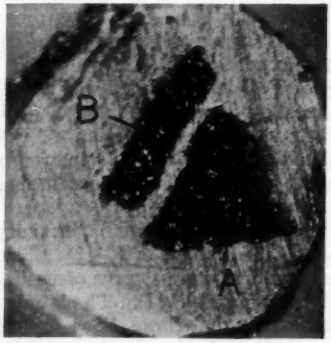

Optical image of powders on Ni-plate
(Cat. No. 4)

3b ×50

Thermo-electronic image of the same sample using a magnetic lens

B grains on the polished surface of the original catalyst.

Under the optical microscope fine particles of A powder are seen aggregated in arabesque figures, dispersed with difficulty probably due to mutual attraction between the magnetized particles (Phot. 4a), while B powder is seen as separated

4a ×50

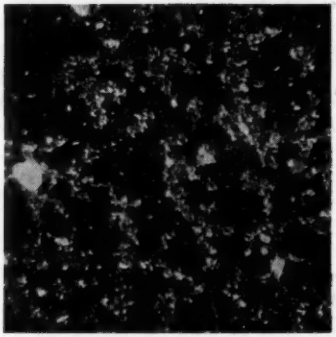

Optical image of powder A
(Cat. No. 4)

particles with rather sharp facets and edges, a fact unexpected from the mere appearance of B grains on the polished surface (Phot. 4b).

4b ×50

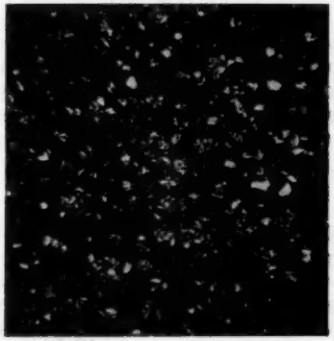

Optical image of powder B
(Cat. No. 4)

The weak ferromagnetic substances can be obtained from all potash-promoted catalysts which give distinct optical and electronic images of B grains. (Table I)

Chemical Compositions of A and B

In the foregoing reports the possible segregation of potash in B grains has merely been assumed from the study of some properties of polished surfaces. This can now be confirmed by analysing A and B powders separately. The results are given in Table II.

TABLE II

Catalyst No.		Weight Percentages of A & B	Oxide Percentages Found in Powder				
			Fe-oxides	Al_2O_3	K_2O	CaO	MgO
3	A	96.1	99.42*	—	0.58	—	—
	B	3.9	97.87*	—	2.13	—	—
4	A	96.9	92.8 (Fe_3O_4)	4.8	0.40 (0.29)**	—	—
	B	3.1	84.5 (Fe_2O_3)	6.3	4.00 (2.95)**	—	—
10	A	95.0	84.4 (Fe_3O_4)	11.3	0.52	0.46	—
	B	5.0	71.6 (Fe_2O_3)	25.0	3.49	2.41	—
12	A	92.0	68.0 (Fe_2O_3) 25.7*** (FeO)	4.9	0.34	—	0.70
	B	8.0	93.14 (Fe_2O_3)	3.4	1.98	—	0.61

* These figures were obtained not by analysis but by subtraction of the weight percentage of potash from one hundred.
** These figures were obtained by the analysis of the sample after boiling for 4 hours in water.
*** These figures obtained by analysis correspond very roughly to Fe_3O_4, so that in other samples shown qualitatively to contain both Fe^{++} and Fe^{+++}, total Fe is assumed to exist in the form of Fe_3O_4.

The alkali content of B is definitely greater than that of A for all the catalysts studied. Here we may tentatively assume that the crystal structure of A is not capable of containing more than about 0,5 per cent of potash, and in the solidifying process B crystals separate out to take over the excers of it. Calcium oxide behaves similarly (Catalyst no. 10), but magnesium oxide does differently (Catalyst no. 12).

X-ray Studies of A and B

Of all A and B specimens listed in Table I, X-ray diffraction photographs were taken using unfiltered Fe-K radiation (Camera diameter: 90 mm). Specimens A from the non-promoted iron oxide (Catalyst no. 1) and from singly promoted catalyst with potash addition (Catalyst no. 3) gave patterns characteristic of magnetite intermingled with some of the strongest lines of α-Fe_2O_3 and FeO respectively, while specimens A from catalysts with alumina addition (Catalyst no. 2, 4, 8–12) always gave the pattern of magnetite only, irrespectively whether they contained other promoters or not. Alumina addition seems to facilitate the formation of spinel lattice of magnetite[7].

Specimen B from a singly promoted catalyst with potash addition (Catalyst no. 3) gave patterns of FeO intermingled with some very strong lines of magnetite. Potash addition seems to favour the formation of FeO, for Fe_2O_3 fused with K_2CO_3 (1:1 in weight) for one hour at about 1100°C also contains FeO in an amount detectable by X-ray.

Specimens B from catalysts containing K_2O and Al_2O_3 (Catalyst no. 4, 10–12) all exhibit complicated diffraction patterns of similar type (denoted by M in Table I). The lattice spacings calculated from these lines and the relative intensities do not correspond to any compound listed in the A. S. T. M. or the Hanawalt tables.[8] However, the comparison of the lines of A and B of catalyst 4 (Phot. 5a, 5b) shows that these two crystal structures are not essentially different.

On both diagrams we notice a few lines exactly in the same positions which may be attributed to indices (044), (004) and (022), or some of the planes most densely packed with O atoms in magnetite structure. The strong lines in Phot. 5a with indices (113) and (115) seem in Phot. 5b to have split into many closely situated lines. Potash added in sufficient quantity seems to change the spinel lattice of magnetite into a slightly modified lattice with reduced degrees of symmetry

7) A possibility of solid solution formation between Fe_3O_4 and γ-Al_2O_3 has been reported by R. W. G. Wyckoff, E. D. Crittenden, *J. Am. Chem. Soc.*, **47**, 2866 (1925); R. Brill, *Z. Elektrochem.*, **38**, 669 (1932).

8) They also do not correspond to $KFeO_2$ or $KAlO_2$, T. F. W. Barth, *J. Chem. Phys.*, **3**, 323 (1935); L. T. Brownmiller, *Am. J. Sci.*, **29**, 260 (1935).

5a (044) (115) (004) (113) (022) powder A (Cat. No. 4)

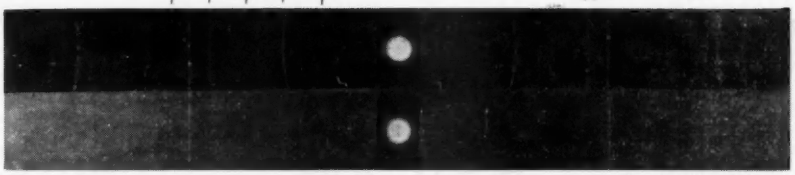

5b powder B (Cat. No. 4)

(thereby probably leaving the closely packed configuration of oxygen atoms almost intact).

Attempts were made to reproduce this interesting M type structure in specimens directly synthesized by fusing for 3 hours at about 1000°C Fe_3O_4 (Catalyst no. 1) with an equal amount of potash and 1, 5, 10, and 20 per cent of Al_2O_3. Of these only one with 5 per cent Al_2O_3 addition gave the M pattern (Phot. 5c).

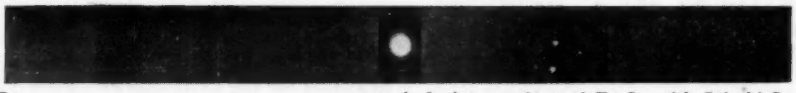

5c potash fusion product of Fe_3O_4 with 5% Al_2O_3

These facts make highly probable our abovementioned assumption that potash added in the course of melting to usual doubly promoted catalysts with K_2O and Al_2O_3 is retained in the spinellattice of magnetite in high dilution and in the M type lattice of B grains in much higher concentration. By the way, when boiled for 4 hours in water, B powder lost about a quarter of the total potash but still retained the M pattern unaltered.

Formerly Okamoto and Kobayashi[9] measured the activation energy for high pressure ammonia synthesis on various kinds of usual doubly promoted catalysts in relation to the amounts of K_2O retained after washing with water at room temperature for one day. They found that the activation energy was large for catalysts with K_2O content less than about 0.5 per cent, and it decreased with increase of K_2O content to a constant minimum value of about 15 Kcals for the K_2O content larger than 0.5 per cent. This fact may be explained by the assumption that the activity of catalysts is determined by A grains which constitute almost the whole mass and can contain K_2O to at most about 0.5 per cent and K_2O soluble in water at room temperature is contained not in A and B but in some other unidentified potassium compounds.

Summary

On the basis of our new finding that B grains on the polished surface (Report 1 and 2) of usual iron synthetic ammonia catalysts are less ferromagnetic than A grains, we attempted to separate magnetically B grains from A grains. The more magnetic fraction (called A powder) and the less magnetic fraction (called B powder) have the following properties:

1. B powder as observed by the surface-electron microscope is as strongly electron-emissive as B grains on the polished surface. This suggests a successful separation.
2. Chemical analysis shows that B powder is far richer in K_2O and CaO than A powder.
3. X-ray diffraction patterns of A powders separated from usual doubly or triply promoted catalysts are identified with that of magnetite, and those of B powders are all similar and complicated, whether they contain CaO or MgO or not. The product of potash fusion of Fe_3O_4 with 5 per cent Al_2O_3 gave the same diffraction pattern as B. Some relation of this new crystal structure to the spinel lattice of magnetite was discussed.

In the next paper will be reported the results of ammonia decomposition tests carried out with A and B powders under atmospheric pressure.

I should like to express my sincere thanks to Professor Nobuji Sasaki for his kind guidance throughout this work; my deep gratitude is also due to assistant R. Kiriyama and I. Taguchi of the laboratory of Professor Nitta, Osaka University, and to Professor J. Kakinoki, Osaka City University, and to Shimazu-Seisakusho Laboratory for taking X-ray diagrams, and to assistant T. Shigematsu of the laboratory of Professor Ishibashi, Kyoto University for his help in chemical analysis.

Department of Chemistry, Faculty of Science, Kyoto University, Kyoto; *Mitsubishi Kasei*

9) T. Okamoto, *J. Soc. of High Pressure Gas Industry* (Japan), **16**, 216 (1952).

Effect of Organic Molecules on the Adsorption of Hydrogen on the Electrode Surface*

By Takashi MUKAIBO and Mitsuru OIKAWA

(Received June 22, 1953)

Introduction

The effect of solvents on the hydrogen overpotential has been discussed recently by J. O'M. Bockris[1)~3)] and A. Wetterholm.[4)] They have obtained many interesting results relating to the mechanism of the hydrogen electrode reaction, and the theoretical presumption on these phenomena has been given. According to these authors,

(a) The solvent effect depends on both the cathode material and the nature of organic solute and therefore does not seem to depend principally upon solvation of the hydrogen ion, which should have some effects according to the slow discharge theories.

(b) The solute layer, held on the surface of the electrode by coulombic or van der Waals adsorption force, affects the velocity of the recombination of hydrogen atoms, which may be the rate-determining step of the electrolytic evolution of hydrogen molecules.

(c) The solvent effect on the adsorption energy of hydrogen molecules on the surface of the working electrode[5)] may change the hydrogen overpotential.

The measurement of the number of metal atoms on the electrode surface covered by organic molecules during the evolution of hydrogen being very difficult, the above theoretical presumption has only poor and indirect experimental evidence.

J.A.V. Butler [6)7)] has proposed the method of measuring the electrode potential in the initial stage of cathodic polarization with a cathode ray or an electromagnetic oscillograph and calculated the number of hydrogen atoms adsorbed on the electrode surface. By this method, we studied about the relation between the hydrogen overpotential and the effect of the adsorption of organic molecules especially in case of a smooth platinum electrode which has been assumed to obey the catalytic mechanism in the cathodic current density between 10^{-3} and 1 A./cm^2.

Under the assumption that the cathode area available for the hydrogen evolution decreases by the steric hindrance of organic molecules adsorbed on the cathode surface, we[8)] estimated the number of surface points covered by organic molecules, by analysing these polarization curves.

Experimental Procedures

The measuring cell was divided into three rooms separated from each other by diaphragms of glass filter. A platinum electrode, having an available area of approximately 3.6 cm^2, was placed between two auxiliary platinum electrodes in the middle room.

The change of the potential difference was recorded with an electromagnetic oscillograph (Yokogawa N-3, D-Type) through a suitably set 1-valve amplifier. At the same time the potential scale was given by a potentiometer through the amplifier.

During experiments air and free oxygen were removed from the apparatus by bubbling hydrogen, purified by passing through heated palladium asbestos in a silica tube. The electrode was first anodically polarized to remove adsorbed hydrogen and to give a constant electrode potential, and then a cathodic current was passed. By this procedure, we obtained curves of good reproducibility. As shown in Fig. 1 three main stages in the initial build up of cathodic polarization have been distinguished, corresponding to the ionisation of adsorbed oxygen (stage α), the charging of a double layer (stage β), and the adsorption of hydrogen at the electrode (stage τ) respectively.

The number of sites of the electrode surface covered by discharged hydrogen atoms can be calculated from the quantity of electricity consumed during the stage τ[9)]. The difference in above numbers before and after the addition of organic molecules to the solution shows the

---

* This paper was read at the annurl meeting of this society on April, 8, 1953.

1) J. J. O'M. Bockris: *Discuss. Farad. Soc.* No. 1, 95 (1947).

2) J. O'M, Bockris and S, Ignatowicz: *Trans, Farad,* **44**, 519 (1948).

3) J. O'M, Bockris and R, Parsons: ibid. **44**, 860 (1948).

4) Allan Wetterholm: ibid. **45**, 861 (1949).

5) R. Parsons and J.O'M. Bockris: ibid. **47**, 914 (1951).

6) R. Pearson and J. A. V. Butler: *Trans. Farad. Soc.* **34**, 1163 (1938).

7) F. P. Bowden: *Proc. Roy. Soc.* **125A**, 446 (1929).

8) M. Oikawa and T. Mukaibo: *J. Electrochem. Soc., Japan.* **20**, 583 (1952).

9) J. A. V. Butler: "Electrocapillarity." p. 178, (1940).

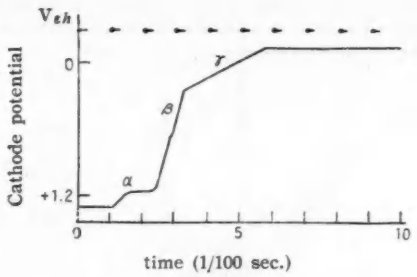

Fig. 1.
Polarization curve of platinum cathode in N. H_2SO_4

number of sites covered by organic molecules.[8] Cathodic current densities were limited between 10^{-3} & 5×10^{-1} A./cm². In this range we can assume that the mechanism of hydrogen electrode reaction belongs to that of the catalytic.[10][11] During the experiments the cell was saturated with pure hydrogen gas, the pressure of which was maintained about one atmosphere.

Results and Discussions

A. Preliminary Experiments. Table I shows the length of stage γ on the smooth platinum electrode in pure N. H_2SO_4 solution. It was found that the length of the stage was almost independent of the current density over the range of $3.0\times10^{-3}\sim1\times10^{-1}$ A./cm².

TABLE I

Cathodic Current Density D.A./cm² $\times10^{-3}$	Stage γ Coul. $\times10^{-5}$	Log D (D, A/cm²)	Electrode Potential V, ε_h
3.2	3.3	−2.49	0.000
5.0	3.3	−2.29	0.015
10.0	3.5	−2.00	0.035
32.0	3.6	−1.49	0.070
100.	3.6	−1.00	0.11

Moreover it was confirmed that the oxygen adsorbed during the anodic polarization was perfectly consumed in the stage α.[8] Though the length of stage α had a wide range of values by the time of duration of the anodic polarization or by the anodic current density, the length of stage γ was almost independent of such conditions, as shown in Table II.

TABLE II

Anodic Polarization (mA.×sec.) /3.6cm²	Cathodic Polarization (A./3.6cm²)	Stage γ (coul.) $\times10^{-5}$
5×30	36.4	3.5
5×60	36.5	3.6
2×30	36.9	3.7
10×20	36.3	3.7
2×20	11.5	3.5
3×30	18.0	3.5

Taking the diameter of a platinum atom as 2.5Å, we calculated the quantity of electricity required to deposit one hydrogen atom on each platinum atom of the electrode surface to be 2.7×10^{-4} coulombs/cm². The same quantity found experimentally by the above mentioned procedure was about 9.7×10^{-4} coulombs per sq. cm. of the apparent surface. This value agrees with the calculated one if we assume the real area of the electrode to be about 3.6 times the apparent area of it. Though there is some uncertainty as to this ratio at the smooth platinum surface, the value 3.6 obtained by us may be reasonable when compared with those estimated by many other authors which lie between 2 and 4[12]. From the values in column 3 and 4 of Table I we get Tafel's constant b of about 0.08.

Then, by adding organic compounds at various concentrations to N. H_2SO_4, we obtained the results shown in Fig. 2 and Fig. 3.

The quantity of electricity consumed in the stage γ is sharply affected by the addition of acetaldehyde; and the larger the concentration of it the smaller becomes the length of the stage.

Fig. 2 shows the relation between the concentration of acetaldehyde in the bulk of the solution and the number of adsorption points covered by molecules of acetaldehyde.

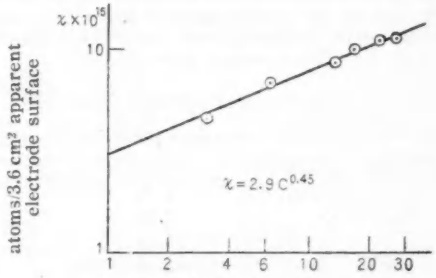

Fig. 2.
Freundlich's adsorption isotherm of the electrode surface (measured at the current density 10mA./cm², 3°C)
x: number of adsorption point covered by acetaldehyde
c: concentration of acetaldehyde (M./l. solution) x and c in log. scale

This figure shows also that the relation fits Freundlich's isotherm very well. The parameters of the equation were determined and are shown also. From Fig. 3 we can see that there exists a parallelism between the adsorption of organic molecules and the electrode potential. This fact suggests to us that the relation between these factors is very important.

10) J. O'M. Bockris and A. M. Azzam: *Trans. Farad. Soc.* **48**, 145 (1952).
11) J. O'M. Bockris: *Chem. Rev.*, **43**, 525 (1948).
12) J. A. V. Butler: "Electrocapillarity" p. 73 (1940).

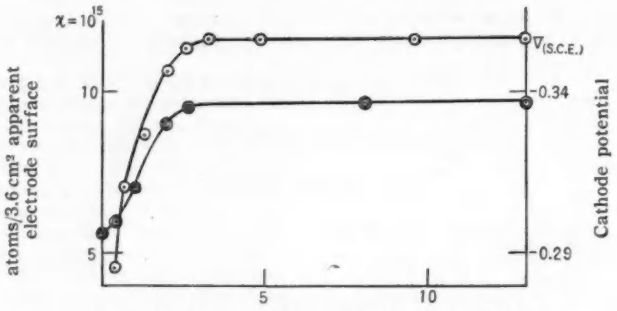

Fig. 3.
The relation between the adsorption of acetaldehyde (⊙) and the cathode potential (◎) (at 3°C)
V: potential in volts referred to the saturated calomel electrode (S.C.E.) the amount of adsorption of acetaldehyde and the electrode potential were all measured at the cathode density 10 mA./cm².

B. Case 1. According to J. O'M. Bockris, an increase of the concentration of an organic compound occurs at the metal-solution interface and this positive adsorption is influenced by several factors, such as the dipole moment of the solute and the properties of the cathode surface. So in the first place we added acetaldehyde to the electrolyte as the organic compound soluble in water and having the dipole moment larger than that of the solvent. Though we feared that acetaldehyde might be reduced at the cathode, it was confirmed by the preliminary experiments that acetaldehyde was not reducible at the platinum cathode in the N. H_2SO_4 solution.[13,14,15]

We measured the hydrogen overpotential on the platinum electrode dipped in the electrolyte containing a different amount of acetaldehyde, under several cathodic current densities.

The results are shown in Table III and Fig. 4.

TABLE III

Composition of Electrolyte	Log D* (D.A./cm²)	Available Area** cm²	Log D'*** (D',A./cm²)	Electrode**** Potential V, ε_h
0.96M. Acetaldehyde/L of N. H_2SO_4	−2.49	1.67	−2.16	0.02
	−2.29	1.94	−2.03	0.03
	−2.00	2.00	−1.70	0.05
	−1.48	2.54	−1.33	0.08
0.48M. Acetaldehyde/L of N. H_2SO_4	−2.49	1.95	−2.23	0.01
	−2.29	2.00	−2.04	0.02
	−2.00	2.25	−1.80	0.04
	−1.67	2.75	−1.56	0.06
	−1.48	3.00	−1.41	0.07

* D: Cathodic current density A./cm² apparent area.
** Cathode area for hydrogen evolution reaction corrected by taking the steric hindrance of organic molecules.
*** D': (D×3.6)/(available area), 3.6cm²: apparent area of the cathode.
**** Considering the exactness of our data, we took the numerical value of the electrode potential to the order of 10 mV when the electrolyte contained organic molecules.

In column 4, D' is the current density corrected by taking the steric hindrance of acetaldehyde into consideration, that is, it was assumed that the surface points covered by organic molecules did not take part in the discharge of hydrogen ions.

As seen in Fig. 4 and 3, the hydrogen overpotential increases with the increase of the concentration of acetaldehyde in accordance with the results of Wetterholm (10^{-3}~10^{-2}A./cm²). Tafel's

13) C. J. Brockman: "Electro Organic Chemistry" p. 287 (1926).
14) V. Stern and S. Polak: *Acta Physicochim U. R. S. S.* **11**, 797 (1939).
15) Böttger: "Physik. Methode d. Anal. Chem" Bd. II. p. 295, (1936).

constant b changes between 0.06~0.08, but after the correction of the effective cathode area which

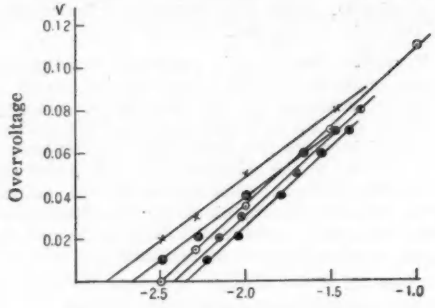

Fig. 4.
Effect of acetaldehyde on the relation between the cathodic current density and the overpotential (at 3°C)
(⊙) $N.H_2SO_4$, b=0.08
(×) 0.96M. acetaldehyde/L $N.H_2SO_4$, b=0.06
(◑) 0.48M. acetaldehyde/L $N.H_2SO_4$, b=0.06
(⊗) after the correction of the current density (0.96M. acetaldehyde/L $N.H_2SO_4$) b=0.08
(●) after the correction of the current density (0.48M. acetaldehyde/L $N.H_2SO_4$) b=0.08

we supposed would diminish by the adsorption of acetaldehyde, b becomes about 0.08, the same value as when there is no addition. Though Tafel's another constant a also changes slightly, we may attribute the main effect of acetaldehyde to the steric hindrance of it on the electrode surface.

Of course we must take account of the effect of the solute on δ, the thickness of the double layer, or the value of ΔH^* (the heat of activation of hydrogen evolution) as J. O'M. Beckris mentioned,[5,16] but according to our experiments the chief effect of the solute seemed to be the steric hindrance.

C. Case II. Next we examined the effect of the addition of ethyl alcohol as the solute having smaller dipole moment than that of water.

The results are shown in Fig. 5 to Fig. 7. In Fig. 5 we can see that the amount of adsorption of ethyl alcohol is very small as compared with the case of acetaldehyde even in the concentrated solution. In Fig. 6 we showed Tafel's lines in

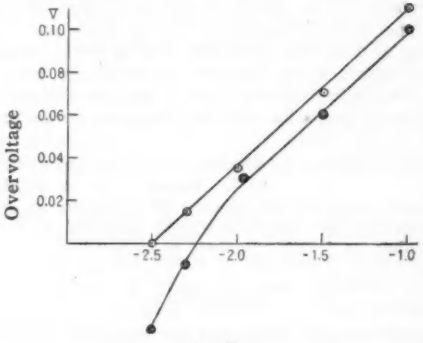

Fig. 6.
Tafel's line on $N.H_2SO_4$ and on the solution of ethyl alcohol (at 3°C)
(⊙) $N.H_2SO_4$
(◑) ethyl alcohol (1.7M./l.$N.H_2SO_4$)

$N.H_2SO_4$ and in the solution of ethyl alcohol. The relation between the electrode potential and the concentration of ethyl alcohol is shown in Fig. 7.

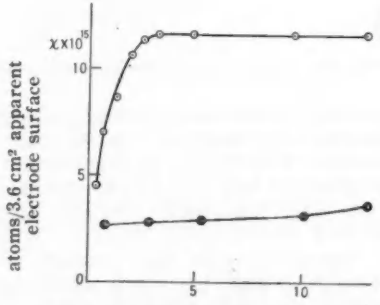

Fig. 5.
Relation between the adsorbed amount of organic compounds and their concentration (at 3°C)
(⊙) acetaldehyde M./L $N.H_2SO_4$
(◑) ethyl alcohol M./L $N.H_2SO_4$ measured at the current density 10 mA./cm²

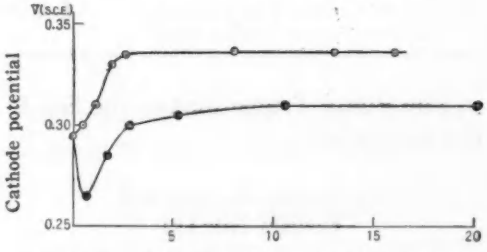

Fig. 7.
The relation between the cathode potential and the concentration of organic compound (at 3°C)
(⊙) acetaldehyde (◑) ethyl alcohol measured at the cathode density 10 mA./cm²

16) P. J. Hillson: *Trans. Farad. Soc.* 48, 462 (1952).

The electrode potential decreases at first, but becomes high with the further increasing concentration of the alcohol. After reaching the value near that in pure $N.H_2SO_4$, it stays there over a wide range of concentration of ethyl alcohol (5~35 M. EtoH/1), then decreases slowly at higher concentrations (ca. 35M./1).

In the concentrated solution of ethyl alcohol, we found that the bending point of the polarization curve in the oscillograph showing the saturation of the adsorption of the hydrogen atom disappears. From this fact, we may attribute the reason of the lowering of the potential in the concentrated solution to the existence of some reaction other than pure hydrogen evolution on the cathode surface. From these we may conclude as follows.

The organic molecules having dipole moments smaller than that of water such as ethyl alcohol are adsorbed very poorly on platinum cathode as shown in this experiment, so the change of electrode potential by its steric hindrance may be small.

Accordingly, the change of the electrode potential in this case may be largely due to another factor such as the change of adsorption energy of discharged hydrogen by the addition of ethyl alcohol, as J. O'M. Bockris proposed.[17,18]

Conclusion

The relation between the electrode potential and the adsorption of organic molecules was studied by measuring the adsorption by the oscillograph. We can divide in two types the effects of organic molecules adsorbed to the surface of the cathode, when the evolution of hydrogen is of catalytic mechanism.

Type I. The organic molecule having the dipole moment greater than that of water is strongly adsorbed on the surface of platinum cathode and by its steric hindrance, the cathode potential becomes less noble with the increase of its addition to the solution. On such a type, by correcting current densities as to the cathode area covered by organic molecules, Tafel's constant and also the potential become almost the same as when there is no addition.

Type II. The organic molecule having the dipole moment smaller than that of water is adsorbed only a little on the electrode and the effect of it on the electrode potential seems rather due to the solvent effect than to the steric hindrance, when the size of the molecule is small.

These conclusions may be reasonable in reference to the discussion of former authors, especially to that of J.O'M. Bockris.[1)~3)]

The expenses incured for this work were met by the Grant in Aid for Fundamental Scientific Research, to which our thanks are due.

Laboratory of Applied Electrochemistry, and Photochemistry Faculty of Engineering, University of Tokyo

17) J. O'M. Bockris & R. Parsons: *Trans. Farad. Soc.*, **44**, 860 (1948).
18) R. Parsons & J. O'M. Bockris: ibid **47**, 914 (1951).

LETTER

The Phase Transitions of the Solid Cyclohexanol*)

By Sei-ichi KONDO and Kiyoshi NOZAKI

(Received June 8, 1953)

Investigations have been made of the dilatometry and the dielectric constant of the pure cyclohexanol mainly on the behavior of the phase transitions at −8.1°C and −28.6°C. These two phase transitions were well studied thermally by Kelly,[1)] and Otsubo,[2)] dielectrically by White and Morgan,[3)] and Smyth,[4)] and structurally with X-rays by Sugawara.[5)]

Cyclohexanol was boiled with calcium oxide for one day, fractionally distilled, warmed again with calcium oxide for about 30 hours and evaporated in a high vacuum into a dilatometer vessel to which distilled and evacuated mercury was introduced. The melting point of this material thus purified

* This research was made in part under the support of the scientific research grant of the Education Ministry.

1) K. K. Kelly; *J. Am. Chem. Soc.*, **51**, 1400 (1929).
2) E. Kanda and Otsubo; read at the annual meeting of the *Chem. Soc. Japan.* in (1952).
3) White and Morgan; *J. Am. Chem. Soc.*, **57**, 2081 (1935).
4) C. P. Smyth and R. W. Crowe; *J. Am. Chem. Soc.*, **73**, 5409 (1951).
5) T. Sugawara; will appear in "X-Sen" Vol. 12 No. (1953).

was 24.2°C.

The results of the experiments are illustrated in Fig. 1. Cyclohexanol is supercooled very easily to the temperature of liquid air. (the full line in Fig. 1.) The volume expansion coefficient of this phase is 4.4×10^{-4} cc/degree, which is in good agreement with the value 4.4×10^{-4} calculated from the lattice constant of the room temperature α phase by Oda[6] and that of the supercooled α phase.[5] When heating it immediately after cooling to the temperature of dry-ice alcohol mixture or liquid air, the volume change at the lower transition point is small and indefinite. (the dotted line in Fig. 1.) When cooled for about one day in liquid air or dry-ice mixture, the

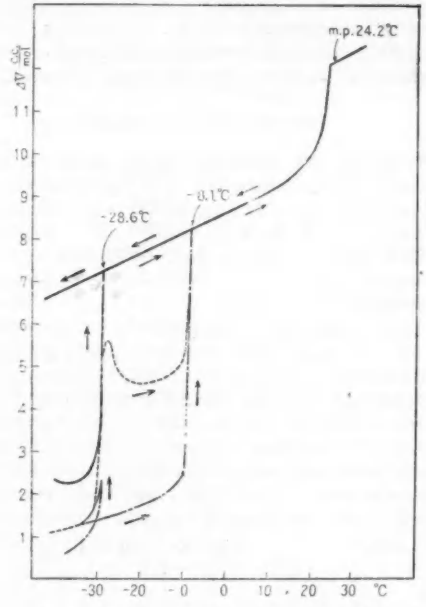

Fig. 1. The volume expansion $\triangle V$ c.c./mol. of the solid cyclohexanol. The full line shows the curve warmed after cooling for 2 hrs. and the dotted and broken lines are those warmed after cooling for 24 hrs. in dry-ice alcohol mixture in each case.

volume difference at this point between the γ phase below −28.6°C. and supercooled α phase is constant in every case, which shows that the phase transition from α to γ phase is apparently completed. The γ phase exists always in our thermal treatment, but disappears when the sample is once more cooled a little below −28.6°C. in the middle of this phase transition, and then there exists only the transition at −8.1°C., the volume change of which is about 5.8 cc/mol. (the broken line in Fig. 1.)

When cyclohexane is mixed with this sample, which is soluble with this in the solid state, the phase transition at −8.1°C. becomes smaller in proportion to the concentration of cyclohexane and disappears at about 10% cyclohexane, and there exists only the transition at −31°C., and the β phase below −8.1°C. may disappear.

The dielectric constant and loss were measured with the modified transformer method. Although the main features are the same as Smyth's experiment, the purity of the sample is better in our case, and the dielectric constant of α phase is 15.0 at 8.2°C. which is smaller than that of Smyth and that of γ phase is 2.41. The dielectric constant of the β phase is slightly less than the γ phase.

These features may probably lead us to such a conclusion that the γ phase is unstable and an intermediate one to the stable β phase, and that this β phase is characterized by an intermolecular O—H···O hydrogen-bond regularly throughout the crystal in contract to the other phases and by mixing cyclohexane the effect of this sort of hydrogen-bond becomes less and the γ phase becomes stable.

It is a pleasure to acknowledge our indebtness to Dr. T. Sugawara of Tohoku University for his kindness in showing us his unpublished data and also to Dr. T. Oda of our University and Dr. S. Seki of Osaka University for their useful discussions.

Laboratory of Physical Chemistry
Osaka Liberal Arts University

6) T. Oda; X-cap, **54**, 2 (1945).

Application of the New equation of state to the Joule-Thomson effect

By Tetsuya ISHIKAWA

(Received July 27, 1953)

In a recent paper[1] I proposed an equation of state which equally satisfies the three criteria for state equations: RT_c/p_cV_c, T_B/T_c and $T_c/p_c\cdot(dp/dT)_c$. One more criterion with technical importance is the Joule-Thomson effect which is formulated thermodynamically

1) This *Bulletin*, **23**, 78 (1953).

by the aid of van der Waals' equation of state, but results in a qualitative formula:

$$\mu=\frac{2a_{corr}/RT-b_{corr}}{C_p},\quad a_{corr}=\frac{27R^2T_c^2}{64p_c},$$

$$b_{corr}=\frac{RT_c}{8p_c} \qquad ...(1)$$

where μ is the Joule-Thomson coefficient, C_p the molecular heat, R the gas constant, and T the temperature, these together with a_{corr} and b_{corr} being expressed in liters, atmospheres, moles, deg. absolute.

I will communicate in this letter the applicability of my equation of state to this problem.

Taking my equation, $p+a/V^2-=RT/(V-b)$, in the deduction of the above formula, it readily follows that

$$\mu=\frac{2aV^{\varepsilon'}/RT-b}{Cp},\quad a=3p_cV_c^2,$$

$$b=V_c/3, \qquad ...(2)$$

here a, b &c. are expressed in the same units as above.

It is noticed here that ε in the preceding paper where V is expressed in cc./mole, and ε' denoted here where V is expressed in liter/mole are related by $\varepsilon=\varepsilon'\times \log V/(\log V+3)$.

From International Critical Tables III, V, and Henning's "Warmetechnische Richtwerte", five available data of H_2, CO_2, N_2, O_2 and air can be taken, among which, however, only air may serve as a test case for pressure effect.

To compare with (2—ε) directly from the equation of state, the test for its validity being the present purpose, estimate ε' from formula (2) and transform it into ε, from which (2—ε) from formula (2) is obtained.

	Hydrogen	
	0°C	100°C
(2—ε) from formula (2)	1.979	2.005
(2—ε) from equation of state	2.000	2.009
	(p=50 atm.)	(p=50 atm.)
Divergence in %	1.1	0.2

	Carbon dioxide	
	0°C	100°C
(2—ε) from formula (2)	1.890	1.910
(2—ε) from equation of state	1.900	1.930
	(extrapolated)	(p=50−1000 atm.)
Divergence in %	0.5	1.0

	Nitrogen	
	0°C	100°C
(2—ε) from formula (2)	1.944	1.965
(2—ε) from equation of state	2.007	2.039
	(p=50−1000 atm.)	(p=50−1000 atm.)
Divergence in %	3.1	3.6

	Oxygen	
	0°C	100°C
(2—ε) from formula (2)	1.941	1.959
(2—ε) from equation of state	1.967	2.026
	(p=36−62 atm.)	(p=100−1000 atm.)
Divergence in %	1.3	3.3

	Air at 0°C			
			p (atm.)	
	1	20	60	100
(2—ε) from formula (2)	1.977	1.969	1.973	1.987
(2—ε) from equation of state	1.987	1.997	2.000	2.002
Divergence in %	0.5	1.4	1.4	0.8

	Air at 100°C			
			p (atm.)	
	1	20	60	100
(2—ε) from formula (2)	1.995	1.995	2.005	2.019
(2—ε) from equation of state	1.986	2.019	2.025	2.029
Divergence in %	0.4	1.2	1.0	0.5

The agreements between these two are fairly good as seen from the above tables, and even the greatest divergence arising in the cases of N_2 and O_2 is less than 4%, where the mean values of $(2-\varepsilon)$ from the equation of state at 50 or 100—1000 atms. are presumably the same as those at 1 atm. These results lead to the conclusion that the Joule-Thomson effect is formulated with accuracy by making use of my equation of state.

Sasebo Commercial Junior College, Sasebo, Nagasaki

Dielectric Properties of Disodium Monohydrogen Phosphate Dodecahydrate, $Na_2HPO_4 \cdot 12H_2O$

By Ryôiti KIRIYAMA and Yusiro SAITO

(Received August 25, 1953)

Using large single crystals we measured the temperature and frequency dependences of the dielectric constants and losses of several hydrated salts. The region of the temperatures measured is from −170°C to the temperature of dehydration and that of frequencies is from 0.3 kc to 3 Mc. For disodium monohydrogen phosphate dodecahydrate, $Na_2HPO_4 \cdot 12H_2O$ (crystal class, C_{2h}), no appreciable anisotropy in its dielectric behaviour is observed. At 3 Mc the dielectric constant perpendicular to (001) is 5.2, monotonously increasing with temperature coefficient 3×10^{-3}. At 0.5 kc, as temperature rises the dielectric dispersion becomes appreciable from about 10°C upward, and ε' reaches a value twice as great as that measured at 3 Mc, accompanying a large conductivity when the temperature is raised to its dehydration temperature 35°C. These are the results obtained with the tin-foiled specimen. On the other hand, in the case of the sandwiched specimen by mica-foils for avoiding the d.c. conductivity, the temperature and frequency dependences of ε' become considerably greater and at 0.5 kc ε' attains to a value of about 70 at 35°C as shown in Fig. 1. The ε' and ε'' values fit in with the Cole-Cole diagram in this dispersion region with distribution parameter α of about 10° (Fig. 2). From the

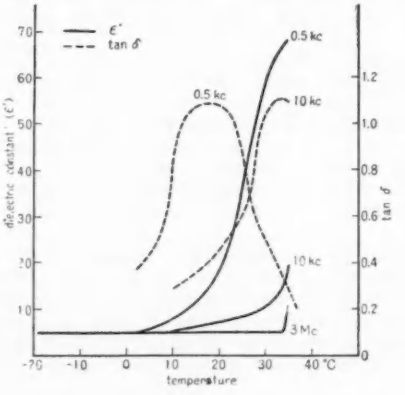

Fig. 1.
Dielectric constant-temperature and loss tangent-temperature curves for $Na_2HPO_4 \cdot 12H_2O$ (perpendicular to (001))

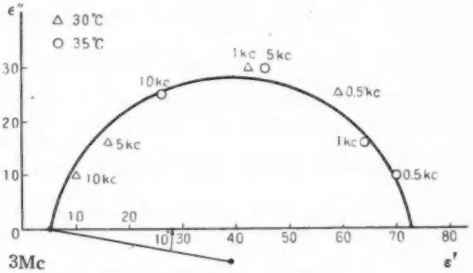

Fig. 2.
Cole-Cole diagram for $Na_2HPO_4 \cdot 12H_2O$ (perpendicular to (001))

relaxation time and its temperature variation, the free energy of activation is obtained to be $\Delta F = 13$ kcal/mole and the enthalpy $\Delta H = 27$ kcal/mole. For the single crystals of $Na_2SO_4 \cdot 10H_2O$ and $Na_2CO \cdot 10H_2O$, we obtained similar results and the single crystal of $Na_2S_2O_3 \cdot 5H_2O$ shows a similar behaviour but to a less extent, and that of $Na_2B_4O_7 \cdot 10H_2O$ no appreciable effects.

All these crystals are very efflorescent, and the dehydrated water molecules are set free from the crystal surfaces and affect the dielectric properties considerably. In the above experiments, we have taken precaution by passing dry air through the measuring cell in order to avoid these effects of dehydrated water as far as possible.

From these measurements and our previous experiments about such behaviours of water of crystallization, it may be concluded that water molecules in these hydrated phosphate, sulphate and carbonate crystals are linked to oxygen atoms in a manner somewhat similar to the water molecules in ice and further the observed dielectric phenomena due to rotation of the water molecules may be originated at some points of lattice defects.

Detailed discussion will be published in this Bulletin.

Department of Chemistry, Faculty of Science, Osaka University, Osaka

Additions and Corrections

Volume 26, 1953

H. Fujita, K. Ninomiya and **T. Homma.** Mechanical Properties of Concentrated Hydrogels of Agar-agar. II.

Page 22. In reference (5), for "Leadermen" read "Leaderman".
Page 23. In col. 1, line 4 from the bottom, for "effect" read "effects".

H. Fujita, and **K. Ninomiya.** Mechanical Properties of Concentrated Hydrogels of Agar-agar. III.

Page 26. In col. 2, line 17, 25, for "parameter" read "parameters".
Page 27. In col. 1, line 4 from the bottom, for "intercepti" read intercept."

M. Ōki. 4,4'-Dimethoxy-α α'-dihalogeno-stilbens.

Page 39. In col. 2, line 30, for "4,4'-dimethoxystilbene" read "4,4'-dimethoxytolane".

S. Yamada, Y. Shimura and **R. Tsuchida.** Spectrochemical Study of Microscopic Crystals. III.

Page 73. In Fig. 1, log ε, for "4.5, 4.0, 3.5, 3.0, 2.5, 2.0" read "4.3, 3.8, 3.3, 2.8, 2.3, 1.8".
Page 74. In Table 1, log ε, for "3.14, 2.66, (3.5), 4.54" read "2.94, 2.46, (3.3), 4.34". In col. 1, line 5 from the bottom, for "shown Fig. 2" read "shown in Fig. 2".
Page 75. In col. 2, line 27 from the bottom, for "much large in" read "much larger in"

T. Sasaki and **M. Muramatsu.** On the Nature of Built-up Film. III.

Page 96. In col. 1, line 14, for "A certain" read "Certain". line 20, for "point of view" read "point of view."
Page 97. In col. 1, line 31, for "observed thet" read "observed that".
Page 98. In col. 1, line 8, for "camelia oil" read "camellia oil".

K. Shinoda. The Effect of Chain Length, Salts and Alcohols on the Critical Micelle Concentration.

Page 102. In col. 1, Equation (2.1), for "C_n/C_{n-1} exp $(-\omega/kT)=1/3$" read "$C_n/C_{n-1}=\exp(-\omega/kT)=1/3$."
Page 104. In col. 2, Table 1, The forth columu, for "Calculated C.M.C." read "Calculated Rate".

R. Senzyu. Untersuchungen über Lignin und Zellstoff. 1.

Page 144. In col. 2, line 11, for "nicht die geeignet" read "nicht geeignet". line 23, for "wird es wie" read "wird es, wie". line 30, for "Ligninsulfosaure" read "Ligninsulfosäure".
Page 145. In reference (14), for "A. Nall". read "A Noll" in col. 2, line 12 from the bottom, for "damit bei Bestimmung" read damit die Bestimmung".
Page 147. In col. 2, line 11 for "Zu die sem" read "Zu diesem".

R. Senzyu. Untersuchungen über Lignin und Zellstoff. II.

Page 148. top, for "Einteilung" read "Einleitung".

Y. Kurita, T. Nozoe and **M. Kubo.** Dipole Moments of Bromotropolones, Thujaplicins and Related Compounds.

Page 242. In col. 1, line 24, for "crystals or whether" read "crystals or."
Page 243. In col. 2, line 5 from the bottom, for "slight dscrepancy" read "slight discrepancy".
Page 244. In col. 1, line 8, for "do not affect" read "does not affect".

T. Nishimura. Antituberculous Compounds. II.

Page 253. In col. 2, line 25, for "butan-3-one" read "butane-3-one". line 28 and Page 254. In col. 2, line 17 from the bottom, for "buten-3-one". read "butene-3-one". title of the sixth section in Experimental, read "1-(p-Nitrophenyl)-2-bromo-1-butene-3-one (VII)". lines 13, 23, for "4-nitro" read "p-nitro" intitle of the seventh section, for "buten-3-one" read "butene-3-one". line 13 from the bottom, for "reprecipi tated" read "reprecipitated".

T. Nishimura. Antituberculous Compounds. III.

Page 262. In col. 2, line 8, for "were washed" read "washed". line 13 from the bottom, for "sopium hydroxide" read "sodium hydroxide".

M. Shimomura and **F. Egami.** Dephosphorylation of Nucleic Acids, Mononucleotides and Casein by Lanthanum and Cerium Hydroxide Gels.

Page 266. In Table 2, the fifth column, for "Periodate consumption Colour intensity of orcinol tert, mole" read "Periodate consumption/colour intensity of orcinol test, mole".

Y. Kurita, S. Seto, T. Nozoe and **M. Kubo.** Dipole Moments of Tropone, 2-phenyltropone, Tropolone Methyl Ether and their Derivatives.

Page 274. In reference (14), for "G. Hazato private communication" read "G. Hazato, private communication".

R. Okawara and **K. Hashitani.** Diallylsilanediol, $(CH_2=CH-CH_2)_2 \cdot Si(OH)_2$.

Page 280. In foot-note, for "excessa mount" read "excess amount".

I. Watanabe and **Y. Kawade.** Purification and Characterization of Tobacco Mosaic Virus.

Page 294. In col. 1, line 2, for "(TMV), by Stanley[1] studies" read "(TMV) by Stanley, studies". line 19, for "preparations by various means among" read "preparations by various means, among".

Page 295. In col. 1, line 2 from the bottom, for "in the case only" read "in the case of TMV-8 only". In col. 2, top line for "pattern of TMV-8, and" read "pattern and".

Page 296. In reference (21), for "2b, 10(81947)" read "2b, 108(1947)".

Page 297. In footnote, line 3, read "sedimentation pattern[18]".

Page 298. In col. 1, line 34, for "to the bes" read "to the best". line 41, for "with the lapse O" read "with the lapse of". line 2 from the bottom, for "to vary various factors" read "to vary by various factors".

M. Fujimoto. Eine Neue Methode zur Darstellung von Eisenrhodanidenlösung mit dem Kationenaustanschenden Harze.

Page 353. In col. 1, top line, for "Um eine" read "Um die".